https://www.mdc-berlin.de/de/veroeffentlichungstypen/clinical-journal-club

Als gemeinsame Einrichtung von MDC und Charité fördert das Experimental and Clinical Research Center die Zusammenarbeit zwischen Grundlagenwissenschaftlern und klinischen Forschern. Hier werden neue Ansätze für Diagnose, Prävention und Therapie von Herz-Kreislauf- und Stoffwechselerkrankungen, Krebs sowie neurologischen Erkrankungen entwickelt und zeitnah am Patienten eingesetzt. Sie sind eingeladen, uns beizutreten. Bewerben Sie sich!

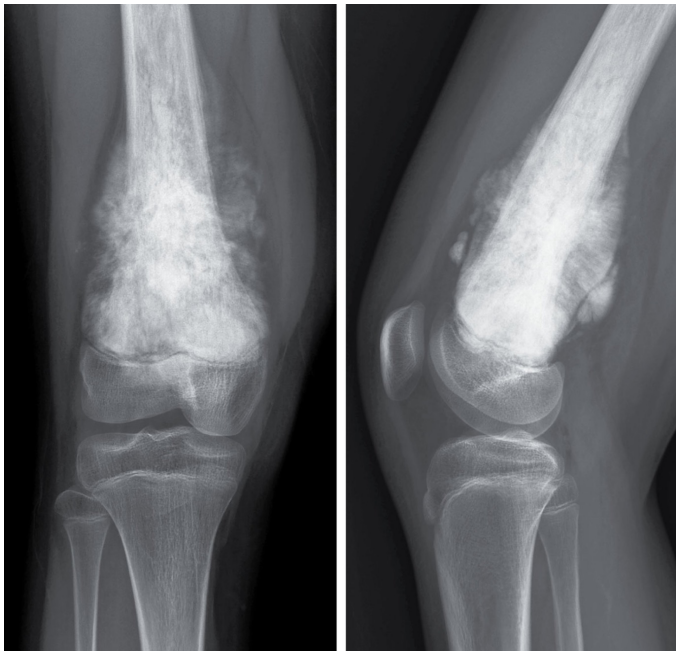

Radiographs showed a metaphyseal osteoblastic lesion with ill-defined margins and cortical destruction in the distal femur. A subsequent magnetic resonance imaging of the knee and a bone biopsy confirmed the diagnosis of high-grade osteosarcoma. Osteosarcoma is the most common primary malignant bone tumor in children. It typically manifests in the second decade of life owing to the rapid bone growth during that stage of development.

An 11-year-old girl presented to the orthopedic clinic with a 1-month history of right thigh pain that worsened at night. Physical examination was notable for soft-tissue swelling over the distal thigh and limited range of motion of the knee on the right side. Which of the following is the most likely diagnosis?

Aneurysmal bone cyst

Chondrosarcoma

Osteoid Osteoma

Osteomyelitis

Osteosarcoma

Atrial fibrillation and the left-atrial appendage

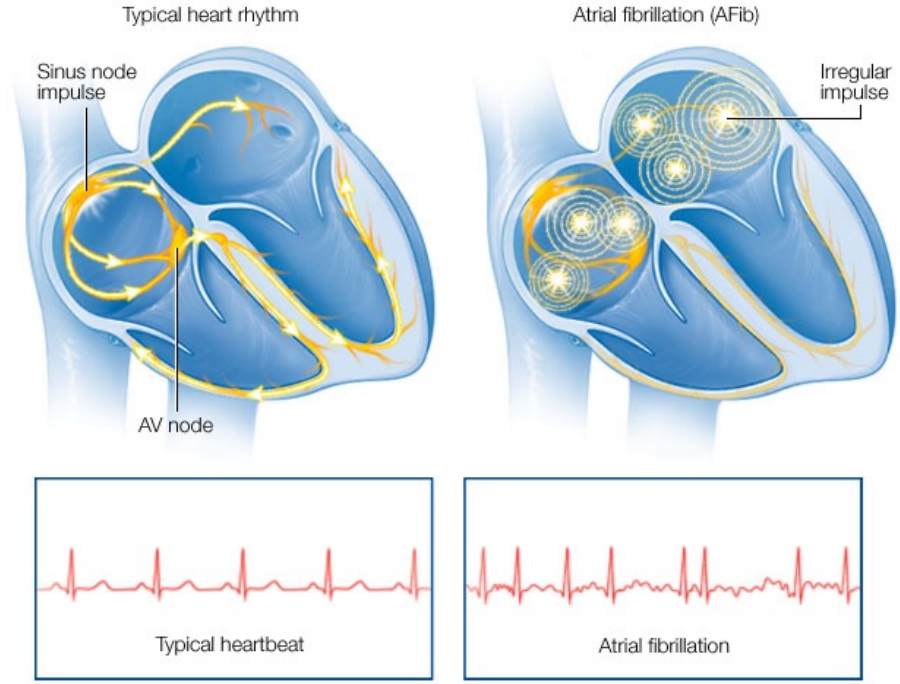

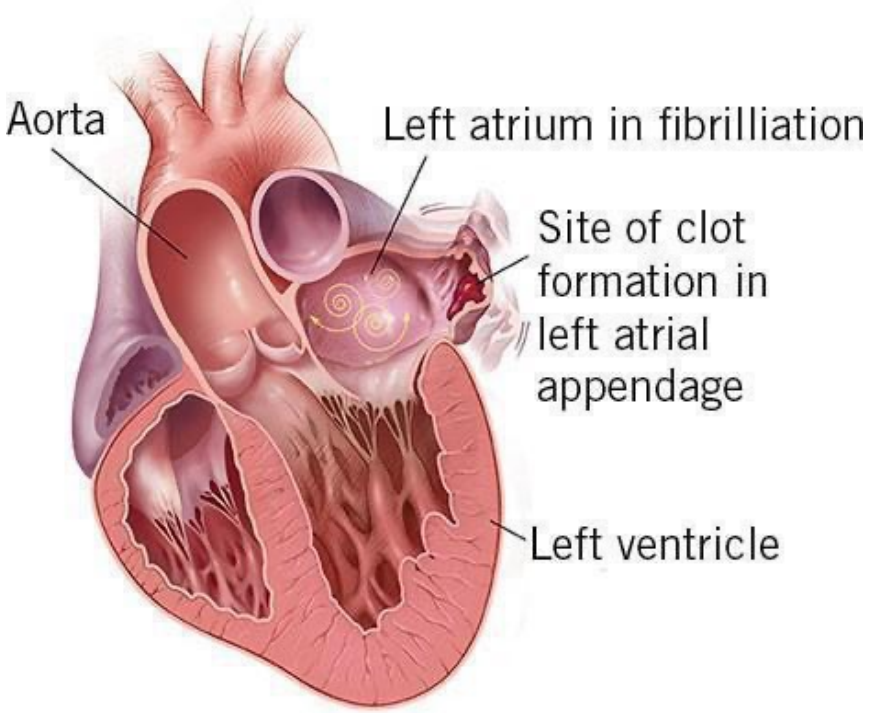

Should the left-atrial appendage be closed?

Das medizinische Prinzip des left atrial appendage closureLAAC

Bei Patienten mit Vorhofflimmern zieht sich der Herzvorhof nicht mehr koordiniert zusammen. Infolgedessen stagniert das Blut, und in über 90 % der Fälle bilden sich gefährliche Blutgerinnsel direkt im linken Vorhofohr (einer kleinen Ausstülpung des Herzens). Wenn sich ein solches Gerinnsel löst, kann es ins Gehirn wandern und einen Schlaganfall auslösen. Der dauerhafte mechanische Verschluss dieses Vorhofohrs verhindert das Entweichen von Gerinnseln in den Blutkreislauf.

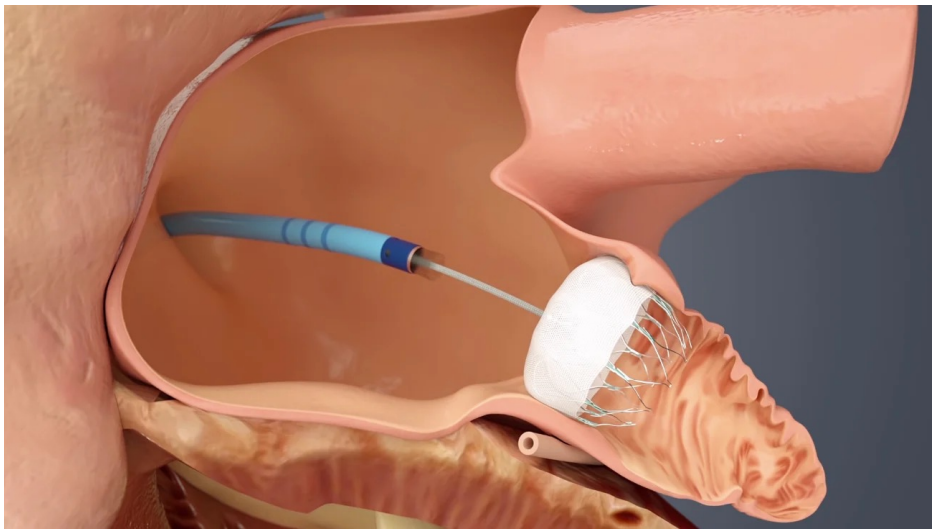

Die WATCHMAN-Produktgenerationen von Boston Scientific

Boston Scientific bietet hochentwickelte Implantate an, die über einen minimalinvasiven Katheterzugriff (meist über die Leistenvene) im Herzen platziert werden.

Left Atrial Appendage Closure or Anticoagulation for Atrial Fibrillation

For patients with atrial fibrillation, the use of oral anticoagulant therapy to prevent stroke is limited by the risk of bleeding. Left atrial appendage closure is considered for patients who are unsuitable candidates for long-term anticoagulation, but its role in patients who are eligible for anticoagulants has not been established.

In this ongoing, prospective, international, randomized trial involving patients with atrial fibrillation who were suitable candidates for anticoagulation, we randomly assigned patients in a 1:1 ratio to receive either device-based left atrial appendage closure (device group) or non–vitamin K antagonist oral anticoagulant (NOAC) therapy (anticoagulation group). The primary efficacy end point — a composite of death from cardiovascular causes, stroke, or systemic embolism — was tested for noninferiority (noninferiority margin, 4.8 percentage points) after 3 years of follow-up. The primary safety end point, non–procedure-related bleeding, was tested for superiority.

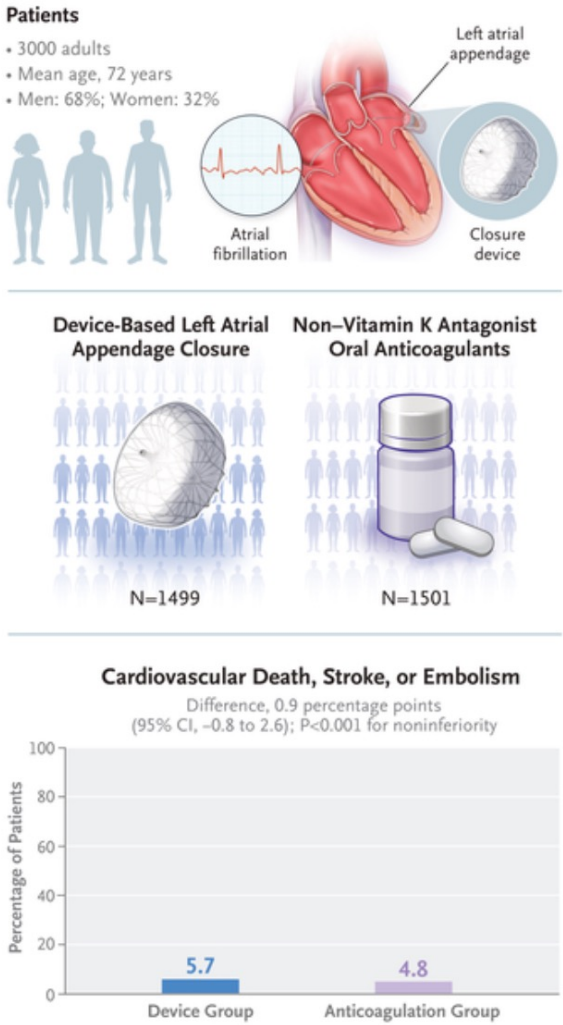

Atrial fibrillation is the most common sustained arrhythmia observed in clinical practice, affecting an estimated 10.5 million persons in the United States and 60 million persons worldwide. A major complication associated with atrial fibrillation is cardioembolic stroke. Non–vitamin K antagonist oral anticoagulant (NOAC) agents are currently the preferred treatment option for patients with atrial fibrillation who are at risk for stroke, but uptake and adherence have been limited by bleeding complications that can accompany NOAC therapy.

A left atrial appendage closure device is currently approved for use in patients who have a rationale to avoid long-term oral anticoagulant therapy. The benefit of left atrial appendage closure has not been well studied in patients who are suitable candidates for NOACs. The CHAMPION-AF (Watchman Flx versus NOAC for Embolic Protection in the Management of Patients with Non-Valvular Atrial Fibrillation) trial was designed to determine whether the use of a left atrial appendage closure device is a reasonable alternative to oral anticoagulation in patients who are eligible for long-term NOAC use. Here, we report the results of an analysis of efficacy and safety after 3 years of follow-up.

Patients

Patients with atrial fibrillation who were at increased risk for stroke (CHA_2DS_2-VASc score of ≥2 for men and ≥3 for women) were eligible for enrollment. The CHA_2DS_2-VASc scale is used to assess the risk of stroke among patients with atrial fibrillation; scores range from 0 to 9, with higher scores indicating a higher risk of stroke. Bleeding risk was assessed with the HAS-BLED score, which reflects the risk of major bleeding among patients with atrial fibrillation receiving anticoagulants; scores range from 0 to 9, with higher scores indicating a greater risk of bleeding. Patients were excluded if they had had a myocardial infarction, stroke, or transient ischemic attack in the 30 days before enrollment or a major bleeding event, defined according to the International Society on Thrombosis and Haemostasis (ISTH) criteria, that had occurred within the previous 30 days.

End Points

The primary efficacy end point was a composite of death from cardiovascular causes (including hemorrhage-related and unexplained deaths), stroke (ischemic or hemorrhagic), or systemic embolism at 3 years.

Characteristic	Anticoagulation Group (N=1501)	Device Group (N=1499)
Age — yr	71.8±7.5	71.6±7.5
Sex — no. (%)		
Male	1027 (68.4)	1014 (67.6)
Female	473 (31.5)	485 (32.4)
Race or ethnic group — no. (%)†		
White	1276 (85.0)	1276 (85.1)
Black	28 (1.9)	35 (2.3)
Hispanic or Latino	42 (2.8)	46 (3.1)
Asian, Native Hawaiian, or Other Pacific Islander	71 (4.7)	64 (4.3)
Other	16 (1.1)	10 (0.7)
Not disclosed	74 (4.9)	71 (4.7)
CHA_2DS_2-VASc score‡		
Average score	3.5±1.3	3.5±1.2
Distribution — no. (%)		
2	349 (23.3)	355 (23.7)
3 to 4	876 (58.4)	864 (57.6)
≥5	276 (18.4)	279 (18.6)
HAS-BLED score§	1.3±0.8	1.3±0.8
Previous ischemic stroke — no. (%)	114 (7.6)	119 (7.9)
Previous hemorrhagic stroke — no. (%)	10 (0.7)	4 (0.3)
Atrial fibrillation pattern — no. (%)		
Paroxysmal	1028 (68.5)	1038 (69.3)
Persistent	382 (25.4)	358 (23.9)
Permanent	91 (6.1)	102 (6.8)
Previous atrial fibrillation ablation — no (%)	704 (46.9)	730 (48.7)
≤3 Months before randomization	71 (4.7)	66 (4.4)
>3 to ≤12 Months before randomization	225 (15.0)	244 (16.3)
>12 Months before randomization	324 (21.6)	347 (23.2)

Primary and Secondary End Points (Kaplan–Meier Estimates) at 3 Years.

End Point	Type of Analysis	Anticoagulation Group (N=1501)	Device Group (N=1499)	Difference (95% CI)	Hazard Ratio (95% CI)	P Value
		no. of patients with event (Kaplan–Meier %)		*percentage points*		
Primary end points						
Efficacy: death from cardiovascular cause, stroke, or systemic embolism†‡	Noninferiority	65 (4.8±0.6)	81 (5.7±0.6)	0.9 (−0.8 to 2.6)	1.20 (0.87 to 1.66)	<0.001
Components of the primary efficacy end point						
Death from cardiovascular cause†		36 (2.7±0.4)	38 (2.7±0.4)	0.0 (−1.2 to 1.2)	1.01 (0.64 to 1.59)	–
Stroke‡		33 (2.5±0.4)	50 (3.6±0.5)	1.1 (−0.2 to 2.4)	1.46 (0.94 to 2.27)	–
Systemic embolism		2 (0.1±0.1)	0	–	–	–
Safety: non–procedure-related bleeding§	Superiority	260 (19.0±1.1)	154 (10.9±0.8)	−8.1 (−10.8 to −5.5)	0.55 (0.45 to 0.67)	<0.001
ISTH major bleeding		87 (6.4±0.7)	71 (5.1±0.6)	−1.4 (−3.1 to 0.4)	0.78 (0.57 to 1.06)	–
Modified ISTH clinically relevant nonmajor bleeding		193 (14.2±0.9)	99 (7.0±0.7)	−7.1 (−9.4 to −4.8)	0.48 (0.37 to 0.61)	–
Secondary end points						
Safety: procedure-related and non–procedure-related ISTH major bleeding	Noninferiority	87 (6.4±0.7)	83 (5.9±0.6)	−0.6 (−2.4 to 1.2)	0.92 (0.68 to 1.24)	<0.001
Net clinical benefit: cardiovascular death, stroke, systemic embolism, or non–procedure-related bleeding†‡§	Noninferiority	300 (21.8±1.1)	215 (15.1±1.0)	−6.7 (−9.6 to −3.8)	0.66 (0.56 to 0.79)	<0.001

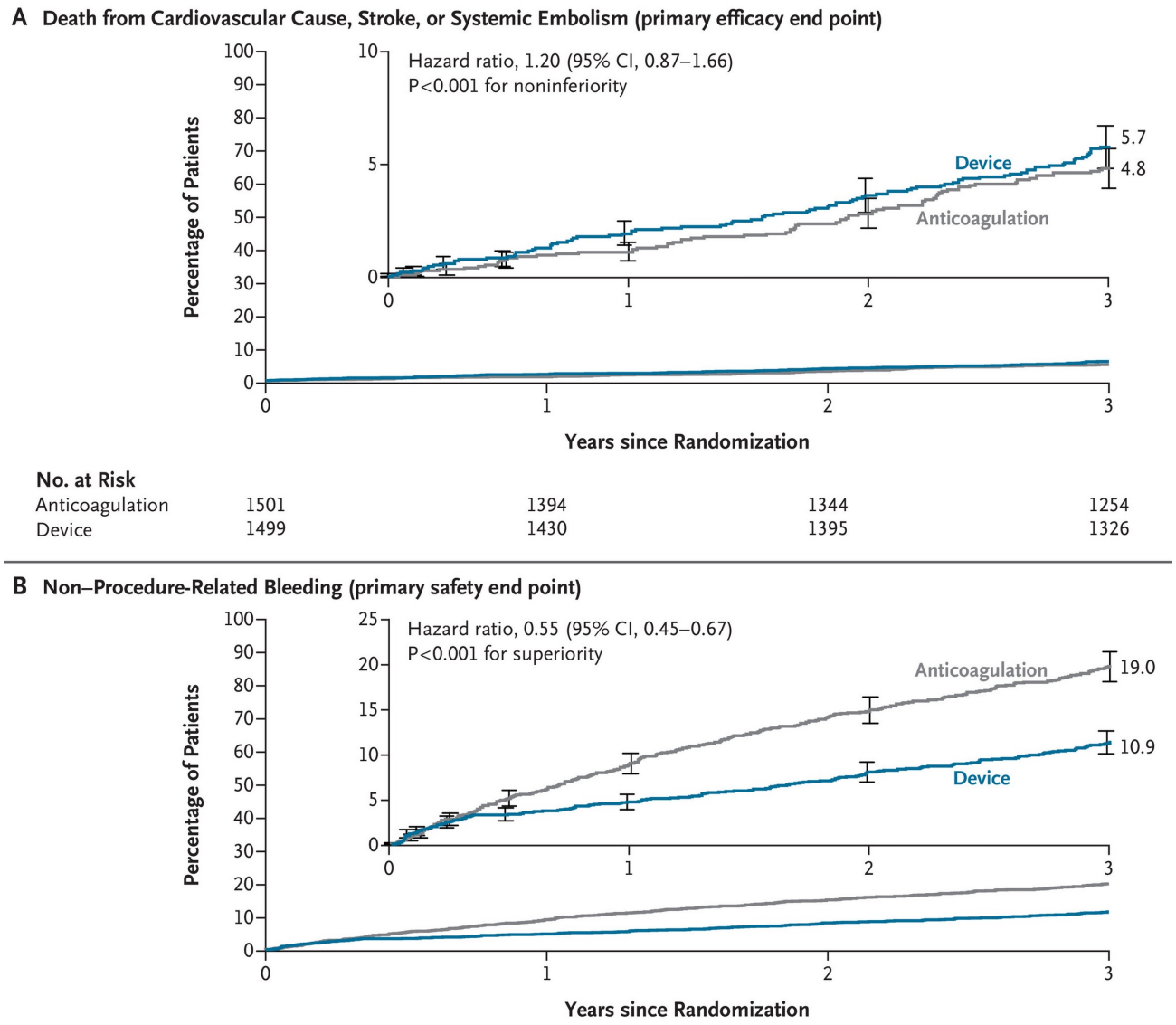

Kaplan–Meier Curves for the Primary End Points.

Panel A shows the 3-year incidence of death from cardiovascular causes, stroke, or systemic embolism (primary composite efficacy end point). Panel B shows the incidence of non–procedure-related bleeding (the primary safety end point), which included major bleeding (as defined by the International Society on Thrombosis and Haemostasis [ISTH]) and clinically relevant nonmajor bleeding (defined according to modified ISTH criteria). The insets show the same data on an expanded y axis. The I bars indicate 1.5 times the standard error.

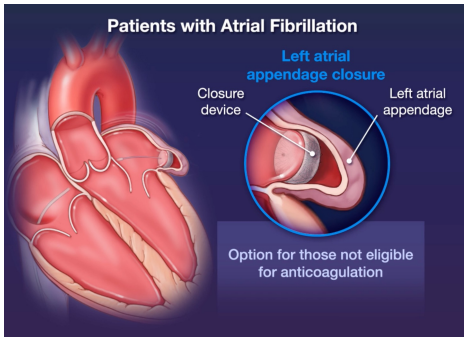

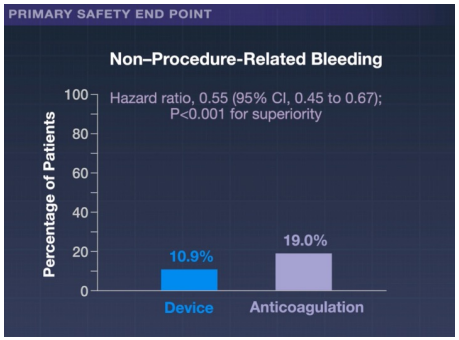

Superiority here

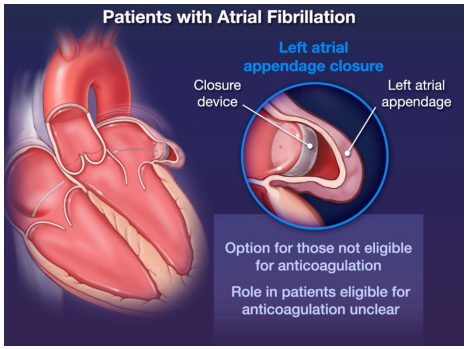

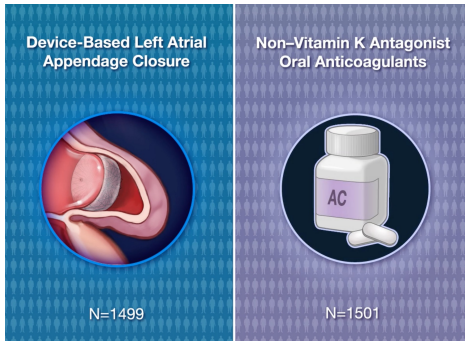

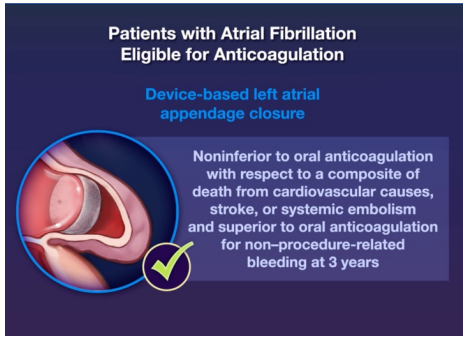

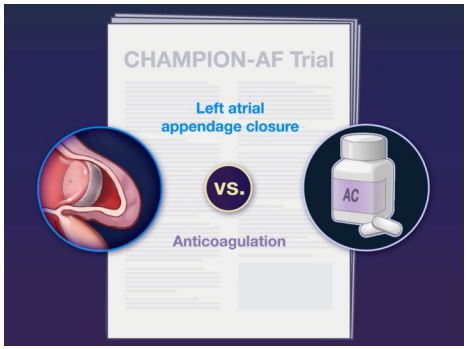

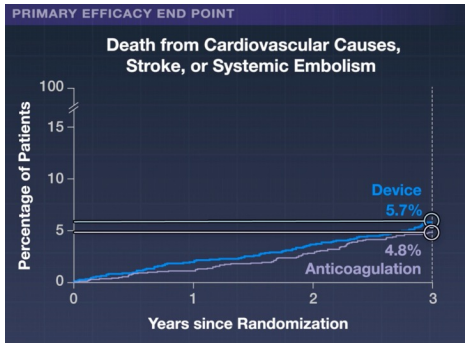

A study from Berlin in April could not show non-inferiority for left atrial appendage closure

Is HFNC worth it?

Die **High-Flow-Sauerstofftherapie** (oft als HFOT oder HFNC für *High Flow Nasal Cannula* bezeichnet) ist eine **nicht-invasive Form der Atemunterstützung**, bei der Patienten ein erwärmtes und befeuchtetes Sauerstoff-Luft-Gemisch mit sehr hohen Flussraten verabreicht wird. Im Gegensatz zur klassischen Sauerstofftherapie (bis zu 15 l/min) bewegt sich der Gasfluss hier üblicherweise zwischen **20 und 60 Litern pro Minute** (teilweise bis zu 70 l/min).

Funktionsweise und Parameter

Das System besteht aus einem Mischer (Air/Oxygen Blender), einem aktiven Befeuchter und einer speziellen, großlumigen Nasenkanüle. Drei wesentliche Parameter lassen sich exakt einstellen:

•**Gasfluss (Flow):** Steuerung des Atemgases in Litern pro Minute.

•**FiO2:** Der exakte Sauerstoffanteil der Einatmungsluft (21 % bis 100 %).

•**Temperatur:** Anwärmung des Gases (meist 31–37 °C) zur Schonung der Schleimhäute

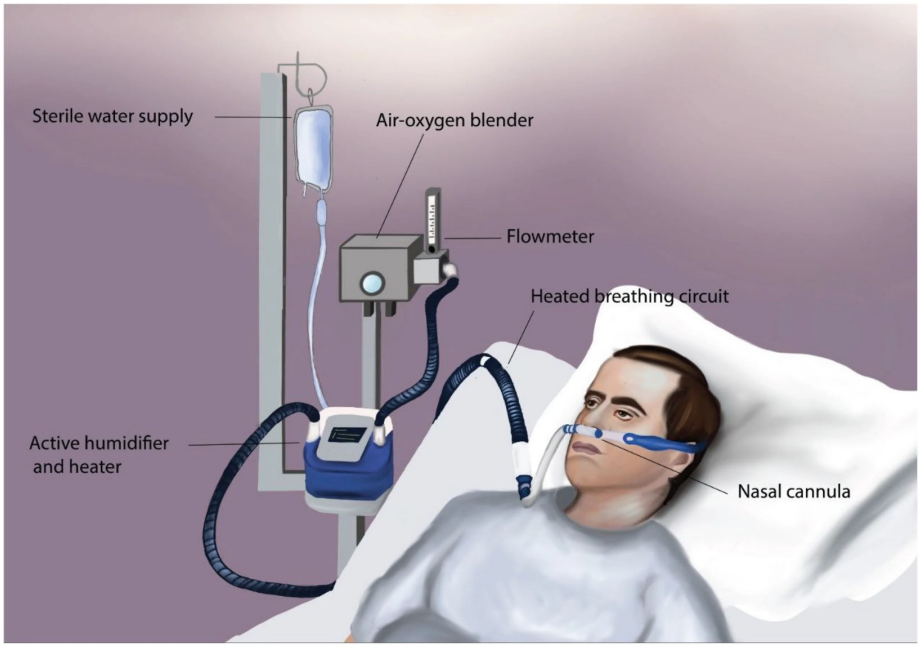

High-Flow Nasal Cannula (HFNC) therapy typically requires **3 to 6 times more pure oxygen** from hospital supply systems than conventional oxygen masks to deliver the same high concentration of oxygen.

High-Flow or Standard Oxygen in Acute Hypoxemic Respiratory Failure

Data are needed on the effect of oxygen delivered through a high-flow nasal cannula, as compared with standard oxygen therapy, on intubation and mortality in patients with acute hypoxemic respiratory failure.

In this multicenter, open-label trial, we randomly assigned patients who had acute hypoxemic respiratory failure to receive high-flow-oxygen or standard-oxygen therapy. All the patients had a ratio of the partial pressure of arterial oxygen to the fraction of inspired oxygen of 200 or less, a respiratory rate of more than 25 breaths per minute, and pulmonary infiltrate on chest imaging. The primary outcome was death by day 28.

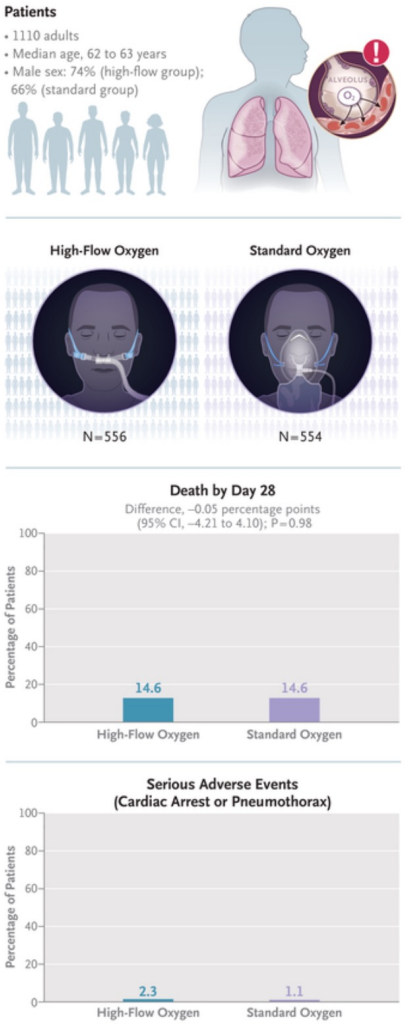

Acute respiratory failure is the leading cause of admission to intensive care units (ICUs), accounting for approximately three quarters of admissions worldwide. Acute hypoxemic respiratory failure in the absence of cardiogenic pulmonary edema or chronic respiratory diseases is caused primarily by viral or bacterial pneumonia and is associated with the worst outcomes.

The administration of oxygen is the first-line therapy and can be given with a standard nonrebreather mask, with high-flow oxygen through nasal cannula, or with noninvasive ventilation through a face mask. The primary goal is to avoid endotracheal intubation, because invasive mechanical ventilation is associated with severe adverse events and can result in high mortality.

Although standard oxygen is the most common approach to treating patients with acute hypoxemic respiratory failure, such therapy is limited in its ability to provide high levels of fraction of inspired oxygen (Fio_2) and to unload inspiratory effort. In contrast, high-flow oxygen and noninvasive ventilation improve oxygenation and relieve patient effort and dyspnea.

Methods

Trial Design and Oversight

The SOHO (Standard Oxygen versus High-Flow Oxygen Therapy in Acute Hypoxemic Respiratory Failure) trial was an investigator-initiated, multicenter, open-label, randomized clinical trial conducted in 42 ICUs.

Trial Population

Consecutive adult patients (≥18 years of age) who had been admitted to an ICU with acute hypoxemic respiratory failure were eligible if they met all the following criteria: a respiratory rate of more than 25 breaths per minute, pulmonary infiltrates on chest imaging, and a ratio of partial pressure of arterial oxygen (Pao_2; measured in mm Hg) to the fraction of inspired oxygen (Fio_2) of 200 or less while breathing oxygen at a flow of 10 liters per minute or more through a nonrebreather mask. For the calculation of the Pao_2:Fio_2 ratio, the Fio_2 was estimated as 0.03×(oxygen flow in liters/min)+0.21.

Interventions

In the high-flow-oxygen group, oxygen was delivered through a heated humidifier (MR850, Fisher and Paykel Healthcare) and was applied continuously through large-bore binasal prongs, with a gas flow rate of at least 50 liters per minute. The Fio_2 was adjusted to maintain oxygen saturation, as measured by a pulse-oximetry level of 92 to 96%.

Outcomes

The primary outcome was death from any cause 28 days after randomization. Key secondary outcomes were endotracheal intubation within 28 days after randomization, the interval between randomization and intubation.

Variables	High-Flow Oxygen (N=556)	Standard Oxygen (N=554)
Age — yr	62±13	63±13
Male sex — no. (%)	411 (73.9)	364 (65.7)
Body-mass index†	28±6	28±6
SAPS II‡	35±13	34±14
Median SOFA score (IQR)§	2 (2–3)	2 (2–3)
Median Clinical Frailty Score (IQR)¶	2 (1–3)	2 (1–3)
Current smoker — no. (%)	72 (12.9)	90 (16.2)
Coexisting illness — no. (%)		
Immunosuppression‖	124 (22.3)	124 (22.4)
Ischemic heart disease	52 (9.4)	53 (9.6)
Chronic lung disease	61 (11.0)	61 (11.0)
Main reason for acute respiratory failure — no. (%)		
Viral pneumonia	300 (54.0)	292 (52.7)
Covid-19	258 (46.4)	259 (46.8)
Bacterial pneumonia	172 (30.9)	180 (32.5)
Fungal pneumonia	17 (3.1)	17 (3.1)
Other reason	67 (12.1)	65 (11.7)
Medication — no. (%)		
Glucocorticoid	343 (62.3)	338 (62.0)
Vasopressor	13 (2.3)	8 (1.4)
Bilateral pulmonary infiltrates — no. (%)	491 (88.3)	478 (86.3)
Clinical measure		
Heart rate — beats/min	92±21	92±22
Respiratory rate — breaths/min	30±5	31±6
Median dyspnea score (IQR) — mm**	33 (9–59)	25 (5–50)
Oxygen flow rate — liters/min	13±3	13±3
Arterial blood gas		
pH	7.45±0.05	7.45±0.06
Pao_2 — mm Hg	76±17	76±16
Pao_2:FIo_2 ratio††	131±32	132±32
$Paco_2$ — mm Hg	35±5	35±5
Arterial pressure — mm Hg		
Systolic	129±22	129±22
Mean	90±15	90±15
Median time between ICU admission and randomization (IQR) — hr	2.5 (1.3–5.9)	2.4 (1.4–6.4)

Primary and Secondary Outcomes.

Outcome	High-Flow Oxygen (N=556)	Standard Oxygen (N=554)	Difference (95% CI)†	P Value
Primary outcome				
Death by day 28 — no. (%)				
Unadjusted analysis	81 (14.6)	81 (14.6)	−0.05 (−4.21 to 4.10)	0.98
Adjusted analysis‡	81 (14.6)	81 (14.6)	−0.28 (−3.88 to 3.33)	—
Secondary outcomes				
Intubation at day 28 — no. (%)	236 (42.4)	268 (48.4)	−5.93 (−11.78 to −0.08)	—
Median time from randomization to intubation (IQR) — hr	24 (10 to 67)	23 (10 to 47)	0.4 (−6.8 to 6.5)	—
Median ventilator-free time at day 28 (IQR) — days§	28 (11 to 28)	26 (10 to 28)	2.0 (0.0 to 4.0)	—
Death — no. (%)				
In ICU	81 (14.6)	82 (14.8)	−0.2 (−4.4 to 3.9)	—
In hospital	94 (16.9)	99 (17.9)	−1.0 (−5.4 to 3.5)	—
By day 90	98 (17.6)	104 (18.8)	−1.2 (−5.7 to 3.4)	—
Median duration of invasive ventilation (IQR) — days	0 (0–9)	0 (0–10)	0.0 (−2.0 to 0.0)	
Median length of stay (IQR) — days				
In ICU	7 (4 to 13)	8 (4 to 15)	−1.0 (−1.0 to 1.0)	—
In hospital	15 (10 to 24)	16 (10 to 26)	−1.0 (−3.0 to 1.0)	—
Analyses performed 1 hr after treatment initiation				
Pao_2 — mm Hg	75±22	82±25	−7.0 (−10.1 to −3.9)	—
Pao_2:FIo_2 ratio	120±41	144±51	−24 (−30.0 to −18.0)	—
$Paco_2$ — mm Hg	34±5	36±5	−2.0 (−2.6 to −1.3)	—
Respiratory rate — breaths/min	26±7	29±7	−3.0 (−3.8 to −2.2)	—
Dyspnea score (IQR) — mm¶‖	25 (9 to 50)	20 (5 to 50)	4.5 (−1.5 to 10.5)	—
Improved grade of patient-perceived dyspnea — no. (%)‖**	275 (49.5)	192 (34.7)	14.9 (8.6 to 21.1)	—

Der normale **PaO_2/FiO_2-Quotient** (auch bekannt als Horovitz-Quotient oder P/F-Ratio) liegt auf Meereshöhe bei gesunden Menschen **zwischen 400 und 500 mmHg**. Ein Wert **über 380 bis 400 mmHg** gilt in der klinischen Praxis allgemein als völlig unauffällig und normal.

Serious Adverse Events and Causes of Death.

Adverse Event or Cause of Death	High-Flow Oxygen (N=556)	Standard Oxygen (N=554)	P Value
Serious adverse events			
Serious adverse events during spontaneous breathing — no. (%)			
Cardiac arrest leading to intubation	3 (0.5)	2 (0.4)	1.00
Pneumothorax	10 (1.8)	4 (0.7)	0.11
Severe complications during intubation procedure — no./total no. (%)			
Cardiac arrest	4/236 (1.7)	4/268 (1.5)	1.00
Severe arterial hypotension*	26/236 (11.0)	24/268 (9.0)	0.44
Pulse-oximetry level of <80%	54/236 (22.9)	68/268 (25.4)	0.52
Serious adverse events after intubation — no. (%)			
Septic shock	50 (9.0)	60 (10.8)	0.31
Ventilator-associated pneumonia	95 (17.1)	104 (18.8)	0.46
Cause of death			
Death at day 90 — no./total no. (%)			0.11
Cardiac arrest in ICU	5/98 (5.1)	12/104 (11.5)	
Refractory hypoxemia in ICU	21/98 (21.4)	13/104 (12.5)	
Refractory shock in ICU	11/98 (11.2)	7/104 (6.7)	
Withdrawal of life-sustaining therapy	38/98 (38.8)	38/104 (36.5)	
Death after ICU discharge	23/98 (23.5)	34/104 (32.7)	

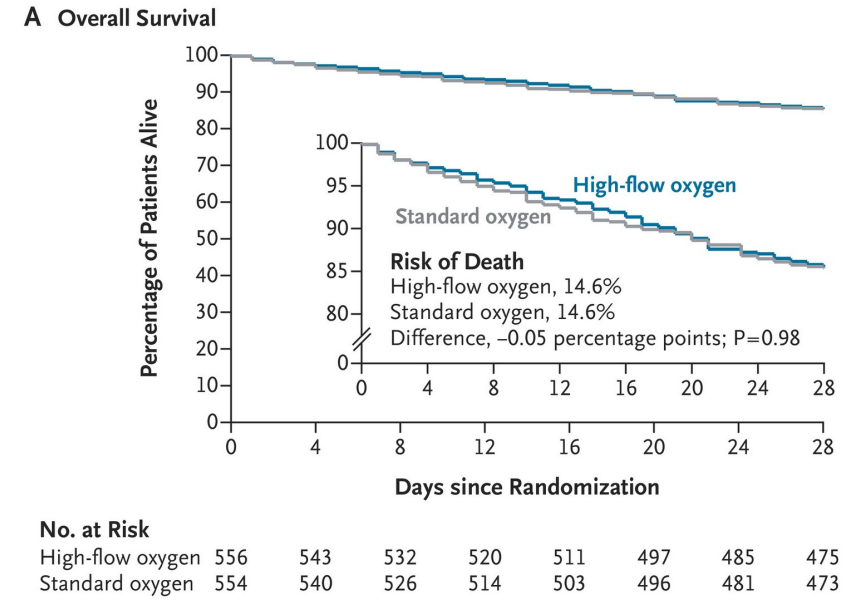

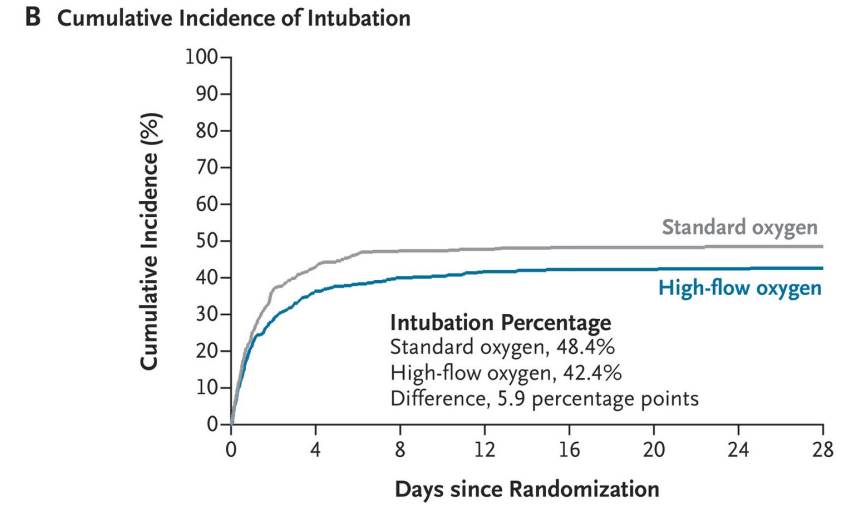

Probability of Survival and Cumulative Incidence of Intubation.

Panel A shows the probability of survival during the first 28 days after randomization in the group that received high-flow oxygen and the group that received standard oxygen. The curves in the inset show the same data on an expanded y axis. Panel B shows the cumulative incidence of intubation during the first 28 days after randomization, with death considered as a competing event.

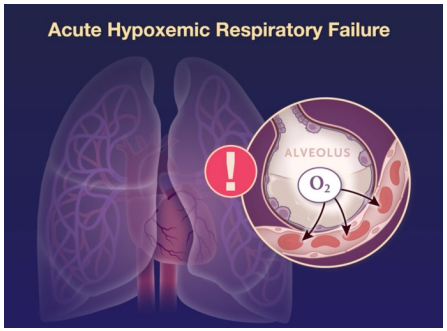

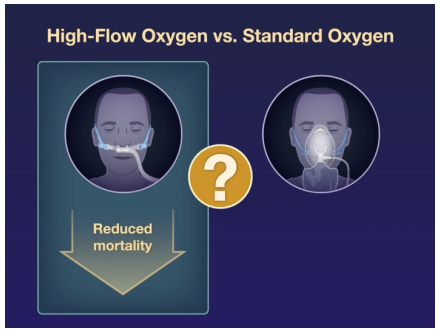

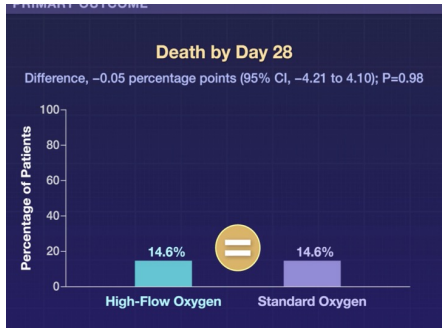

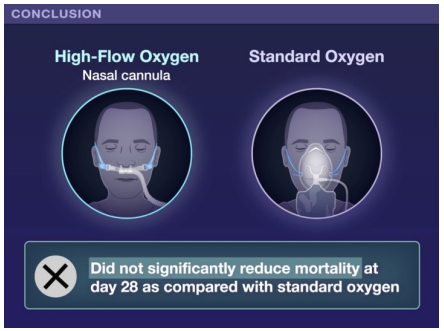

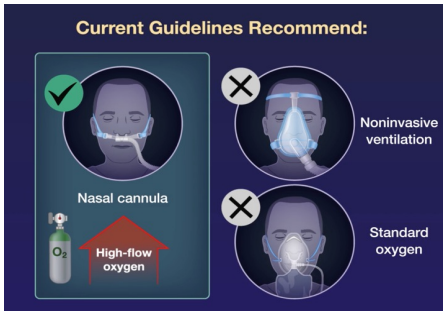

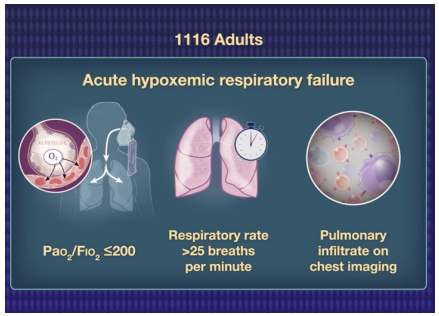

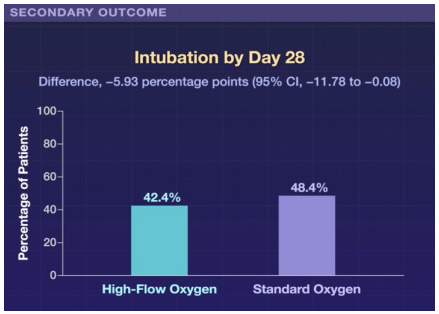

High-flow oxygen was not better thtan a mask

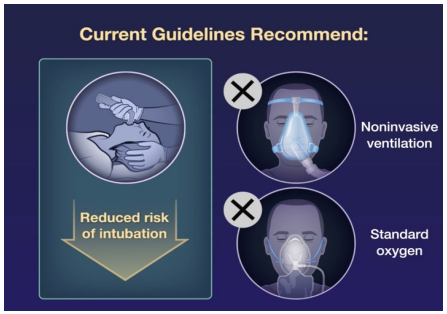

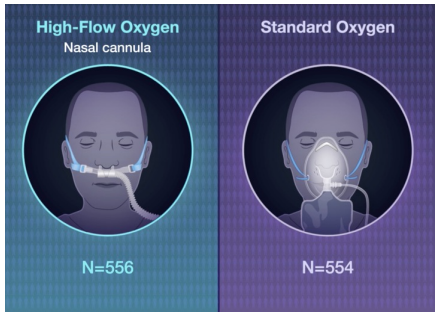

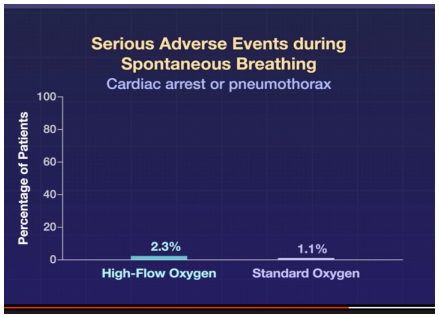

Acute myelogenous leukemia and old-old people

Der Begriff **"Old-Old" (die Hochbetagten)** bezeichnet in der Gerontologie (Altersforschung) die Altersgruppe der Menschen, die **85 Jahre und älter** sind.

Die Akute Myeloische Leukämie (AML) ist eine schnell fortschreitende Form von Blutkrebs, die das blutbildende System befällt. Entartete, unreife weiße Blutkörperchen verdrängen gesunde Blutzellen. Sie erfordert eine sofortige Diagnose und intensive Therapie in spezialisierten Zentren.

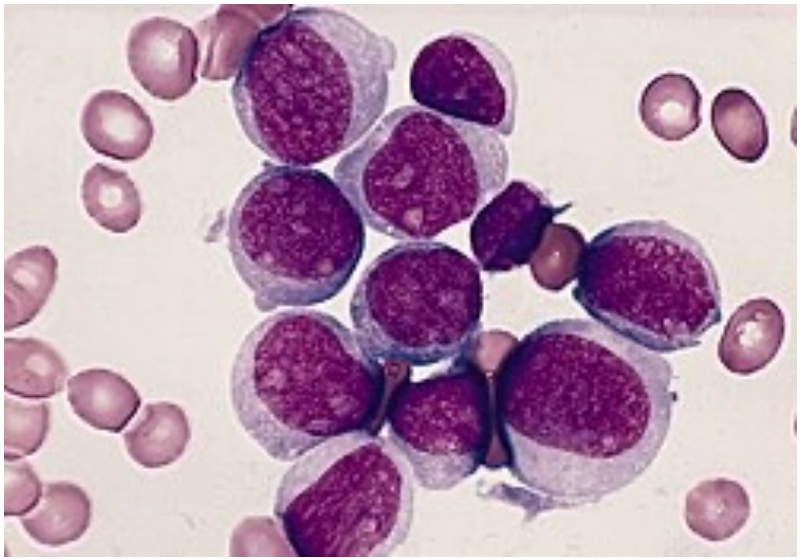

Diagnostik und Behandlung

Verdachtsfälle werden umgehend durch ein großes Blutbild und eine Knochenmarkpunktion abgeklärt. Die Therapie gliedert sich meist in zwei Phasen:

1.Induktionstherapie: Eine hochdosierte Chemotherapie im Krankenhaus, um die Leukämiezellen zurückzudrängen.

2.Konsolidierungstherapie: Weitere Chemotherapien oder eine Stammzelltransplantation (bei Hochrisikopatienten), um Rückfälle zu verhindern.

Decitabin/Cedazuridin ist eine fixe kombinationstherapie in Tablettenform, die zur Behandlung bestimmter Formen von **Blut- und Knochenmarkskrebs** eingesetzt wird.

- **Decitabin (35 mg):** Ein hypomethylierendes Antineoplastikum (DNA-Methyltransferase-Inhibitor). Es schleust sich in die DNA von Krebszellen ein und reaktiviert Gene, die das Tumorwachstum hemmen, wodurch die krankhafte Vermehrung der unreifen Blutzellen gestoppt wird.

- **Cedazuridin (100 mg):** Ein Enzymhemmer (Cytidin-Deaminase-Inhibitor). Decitabin wird im Magen-Darm-Trakt normalerweise sehr schnell durch das Enzym Cytidin-Deaminase abgebaut und wirkt oral alleine nicht. Cedazuridin blockiert dieses Enzym vorübergehend, sodass das Decitabin intakt in den Blutkreislauf gelangt und dieselbe Wirkung wie eine Infusion erzielen kann.

Venetoclax ist ein moderner, zielgerichteter Arzneistoff aus der Gruppe der **Bcl-2-Hemmer**, der zur Behandlung bestimmter Formen von **Blutkrebs** eingesetzt wird. Im Gegensatz zur klassischen Chemotherapie bekämpft er Krebszellen, indem er gezielt ein Überlebensprotein in den Tumorzellen blockiert und so deren natürlichen Zelltod (Apoptose) einleitet

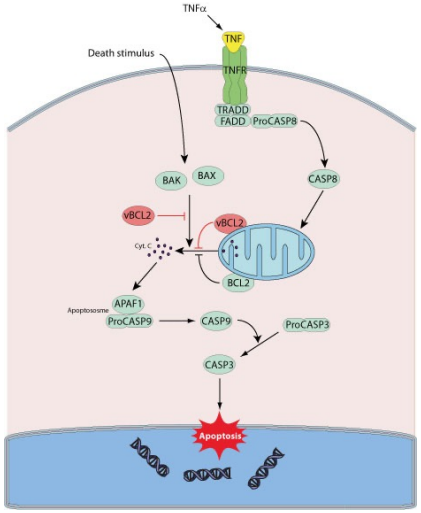

All-Oral Treatment of Newly Diagnosed Acute Myeloid Leukemia

For patients with acute myeloid leukemia (AML) who are 75 years of age or older or who are ineligible for intensive induction chemotherapy, azacitidine or decitabine plus venetoclax is the standard of care, but parenteral administration imposes a burden on patients and providers. Oral decitabine–cedazuridine, approved in Europe for AML, has pharmacokinetic properties equivalent to those of intravenous decitabine but provides limited survival benefit as monotherapy.

In this phase 1–2, open-label, multicenter, nonrandomized trial, we assigned patients with newly diagnosed AML who were 75 years of age or older or who were ineligible for intensive chemotherapy to receive oral decitabine–cedazuridine plus oral venetoclax. To mitigate myelosuppression observed in phase 1, schedule adjustments were encouraged in phase 2b after bone marrow blast clearance. The primary end points were the venetoclax area under the curve from 0 to 24 hours and maximum observed concentration with or without decitabine–cedazuridine (measures of drug interaction) on days 5 and 15 of cycle 2 (phase 1–2a) and complete response (phase 2a–b).

Conclusions

Among patients with newly diagnosed AML who were ineligible for intensive chemotherapy, all-oral decitabine–cedazuridine plus venetoclax caused no drug interactions and resulted in a complete response in nearly half the patients, with myelosuppressive effects.

Patients with acute myeloid leukemia (AML) who are ineligible for intensive induction chemotherapy have limited therapeutic options. Venetoclax, a selective inhibitor of B-cell lymphoma 2 (BCL-2), plus azacitidine, a hypomethylating agent, is approved in the United States and European Union (EU) for patients with AML who are 75 years of age or older or who have coexisting conditions that preclude standard chemotherapy. Decitabine, another hypomethylating agent, is also approved with venetoclax on the basis of similar efficacy in a phase 1b study. Azacitidine and decitabine have limited overall survival benefit as single agents. The current standard of care involves daily parenteral administration of decitabine or azacitidine in a health care setting, for 5 to 7 days per cycle. Treatment is ongoing until the occurrence of unacceptable toxic effects or disease progression and is associated with substantial time, logistic, and quality-of-life challenges for patients, caregivers, and providers. ASCERTAIN-V (ASTX727-07) is a phase 1–2 clinical trial designed to investigate the safety and efficacy of all-oral decitabine–cedazuridine plus venetoclax in patients with newly diagnosed AML who are 75 years of age or older or who have coexisting conditions that preclude intensive chemotherapy. Our objective was to use the enhanced flexibility of an all-oral regimen to optimize outcomes while mitigating regimen-related burdens.

The trial included patients with newly diagnosed AML according to World Health Organization criteria who were 75 years of age or older or who were 18 years of age or older and had at least one coexisting condition that precluded the use of intensive chemotherapy: severe cardiac or pulmonary disorder, creatinine clearance of 30 to less than 45 ml per minute, moderate hepatic impairment (total bilirubin level, >1.5 to 3.0 times the upper limit of the normal range), or an Eastern Cooperative Oncology Group (ECOG) performance-status score (on a 5-point scale in which higher scores reflect greater disability) of 2 (phase 1) or 2 or 3 (phase 2).

Trial Design and Regimens

All the patients received decitabine–cedazuridine (35 mg of decitabine and 100 mg of cedazuridine) on days 1 through 5 and venetoclax at dose of 400 mg daily in 28-day cycles after initial ramp-up in cycle 1 to reduce tumor lysis syndrome (day 1, 100 mg; day 2, 200 mg, and day 3 or later, 400 mg).

End Points and Assessments

The trial had pharmacokinetic (phases 1 and 2a) and efficacy (phase 2b) end points. The phase 1 primary end points were the effect of decitabine–cedazuridine on venetoclax pharmacokinetics and potential drug–drug interactions, as assessed by the venetoclax area under the curve from 0 to 24 hours ($AUC_{0–24}$) and maximum observed concentration (C_{max}) with or without decitabine–cedazuridine on days 5 and 15 of cycle 2. Secondary end points in phase 1 were decitabine and cedazuridine $AUC_{0–24}$ and C_{max} on day 5 with venetoclax in cycle 2.

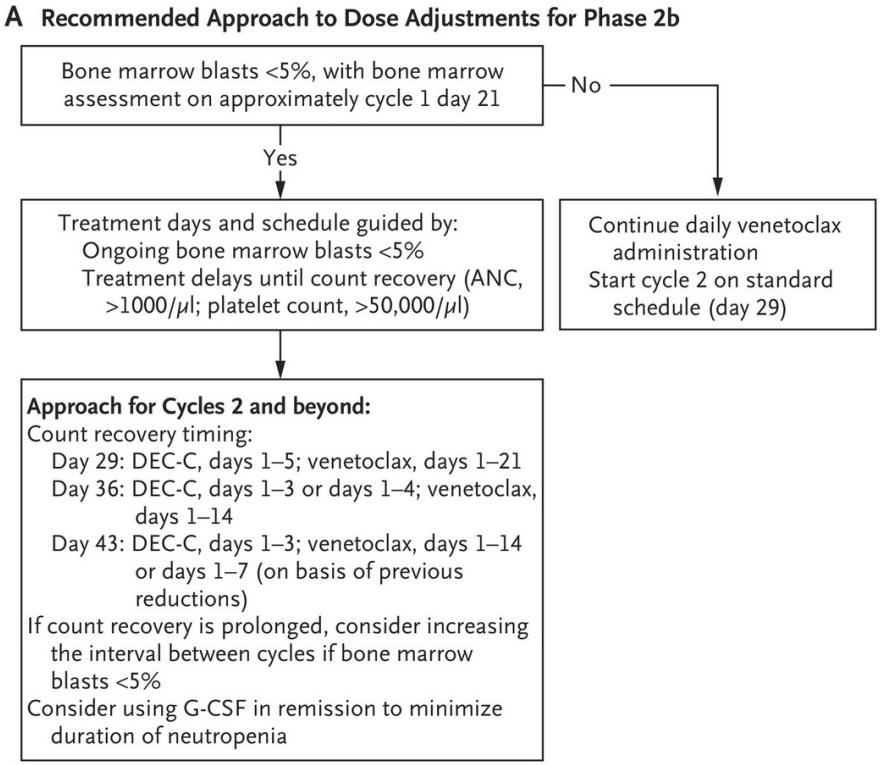

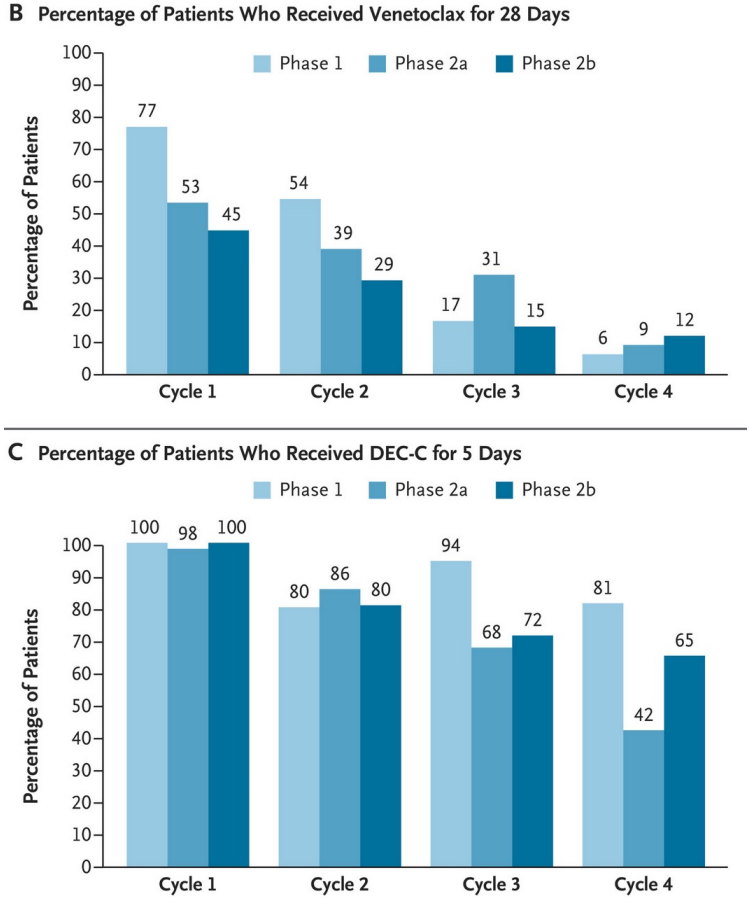

Recommended Approach to Dose Adjustments for Phase 2b and Effect on Number of Days of Treatment Administration.
ANC denotes absolute neutrophil count, DEC-C decitabine–cedazuridine, and G-CSF granulocyte colony-stimulating factor.

Characteristic	Phase 1 (N=30)	Phase 2a (N=58)	Phase 2b (N=101)
Median age (range) — yr	78.0 (66–87)	75.0 (56–91)	78.0 (63–88)
Sex — no. (%)			
Male	16 (53)	33 (57)	61 (60)
Female	14 (47)	25 (43)	40 (40)
ECOG performance-status score — no. (%)†			
0	1 (3)	3 (5)	27 (27)
1	18 (60)	24 (41)	52 (51)
2	11 (37)	28 (48)	18 (18)
>2	0	3 (5)	3 (3)
Missing	0	0	1 (1)
Cytogenetic classification according to ELN 2017 criteria — no. (%)			
Favorable	0	2 (3)	1 (1)
Intermediate	23 (77)	40 (69)	66 (65)
Adverse	5 (17)	13 (22)	24 (24)
Test failed or missing	2 (7)	3 (5)	10 (10)
Mutation profiling according to sequencing — no. (%)‡			
TP53	NA	3 (5)	17 (17)
IDH1	NA	6 (10)	6 (6)
IDH2	NA	6 (10)	12 (12)
FLT3-ITD	NA	NA	11 (11)
KMT2A fusions	NA	2 (3)	0
NPM1	NA	8 (14)	13 (13)
KRAS	NA	3 (5)	12 (12)
NRAS	NA	6 (10)	11 (11)
NPM1/FLT3	NA	2 (3)	4 (4)
≥2 Reasons for ineligibility to receive intensive chemotherapy — no. (%)	NA	10 (17)	19 (19)

Summary of Responses

Variable	Phase 1 (N=30)	Phase 2a (N=58)	Phase 2b (N=101)
Complete response — % (95% CI)	40 (23–59)	38 (26–52)	47 (36–57)
Complete response with incomplete hematologic recovery — % (95% CI)	23 (10–42)	28 (17–41)	17 (10–26)
Complete response with partial hematologic recovery — % (95% CI)	17 (6–35)	21 (11–33)	5 (2–11)
Complete response or complete response with incomplete hematologic recovery — % (95% CI)	63 (44–80)	66 (52–78)	63 (53–73)
Complete response or complete response with partial hematologic recovery — % (95% CI)	57 (37–74)	59 (45–71)	51 (41–62)
Complete response, complete response with incomplete hematologic recovery, or complete response with partial hematologic recovery — % (95% CI)	63 (44–80)	66 (52–78)	63 (53–73)
Complete response that was sustained at 12 mo — % (95% CI)	75 (41–91)	71 (47–86)	75 (57–87)
Median time to complete response (range) — mo	1.9 (0.9–9.6)	2.4 (0.8–12.2)	2.4 (0.7–15.3)

Safety Summary.

Event	Phase 1 (N=30)		Phase 2a (N=58)		Phase 2b (N=101)	
	All Grades	Grade ≥3	All Grades	Grade ≥3	All Grades	Grade ≥3
	number of patients (percent)					
Any adverse event	30 (100)	26 (87)	58 (100)	53 (91)	100 (99)	99 (98)
Treatment-related adverse event*	22 (73)	19 (63)	42 (72)	37 (64)	81 (80)	73 (72)
Serious adverse event	19 (63)		45 (78)		85 (84)	
Treatment-related serious adverse event*	7 (23)		16 (28)		36 (36)	
Adverse event leading to treatment discontinuation	0		6 (10)		9 (9)	
Adverse event leading to treatment interruption	14 (47)		38 (66)		69 (68)	
Adverse event leading to dose reduction	7 (23)		5 (9)		14 (14)	
Adverse event leading to death	3 (10)		7 (12)		16 (16)	
Most frequent treatment-related adverse events*†						
Hematologic						
Anemia	6 (20)	6 (20)	15 (26)	13 (22)	33 (33)	30 (30)
Neutropenia	1 (3)	1 (3)	13 (22)	13 (22)	26 (26)	26 (26)
Febrile neutropenia	0	0	14 (24)	14 (24)	25 (25)	25 (25)
Platelet count decreased	11 (37)	11 (37)	17 (29)	17 (29)	27 (27)	25 (25)
Thrombocytopenia	2 (7)	2 (7)	6 (10)	5 (9)	22 (22)	20 (20)
Neutrophil count decreased	16 (53)	16 (53)	16 (28)	16 (28)	21 (21)	20 (20)
White-cell count decreased	5 (17)	5 (17)	17 (29)	17 (29)	15 (15)	15 (15)
Nonhematologic						
Constipation	10 (33)	1 (3)	6 (10)	0	8 (8)	0
Nausea	6 (20)	0	10 (17)	0	20 (20)	0

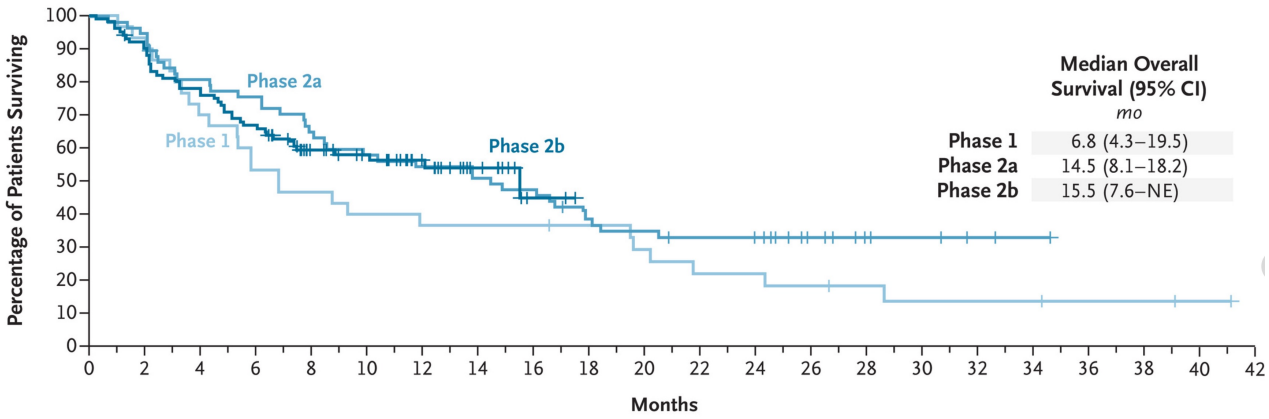

Not a bad treatment for the „old-old“

Discussion

Among patients with newly diagnosed AML who were ineligible for intensive chemotherapy, the all-oral regimen of decitabine–cedazuridine plus venetoclax resulted in a complete response in 47%, either a complete response or complete response with incomplete hematologic recovery in 63%, and a median overall survival of 15.5 months, with expected levels of myelosuppression. As expected on the basis of in vitro risk assessments, pharmacokinetic results confirmed no drug–drug interactions between oral decitabine–cedazuridine and venetoclax, and no new safety signals were observed. In phase 2b, although cross-trial comparisons must be interpreted cautiously, decitabine exposure after coadministration of decitabine–cedazuridine plus venetoclax appeared to be generally similar to the reported results for decitabine–cedazuridine alone in the ASTX727-02 trial. Toxic effects with oral decitabine–cedazuridine and venetoclax were as anticipated, as were 30-day and 60-day mortality in this patient population.

CAR-T-Zellen (Chimäre Antigenrezeptor-T-Zellen) sind gentechnisch veränderte Immunzellen, die gezielt zur Bekämpfung von Krebs eingesetzt werden. Bei dieser Form werden körpereigene T-Lymphozyten (Abwehrzellen) aus dem Blut isoliert, im Labor modifiziert und anschließend dem Patienten zurückgegeben. Sie gelten als einer der bedeutendsten Durchbrüche in der modernen Onkologie.

Der Behandlungsablauf in Einzelschritten

1.Zellgewinnung (Leukapherese): Dem Patienten wird über eine Blutwäsche Blut entnommen, um die T-Zellen herauszufiltern.

2.Labor-Modifikation: Ein harmloses Virus transportiert das neue CAR-Gen in die Zellen.

3.Vermehrung: Die modifizierten Zellen werden im Labor millionenfach vermehrt, was in der Regel mehrere Wochen dauert.

4.Lymphodepletion: Der Patient erhält eine milde Chemotherapie, um Platz für die neuen Abwehrzellen zu schaffen.

5.Infusion: Die CAR-T-Zellen werden wie eine Bluttransfusion in die Blutbahn zurückgeführt

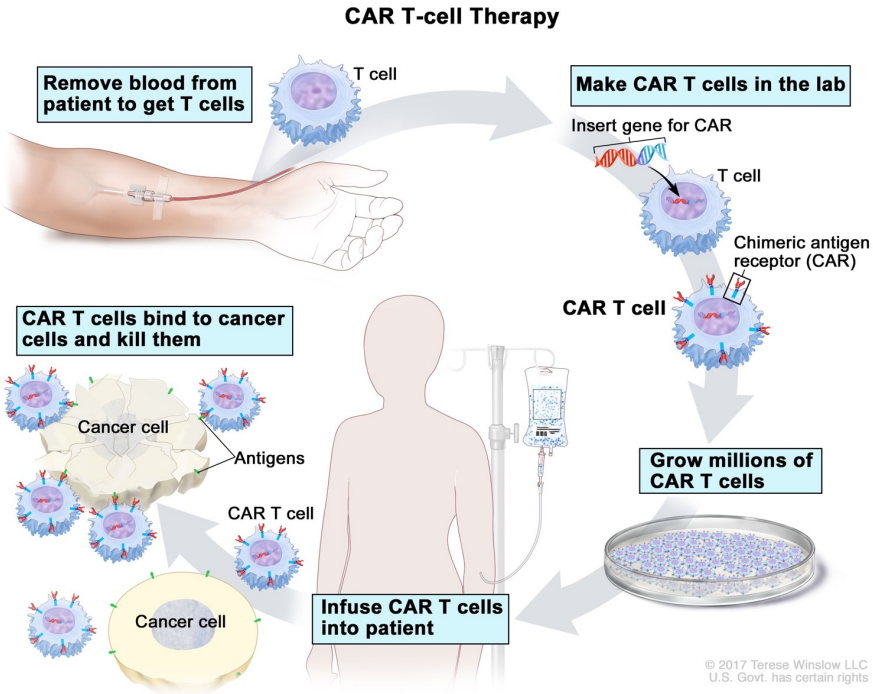

Kidney Transplantation in Two Highly Sensitized Candidates after CAR T-Cell Therapy

Summary

HLA sensitization poses a major challenge to kidney transplantation for patients with end-stage kidney disease, especially for highly sensitized candidates. Attempts at antibody elimination (desensitization) have had inconsistent efficacy and have often failed to produce sustained reductions in anti-HLA antibodies in patients with the highest level of sensitization (calculated panel-reactive antibody score, ≥99.9%). We now report the results for the safety run-in cohort of a multicenter phase 1 clinical study evaluating the safety and efficacy of combined CD19-targeted and B-cell maturation antigen (BCMA)–targeted chimeric antigen receptor (CAR) T cells in eliminating the cellular sources of preformed anti-HLA antibodies (ClinicalTrials.gov number, NCT06056102). Kidney transplantation was performed in two highly sensitized candidates after desensitization with the use of dual CAR T-cell therapy.

More than 91,000 candidates currently await kidney transplantation in the United States; approximately 5000 of these candidates have a high level of sensitization to HLA, which makes transplantation immunologically challenging. HLA sensitization is quantified with the calculated panel-reactive antibody (cPRA) score, the estimated percentage of deceased donors with whom a candidate is incompatible owing to the presence of prohibitive anti-HLA antibodies. Very highly sensitized candidates (cPRA score, ≥99.9%) have the longest waiting times, the lowest likelihood of undergoing transplantation, and the highest risk of death occurring while they are on the waiting list.

Options are being investigated that target either B cells or plasma cells, including treatment with proteasome inhibitors; antibodies against CD20, interleukin-6, or CD38; or T-cell–engaging bispecific antibodies. Given that chimeric antigen receptor (CAR) T-cell therapy has been successful in the treatment of B-cell and plasma-cell cancers, we tested the use of CAR T cells to deplete both B cells and plasma cells and to promote a durable reduction in the level of anti-HLA antibodies in order to facilitate kidney transplantation in highly sensitized candidates.

Methods

We initiated a multicenter phase 1 clinical study evaluating the safety and efficacy of the combination of CD19-targeted CAR T cells and B-cell maturation antigen (BCMA)–targeted CAR T cells in eliminating the cellular sources of alloantibodies, namely memory B cells and plasma cells, as a desensitization strategy in candidates for kidney transplantation with a cPRA score of 99.9% or higher.

All the patients enrolled in the study are to receive an infusion of both CD19-targeted CAR T cells and BCMA-targeted CAR T cells, preceded by lymphodepleting chemotherapy. In the safety run-in cohort (two patients), the dose for both CAR T-cell products (5×10^7 CAR+ cells) was one tenth of the dose that had been used in previous oncology trials, and the lymphodepleting chemotherapy regimen was milder, with cyclophosphamide administered at a dose of 375 mg per square meter of body-surface area daily for 3 days.

The two patients in the safety run-in cohort also underwent five sessions of plasmapheresis, which began 1 month after the CAR T-cell infusion. Each session of plasmapheresis was followed by an infusion of low-dose IVIG (100 mg per kilogram of body weight) that was administered to accelerate the clearance of circulating alloantibodies. Testing for anti-HLA antibodies was performed with a single-antigen bead assay (One Lambda).

(**A**) Serum creatinine pre- and post- CAR T infusion and post-transplant. (**B**) Photomicrograph of renal allograft at day 62 post-transplant. Banff scores: t0, i0, v0, ptc0, g0, ci0, ct0, cv0, cg0.

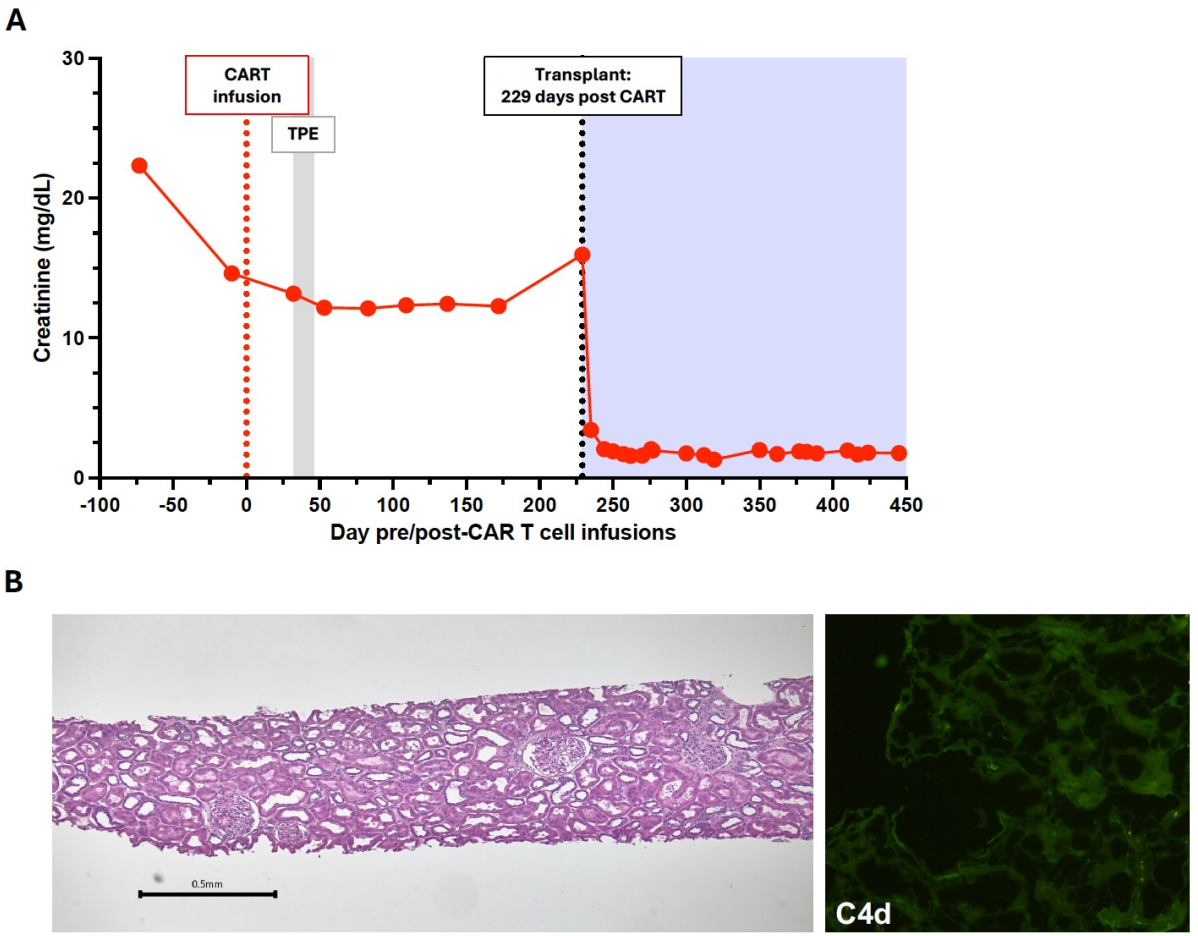

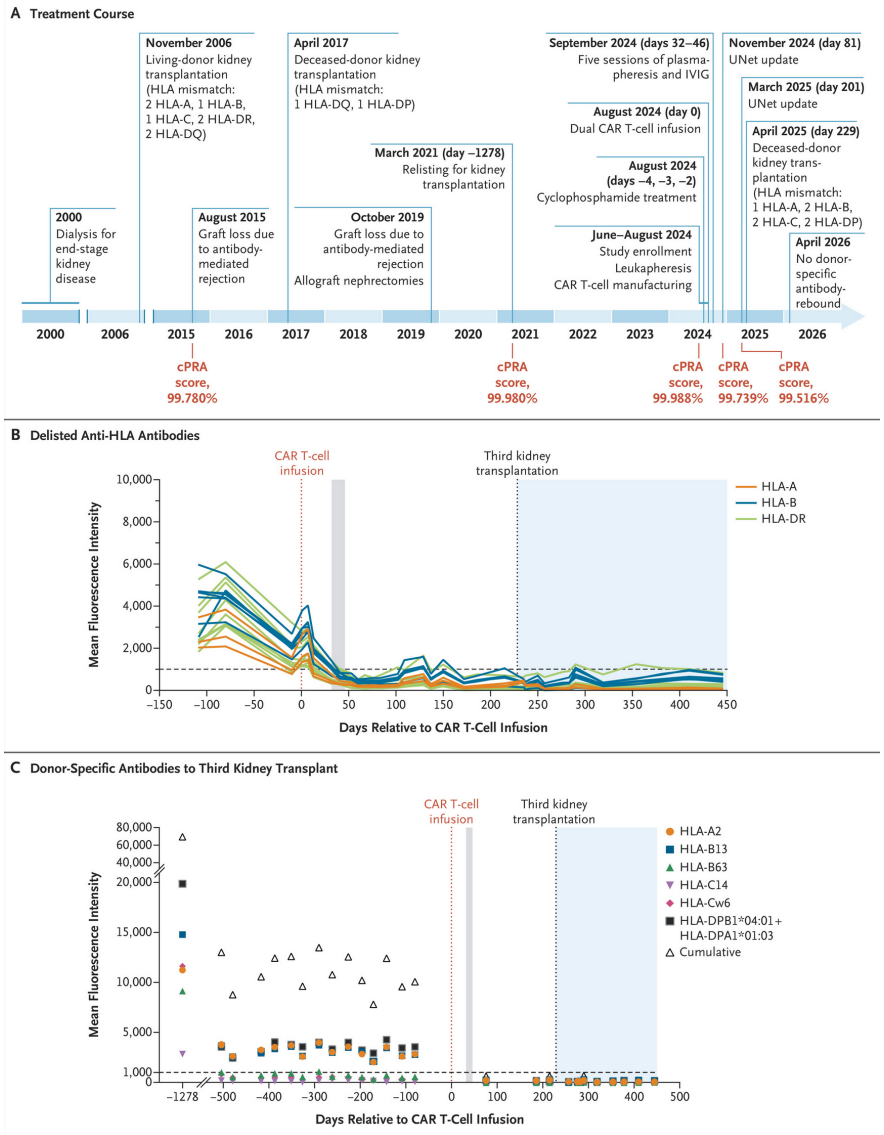

Treatment Course and Anti-HLA Antibody Levels in Patient 1.

Panel A shows the treatment course and calculated panel-reactive antibody (cPRA) scores before and after the infusion of chimeric antigen receptor (CAR) T cells in Patient 1. The cPRA score is the estimated percentage of deceased donors with whom a candidate is incompatible owing to the presence of prohibitive anti-HLA antibodies. Panel B shows levels of antibodies to HLA antigens that were eventually delisted in the patient, before and after the CAR T-cell infusion. Panel C shows levels of donor-specific antibodies to the third kidney transplant before and after the CAR T-cell infusion. In Panels B and C, the horizontal dashed line indicates the threshold (<1000 mean fluorescence intensity) at which an anti-HLA antibody was considered to be eliminated and the corresponding HLA antigen could be removed from the patient's listing in UNet, an online database system developed by the United Network for Organ Sharing. Gray shading indicates the period in which five sessions of plasmapheresis and intravenous immune globulin (IVIG) were administered; blue shading indicates the post-transplantation period.

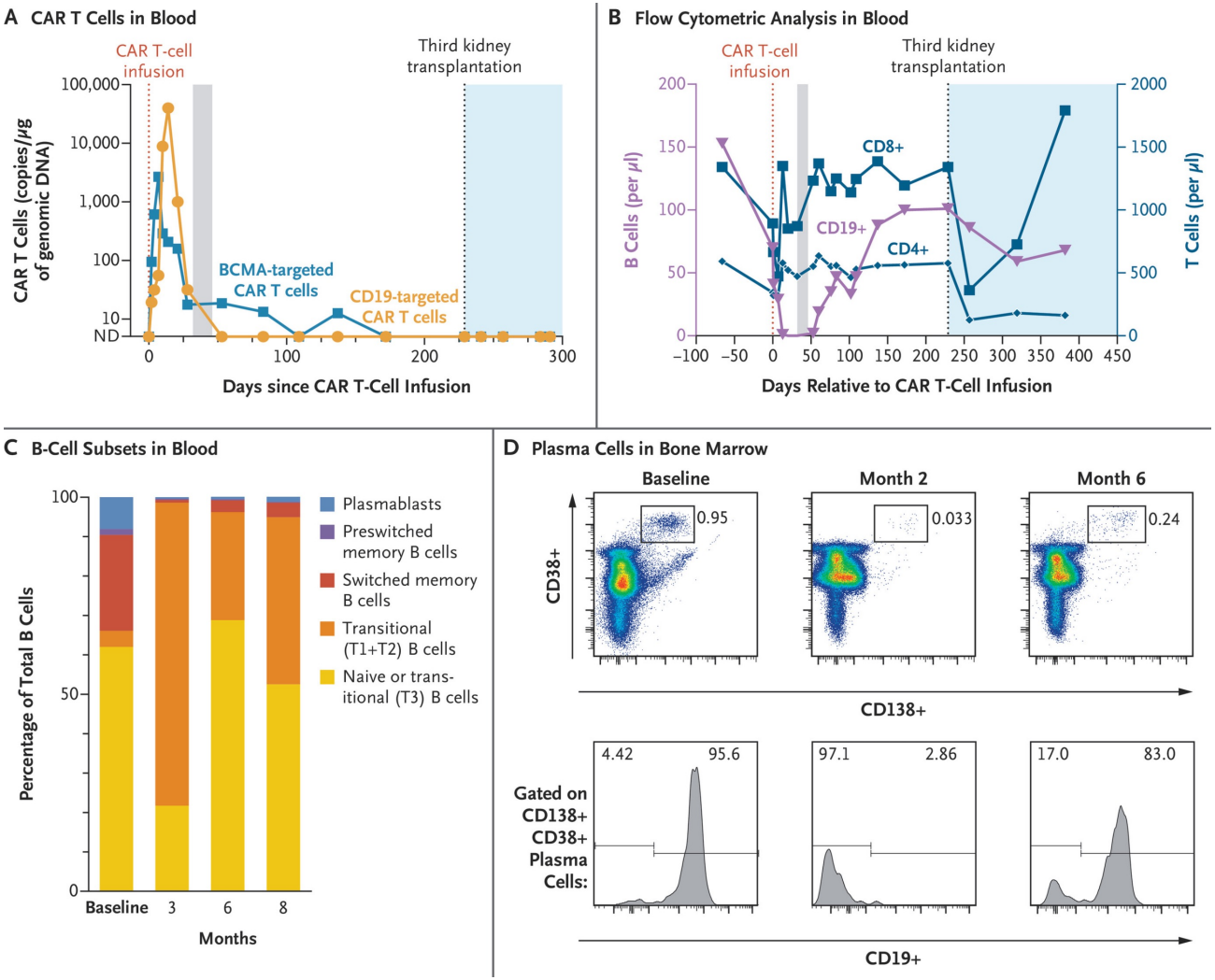

CAR T-Cell Pharmacokinetics and Pharmacodynamics in Patient 1.

Panel A shows levels of CAR T cells in blood after the infusion. ND denotes not detected. Panel B shows the results of flow cytometric analysis in blood before and after the CAR T-cell infusion, including levels of B cells and T cells. The normal ranges are as follows: CD19+ B cells, 91 to 610 per microliter; CD4+ T cells, 430 to 1800 per microliter; and CD8+ T cells, 210 to 1200 per microliter. In Panels A and B, gray shading indicates the period in which five sessions of plasmapheresis and IVIG were administered; blue shading indicates the post-transplantation period. Panel C shows the distribution of B-cell subsets before and after the CAR T-cell infusion. In Panel D, the top row shows the percentage of plasma cells in total nucleated cells in bone marrow, and the bottom row shows the percentage of CD138+CD38+ plasma cells with CD19 expression, before and after the CAR T-cell infusion.

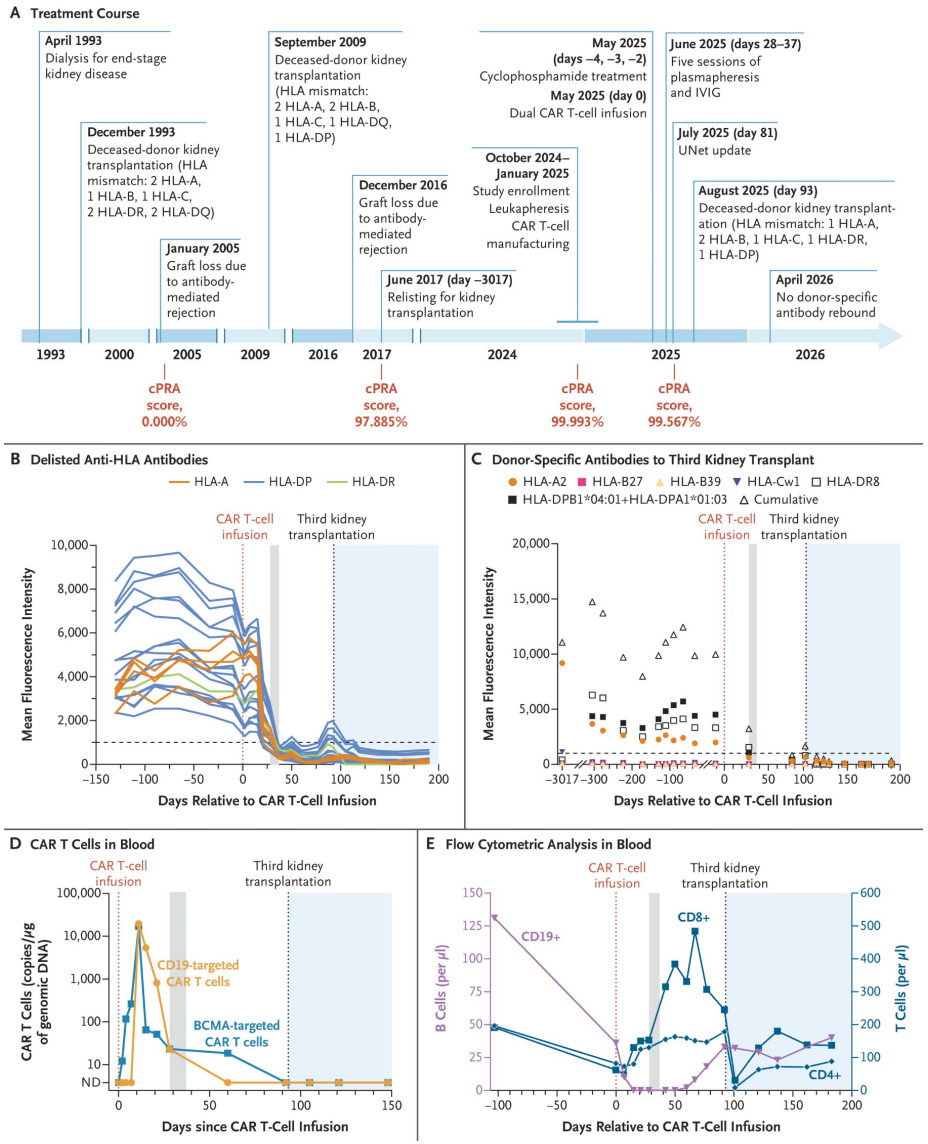

Treatment Course, Anti-HLA Antibody Levels, CAR T-Cell Levels, and Flow Cytometric Analysis in Patient 2.

Panel A shows the treatment course and cPRA scores before and after the CAR T-cell infusion in Patient 2. Panel B shows levels of antibodies to HLA antigens that were eventually delisted in the patient, before and after the CAR T-cell infusion. Panel C shows levels of donor-specific antibodies to the third kidney transplant before and after the CAR T-cell infusion. In Panels B and C, the horizontal dashed line indicates the threshold (<1000 mean fluorescence intensity) at which an anti-HLA antibody was considered to be eliminated and the corresponding HLA antigen could be removed from the patient's UNet listing. Panel D shows levels of CAR T cells in blood after the infusion. Panel E shows the results of flow cytometric analysis in blood before and after the CAR T-cell infusion, including levels of B cells and T cells. The normal ranges are as follows: CD19+ B cells, 91 to 610 per microliter; CD4+ T cells, 430 to 1800 per microliter; and CD8+ T cells, 210 to 1200 per microliter. In Panels B through E, gray shading indicates the period in which five sessions of plasmapheresis and IVIG were administered; blue shading indicates the post-transplantation period.

Discussion

These initial results for the safety run-in cohort of our phase 1 clinical study suggest further expansion of the growing list of clinical applications for CAR T cells beyond oncology. Like most patients who are treated with CAR T cells for autoimmune conditions, the two patients in the safety run-in cohort had no apparent high-grade adverse events, a finding that we speculate is due to the lower antigenic burden in these patients than in those with hematopoietic cancers. CAR T-cell therapy in these patients led to deep but transient B-cell depletion. The preservation of preexisting protective antibodies in Patient 1 suggests that plasma-cell depletion was incomplete yet sufficient to yield a reduction in all alloantibodies, with many decreasing to an undetectable level. Of note, this treatment enabled lowering of the cPRA score in both patients, which led to kidney offers and ultimately to transplantation.

Kidney Transplantation after Clearing Anti-HLA Antibodies with CD19 CAR T Cells

We report the clinical course of a broadly HLA-sensitized patient in whom anti-CD19 chimeric antigen receptor (CAR) T-cell therapy enabled successful kidney transplantation. Kidney failure developed in a 35-year-old woman who, during childhood, had hemolytic uremic syndrome caused by enterohemorrhagic *Escherichia coli*. She received a kidney transplant from her mother at 21 years of age; however, the graft failed after 11 years owing to chronic active antibody-mediated rejection refractory to plasmapheresis, intravenous immune globulin therapy, and rituximab. The failed graft was not removed. The patient had never been pregnant and had not received any cell-containing blood transfusions.

The probability of finding an HLA-matched, ABO-compatible donor within the Eurotransplant network was 0.08%. Given this low probability, the patient was enrolled in a compassionate-use protocol to receive KYV-101, a fully human anti-CD19 CAR T-cell product, to enable her to undergo a second kidney transplantation. After lymphodepletion at a hemodialysis-adapted dose, the patient received 1×10^8 anti-CD19 CAR T cells. She had grade 1 cytokine release syndrome (peak temperature, 38.5°C), which responded to four administrations of tocilizumab; no neurologic or hematologic toxic effects were observed. CAR T-cell expansion was adequate, with persistent, deep B-cell depletion. Before she received CAR T-cell therapy, the patient had anti-HLA antibody levels with mean fluorescence intensities greater than 5000 against 88 out of 119 HLA I and HLA II antigens tested.

Overview of the Ingenui-T process for CAR T-cell manufacturing. Ingenui-T begins with the collection of whole blood from the patient. T cells are simultaneously enriched and activated directly from non-cryopreserved whole blood, then seeded in optimized culture media. The T cells undergo lentiviral transduction with a vector encoding the identical anti-CD19 CAR used in KYV_101 (Kyverna Therapeutics). After transduction, the cells are harvested, debeaded, formulated into final product containers.

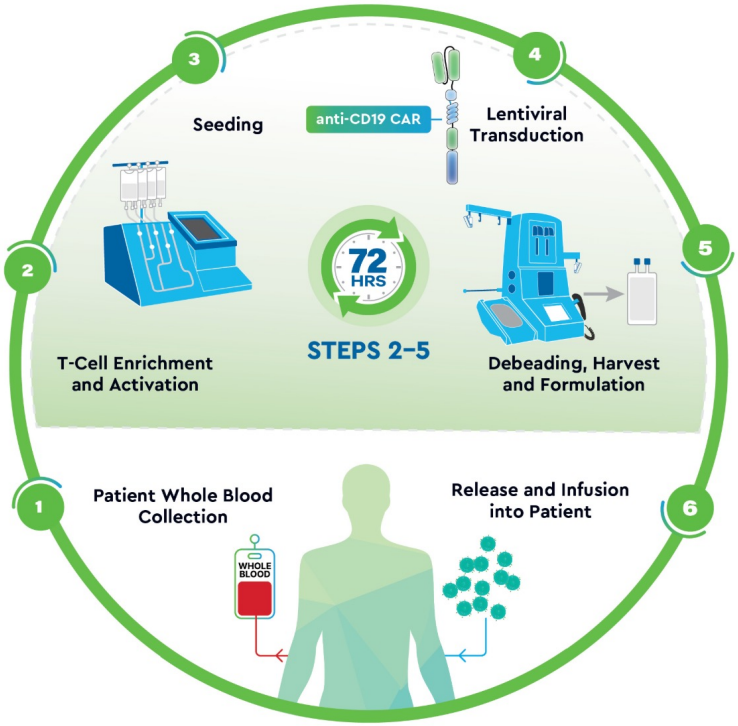

KYV-101 (mivocabtagene) is an investigational, fully human autologous **CD19 CAR T-cell therapy** developed by Kyverna Therapeutics. Unlike traditional oncology CAR T-cells, it is primarily designed to treat severe **B-cell driven autoimmune diseases** by deeply depleting pathogenic B-cells and resetting the immune system.

Key Details & Mechanisms

•**The Design:** It is the only CD19 CAR T-cell in the autoimmune space featuring a fully human design with a CD28 co-stimulatory domain, which minimizes immunogenicity and is associated with an improved safety profile.

•**Indication Pipeline:** It is currently in Phase 1/2 and Phase 2/3 clinical trials for conditions such as:

- Multiple Sclerosis (including progressive forms)
- Lupus Nephritis
- Myasthenia Gravis
- Stiff Person Syndrome
- Systemic Sclerosis

•**Clinical Advantages:** By targeting CD19, the therapy penetrates deep into tissues and the central nervous system to clear out the malfunctioning B-cells responsible for autoimmune attacks.

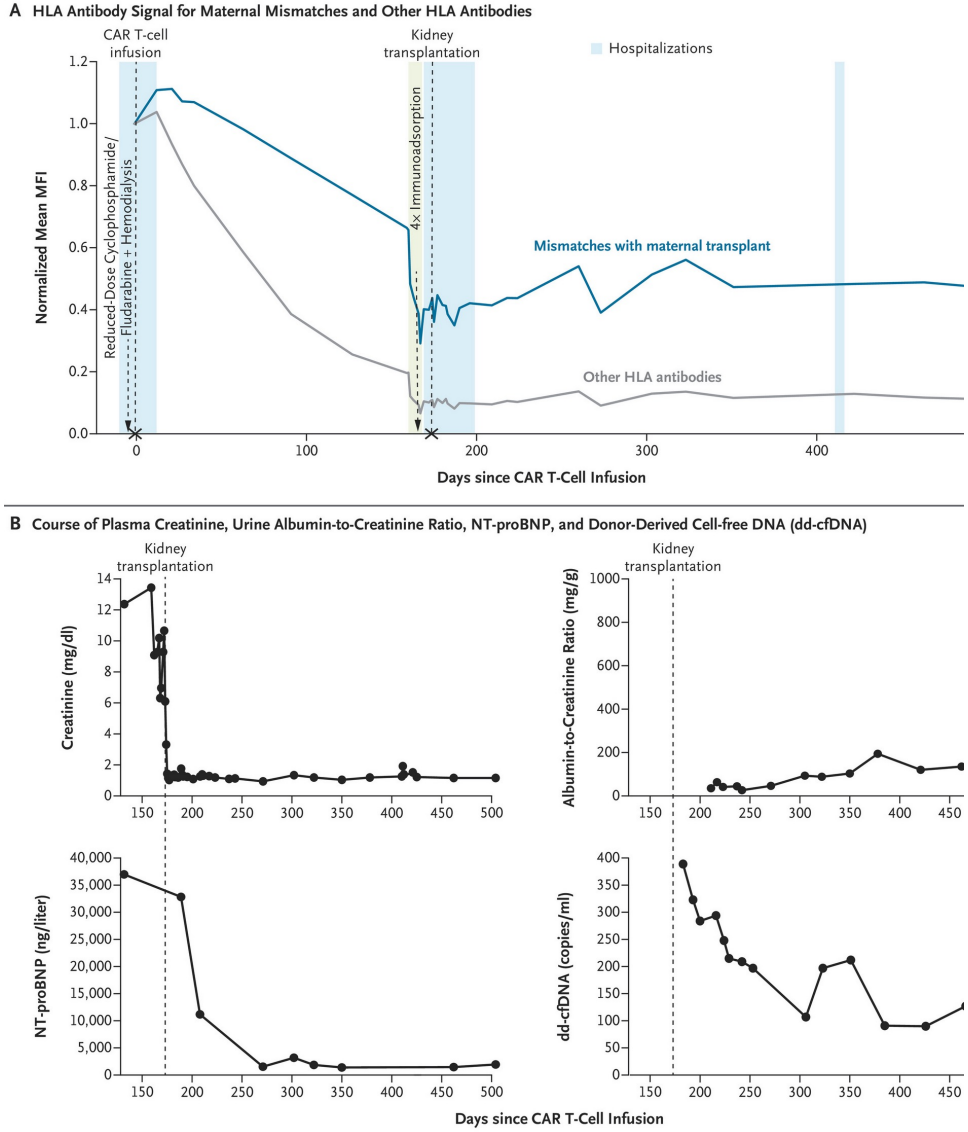

Broad HLA Desensitization for Cross-Reactive HLA Antibodies after Anti-CD19 CAR T-Cell Therapy.

Panel A shows HLA antibody signals for maternal mismatches and other HLA antibodies in the study patient. Lines indicate normalized time series of mean fluorescence intensity (MFI) for mismatches with the previous transplant from the patient's mother (HLA alleles A*01:01, B*57:01, DQB1*03:03, C*06:02, and DRB1*07:01) (blue line) and all other HLA antibodies (black line). Values are normalized to the first chronological sample (at 1.0 on the y-axis). Values greater than 1 indicate an increase relative to baseline, and values less than 1 indicate a decrease relative to baseline. Panel B shows changes over time in the plasma creatinine level, urine albumin-to-creatinine ratio (albuminuria), N-terminal pro-B–type natriuretic peptide (NT-proBNP) level, and donor-derived cell-free DNA (dd-cfDNA) level. Data points indicate individual measurements.

Transplantation was uncomplicated. Primary graft function was observed, with serum creatinine levels reaching 1.2 mg per deciliter (106.1 µmol per liter) by postoperative day 7. Albuminuria stabilized at albumin-to-creatinine ratio levels of less than 300 mg per gram during follow-up. Donor-derived cell-free DNA levels remained low with maintenance immunosuppression. CAR T cells persisted 15 months after infusion. Hypogammaglobulinemia warranted intermittent immune globulin therapy. No infectious complications other than a self-limiting infection with severe acute respiratory syndrome coronavirus 2 occurred. This case provides proof-of-principle that anti-CD19 CAR T-cell therapy can enable kidney transplantation in patients with broad HLA sensitization by inducing a profound, durable contraction of cross-reactive anti-HLA antibodies.

CAR T is an option for transplant
patients who otherwise have none

AAV not so harmless?

Unter **AAV-Integration** versteht man das Einschleusen des Erbguts von **Adeno-assoziierten Viren** in das Genom einer Wirtszelle. Während das Wildtyp-Virus (WT-AAV) sich gezielt an einer bestimmten Stelle integrieren kann, verbleiben die in der Gentherapie eingesetzten rekombinanten Vektoren (rAAV) überwiegend als freie Erbgutringe außerhalb der Chromosomen. Dennoch kommt es bei rAAV zu seltenen, zufälligen Integrationsereignissen, die im Fokus der aktuellen Sicherheitsforschung stehen.

Mechanismen der rAAV-Integration

Obwohl rAAV-Vektoren als nicht-integrierend gelten, liegt die Integrationsrate bei etwa 0,1 % bis 1 % aller transduzierten Zellen.

1.DNA-Doppelstrangbrüche: rAAV nutzt zelleigene Reparaturmechanismen an bereits vorhandenen DNA-Schäden oder gezielten Schnitten aus.

2.Reparaturwege: Die Integration erfolgt primär über die nicht-homologe Endverknüpfung (NHEJ) oder durch homologe Rekombination.

3.Genomische Hotspots: Insertionen finden bevorzugt in aktiv transkribierten Genen oder regulatorischen Bereichen statt.

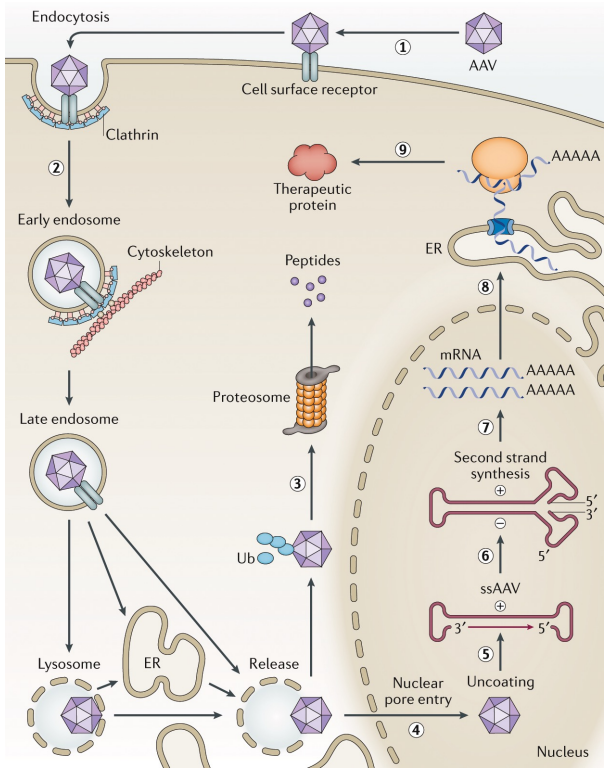

Neuroepithelial Tumor with AAV Integration after Intracisternal Magna Vector Delivery

Summary

Recombinant adeno-associated virus (AAV) vectors are predominantly nonintegrating, but rare genomic integration events have been associated with oncogenesis in neonatal murine models. Here we report a case of a neuroepithelial tumor that developed in a 5-year-old boy with severe mucopolysaccharidosis type I (MPSI, Hurler subtype) 4 years after intracisternal magna administration of AAV serotype 9 gene therapy. The patient underwent successful resection of the primary tumor. Postoperatively, he has continued to have advanced cognitive function for his age, a finding that indicates mitigation of MPSI. Molecular analysis of the tumor showed clonal integration of rearranged AAV vector elements into the gene *PLAG1* and expression of a chimeric AAV-PLAG1 transcript.

Das **PLAG1**-Gen (Pleomorphic Adenoma Gene 1) ist ein Proto-Onkogen auf Chromosom 8 (8q12), das für einen Zinkfinger-Transkriptionsfaktor kodiert. Es ist entscheidend für das fötale Wachstum und die frühe Embryonalentwicklung, wird im erwachsenen Körper jedoch normalerweise nicht exprimiert.

Case Report

Severe MPSI is a lysosomal storage disorder that results from a deficiency of the enzyme α-L-iduronidase (IDUA) and is caused by variants in *IDUA*. Without treatment, MPSI leads to progressive glycosaminoglycan accumulation with multisystem involvement, cognitive decline, and early death. In this patient, MPSI was detected through newborn screening, and he underwent cord-blood hematopoietic stem-cell transplantation (HSCT) from an unrelated donor at 4 months of age. At 10 months of age, the level of donor chimerism had decreased to 27%, and it remained stable thereafter. At 13 months of age, he enrolled in a phase 1–2 gene therapy trial and received RGX-111, an AAV9 vector consisting of a cytomegalovirus enhancer and chicken β-actin (CBA) promoter (i.e., a CAG promoter) that was designed to drive expression of *IDUA*. The vector was administered by means of ICM injection at a total dose of 3.8×10^{13} vector genomes (vg).

Four years after administration of RGX-111, routine neuroimaging for MPSI identified an intraventricular mass measuring 4 cm by 2 cm by 2 cm. Analysis of cerebrospinal fluid showed no evidence of tumor dissemination. A biopsy of the tumor showed indeterminate histologic features with a Ki-67 proliferation index of 5 to 10%. Clinical genomic analysis confirmed that the tumor did not originate from the HSCT donor. Methylation profiling suggested a *PLAGL1*-driven tumor, although no *PLAGL1* fusion was detected. RNA sequencing revealed that the *PLAG1* expression in this patient's tumor was 298 times as high as that in other tumors of the CNS in the CNS tumor cohort at the Children's Hospital of Philadelphia.

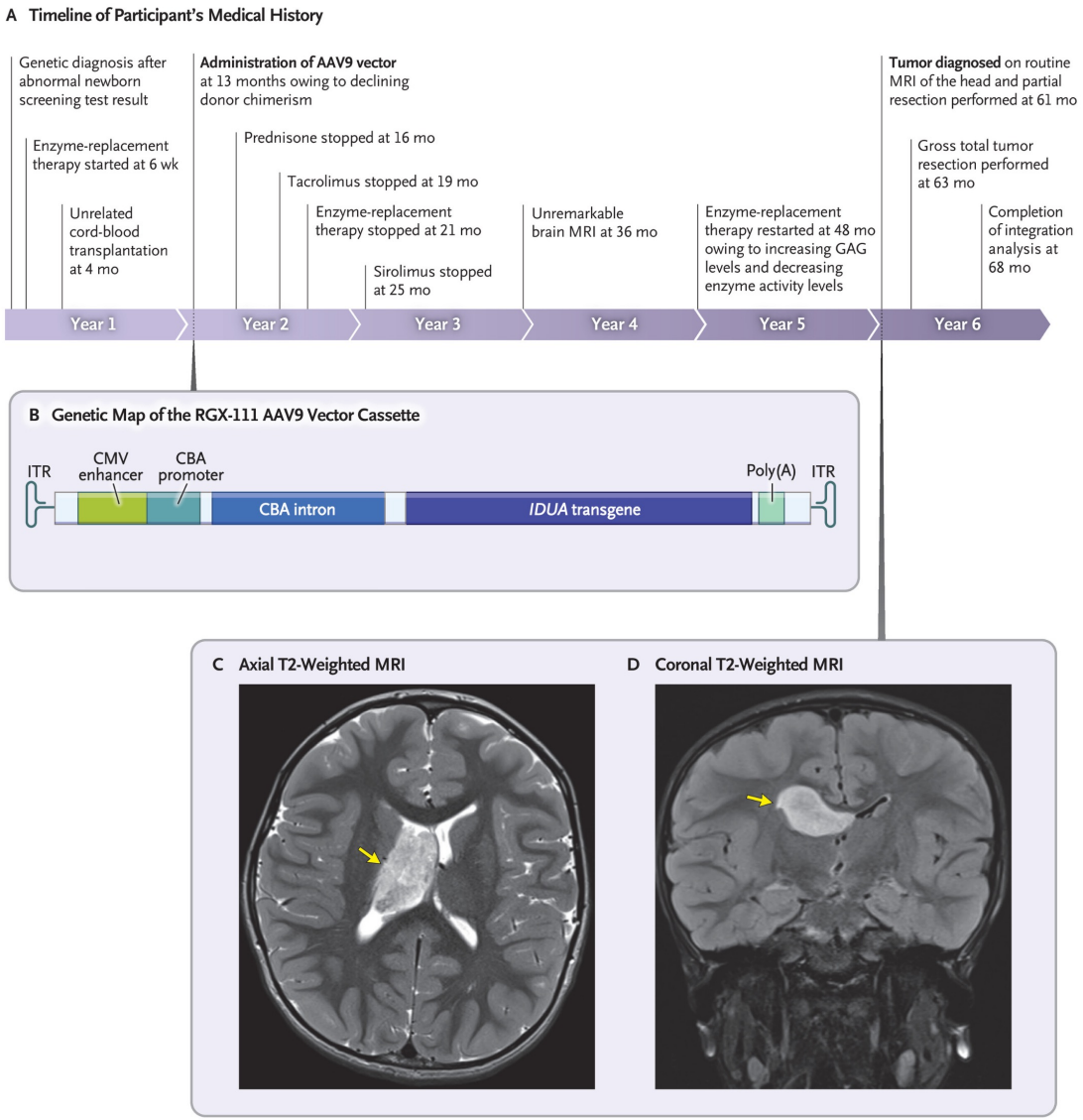

Patient Medical History, Gene Therapy Vector, and Diagnostic Imaging.

Panel A shows a summary timeline of the patient's medical history. Panel B shows a genetic map of the adeno-associated virus serotype 9 (AAV9) vector cassette, which includes a cytomegalovirus (CMV) enhancer, a chicken β-actin (CBA) promoter, and an α-L-iduronidase (*IDUA*) transgene. MRI of the head performed 4 years after treatment with RGX-111 revealed an intraventricular mass. Panel C shows an axial T2-weighted spin–echo sequence, and Panel D shows a coronal T2-weighted turbo inversion recovery magnitude sequence; a mass expanding the right lateral ventricular body with leftward ventricular deviation (Panels C and D, arrows) is present. GAG denotes glycosaminoglycan, and ITR inverted terminal repeat.

Molecular Analyses

RNA sequencing data from tumor tissue showed a fusion of *PLAG1* exon 5 to AAV vector sequences, with the vector CBA splice donor joined to the *PLAG1* exon 5 splice acceptor. The resulting transcript was predicted to encode a *PLAG1* derivative containing five zinc-finger DNA-binding domains and a C-terminal transcriptional activation domain, previously reported to function as a transcriptional activator. To validate this hypothesis, two additional independent RNA samples purified from tumor tissue were analyzed by means of reverse-transcriptase–polymerase-chain-reaction (RT-PCR) assay targeting the fusion junction. An amplification product of the expected size was detected in both samples but not in the control tissue; sequencing of the complementary DNA products confirmed the AAV splice donor–*PLAG1* exon 5 acceptor structure.

These data imply that integrated AAV DNA may drive expression of *PLAG1*. To investigate this theory, single-molecule long-read genome sequencing (PacBio) was performed on genomic DNA from tumor samples. Analysis identified truncated and rearranged AAV vector sequences integrated into intron 4 of *PLAG1* on chromosome 8. The integrated structure contained a duplication of the vector promoter–enhancer sequence, the CBA splice donor, fragments of the *IDUA* transgene, a fragment of DNA from human chromosome 10, and a short duplication of intron 4 sequences. The integrated AAV DNA consisting of the enhancer–promoter–splice donor was oriented to support initiation of transcription and generation of the observed spliced chimeric RNA product linking AAV cassette DNA and *PLAG1* exon 5.

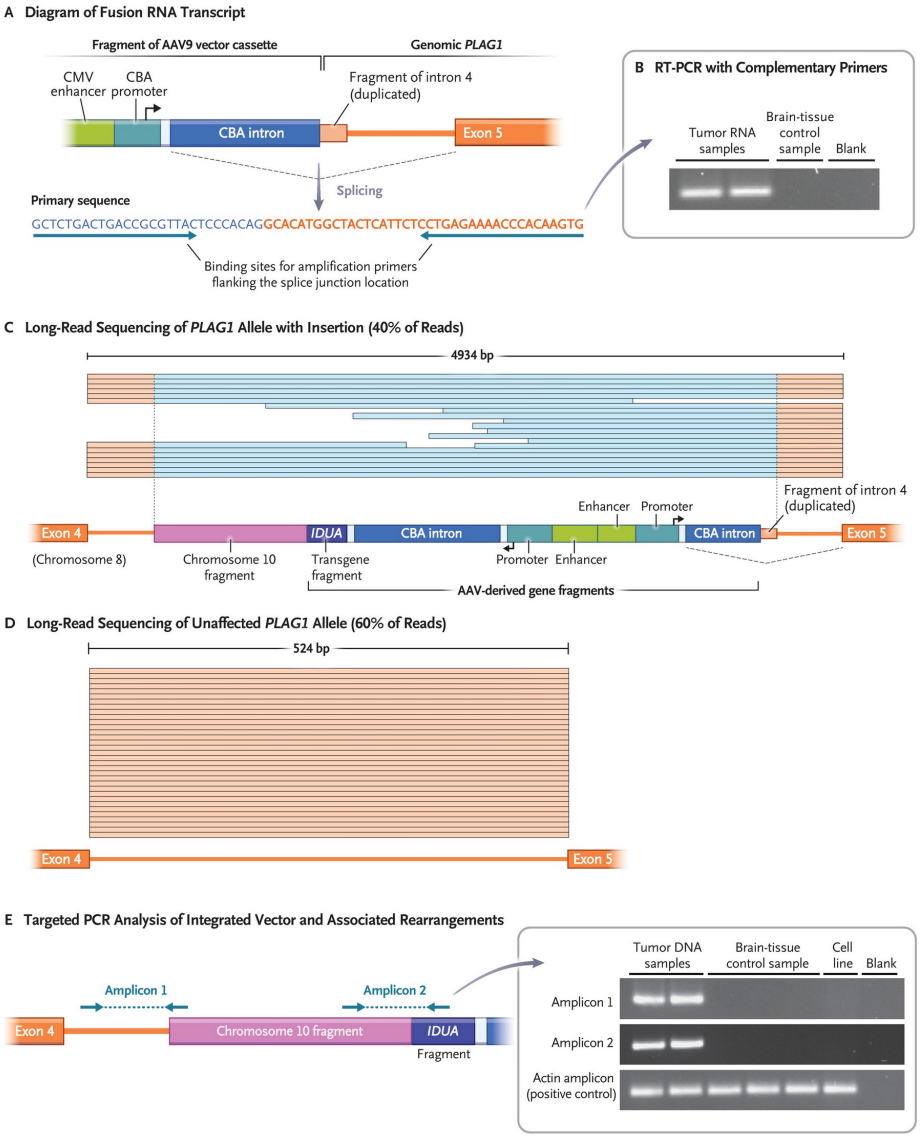

Molecular Analysis of the Tumor.

Panel A shows a diagram of the fusion RNA transcript consisting of the vector cassette DNA encoding a CBA splice donor joined to the genomic *PLAG1* exon 5 splice acceptor. The primary sequence is shown beneath the diagram, which is color coded (vector cassette DNA in blue, *PLAG1* in orange) to indicate the origin of the sequence segments. Arrows indicate binding sites for amplification primers. Panel B shows the results of a reverse-transcriptase–polymerase-chain-reaction (RT-PCR) assay, which was used with primers complementary to sequences flanking the splice junction to query the presence of the fusion transcript. Two RNA samples purified from different tumor sites were compared with the patient's unaffected brain tissue; an amplification product is seen in both tumor samples but not in the control tissue. Panel C shows single-molecule long-read sequencing data identifying the integrated structure in chromosome 8 that contains rearranged vector sequences, including an inverted duplication of the CBA promoter–enhancer and CBA splice donor, fragments of the *IDUA* transgene, a fragment of nonvector DNA from chromosome 10, and a short duplicated fragment of *PLAG1* intron 4. This structure was present in 40% of the reads. A schematic of the integrated structure is shown below the read data. Panel D shows results for the unaffected *PLAG1* allele (60% of the reads). Panel E shows the results of targeted PCR analysis, which was used to confirm the structures of the integrated vector and the associated rearrangements. Amplicon 1 targeted the intron 4–chromosome 10 junction, and amplicon 2 targeted the junction between chromosome 10 and the *IDUA* fragment; the actin amplicon targeted the cellular actin gene and serves as a positive control. The samples include two different tumor samples (lanes 1 and 2), three regions of healthy brain tissue from the same patient (lanes 3 through 5), DNA from the 293T human cell line (lane 6), and a blank control (lane 7). The PCR amplification products are shown on an ethidium bromide–stained gel. The Bio-Rad Gel Documentation System (Image Lab software, version 5.1) incorporated red highlights to indicate overexposed regions; to better represent the original gel, the red highlights have been edited back to white in the published image.

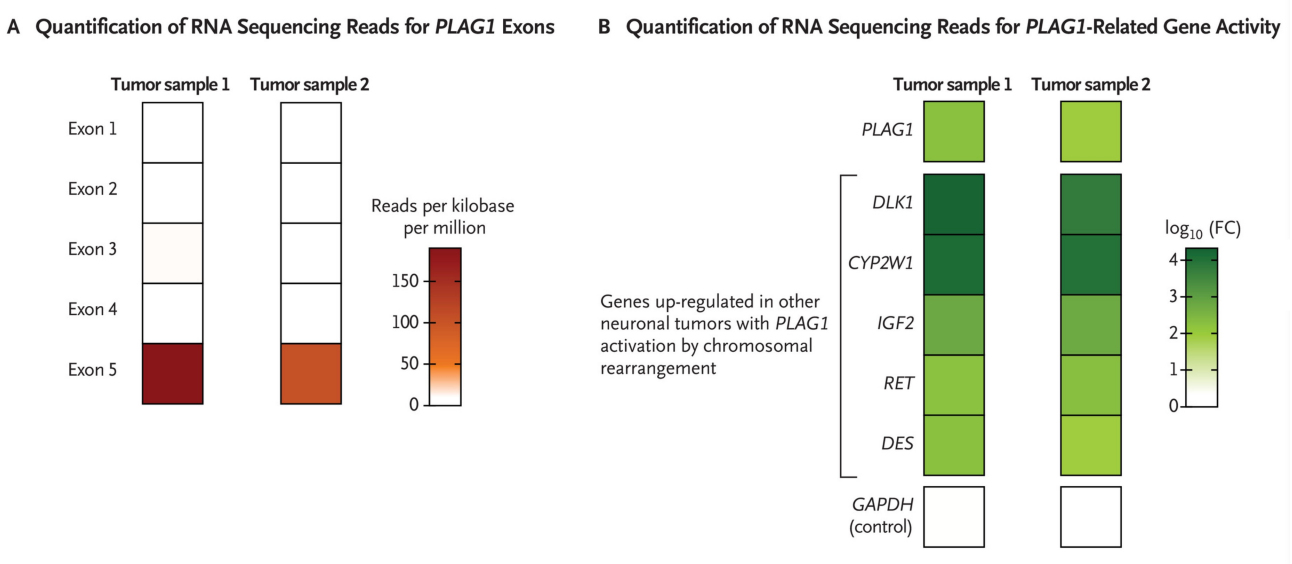

Investigation of Tumor Gene Expression with RNA Sequencing Data.
Panel A shows the quantification of RNA sequencing reads (reported as the number of reads per kilobase per million; red color scale) for each of the *PLAG1* exons. Panel B shows the gene activity for five genes (*IGF2*, *DLK1*, *DES*, *CYP2W1*, and *RET*), which have been previously reported[11] to be up-regulated in neuronal tumors with chromosomal rearrangements associated with *PLAG1* up-regulation. *GAPDH* serves as a housekeeping gene control. The factor change (FC) in the tumor as compared with healthy cortex is shown in green on a log scale. In each panel, read frequencies were compared with each of two neuronal tumor samples and a matched cortex control sample from the same patient.

Discussion

This case shows that the detection of integrated AAV vector DNA is technically challenging, in part because of truncations and rearrangements of vector DNA. The fact that integration was identified in this patient through a combination of long-read DNA sequencing, targeted PCR amplification, and RNA sequencing underscores the importance of using multiple complementary methods. Ideally, future evaluation of possible genotoxic effects associated with AAV therapy will involve multiple orthogonal assessment methods. In this study, adequate tissue samples enabled extensive analysis; however, adequate tissue is not always available. For example, in a recent study, AAV vector sequences were found in the tumor cells of a patient; however the limited availability of tissue precluded a definitive conclusion.

Data from three decades of experience with more than 6000 patients have shown that AAV gene therapy is associated with a favorable safety profile and clinical benefits among diverse patient populations. That said, our findings support the hypothesis that rare AAV integration can contribute to human oncogenesis, which emphasizes the need to optimize gene delivery methods and monitor transduced tissues after treatment.

AAV is „not bad“ but can
cause complications

As the U.S. Secretary of Health and Human Services (HHS), Robert F. Kennedy Jr. has used his position to aggressively reshape federal vaccine policy and public health recommendations. He has consistently promoted vaccine skepticism—including widely debunked claims linking vaccines to autism—and overhauled the U.S. immunization infrastructure

Childhood Vaccine Hesitancy

Summary

Vaccine hesitancy exists along a spectrum; most parents with hesitancy are motivated to protect their children but are often concerned about safety. Routine childhood vaccines recommended by the American Academy of Pediatrics have substantially reduced the incidence of disease and maintain a strong safety record. Clinicians are the most trusted source of vaccine information, and clear, confident recommendations are closely linked to higher uptake. Presumptive communication approaches are more effective than open-ended approaches, especially when paired with respectful dialogue. Empathy-driven, patient-centered strategies, including motivational interviewing, help address concerns, counter misinformation, and build trust while preserving relationships that may encourage future vaccination decisions.

A 12-month-old child presents with his mother for a well-child visit. His growth and development are on schedule and his physical examination is normal. After discussing routine issues including sleep, nutrition, safety, and dental hygiene, you mention that he is due for his routine childhood vaccines. He has received all previously recommended vaccines. His mother, however, responds, "We don't want to do the MMR vaccine." She explains that their 2-year-old son was recently diagnosed with autism, and she believes the measles–mumps–rubella (MMR) vaccine may have caused it. How would you handle this situation?

The Clinical Problem

Vaccines are victims of their own success. Childhood vaccines have provided the greatest contribution to improved infant survival during the past 50 years, with 154 million deaths averted. Most parents today have not nursed their children through measles, polio, diphtheria, or other vaccine-preventable diseases rarely seen today. There was a time when children in iron lungs filled pediatric wards and struggled to breathe because of paralysis of their respiratory muscles caused by polio, with no vaccine available to prevent the disease. Now, some parents fear vaccines more than the diseases they prevent, often because of widely debunked falsehoods, such as the myth that vaccines cause autism. The science is abundantly clear that the benefits of vaccines far outweigh the potential risks, yet parents still question the safety of vaccines and often decline them. Why is this?

Childhood Vaccine Hesitancy

- Vaccine hesitancy exists on a spectrum; most parents who are hesitant want to protect their children but often have safety concerns.
- Vaccines included in the routine childhood schedule recommended by the American Academy of Pediatrics have dramatically decreased the incidence of disease and have a strong safety record.
- Clinicians remain the most trusted influence on parental vaccine decisions; a strong, confident recommendation from a trusted clinician is highly associated with vaccine uptake.
- Presumptive vaccine recommendations (e.g., “Sarah is due for three vaccines today”), followed by respectful engagement when concerns arise, are more effective than conversational approaches (“What do you think about vaccinating today?”) in improving vaccine uptake.
- Empathy-based, patient-centered communication — including motivational interviewing — can build trust, address misinformation, and support informed decision making.
- Maintaining rapport matters, even when vaccination is declined; continuing the conversation can influence future acceptance and broader community protection.

The Behavioral and Social Drivers Framework.

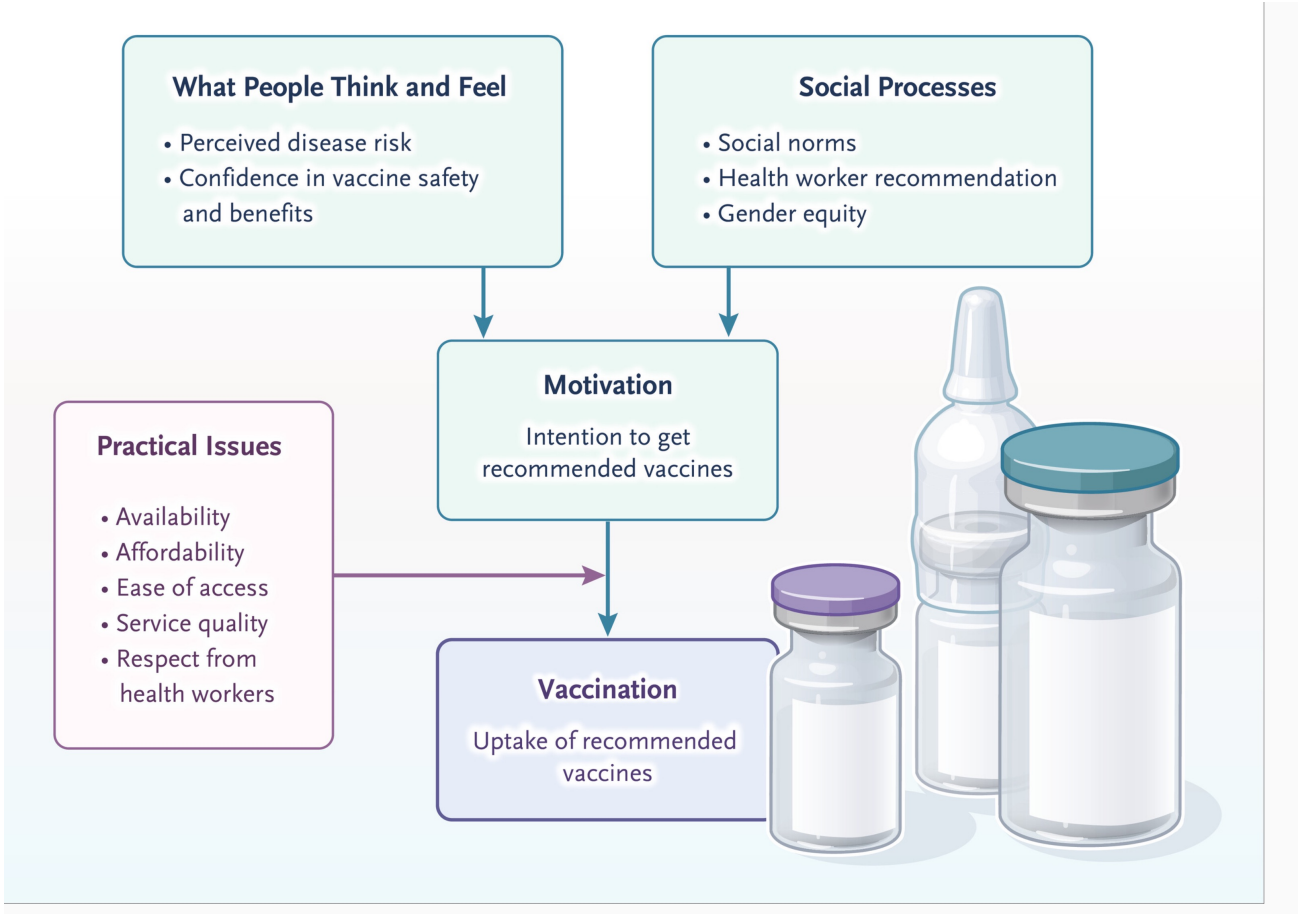

Routine U.S. Childhood Vaccines Recommended by the American Academy of Pediatrics: Effectiveness, Disease Burden, and Safety.

Vaccine	Effectiveness	Prevaccine Burden in the United States	Recent Cases, Hospitalizations, or Deaths	Known Serious Adverse Events†
Diphtheria–tetanus–pertussis				None‡
Diphtheria	>95%	20,000–30,000 cases/yr, 1880–3000 deaths/yr	Incidence near zero	
Tetanus	Near complete protection	Approximately 550 deaths/yr in the 1940s	<30 cases/yr, mostly in unvaccinated persons	
Pertussis	71–85% with acellular vaccine	Hundreds of thousands of cases per year, 4000–7000 deaths/yr	Sporadic outbreaks, far lower incidence than before vaccine	
Paralytic polio	>99% against paralytic disease	Approximately 15,000–20,000 cases/yr; 1800–3000 deaths/yr	Incidence near zero, eliminated domestically	None§
Measles–mumps–rubella				1 Febrile seizure above the background incidence per approximately 2300 doses, 1 case of acute immune thrombocytopenic purpura above the background incidence per approximately 38,000 doses
Measles	Approximately 97% after two doses	500,000–750,000 cases/yr, 400–500 deaths/yr	Sporadic outbreaks and imported cases; 2288 confirmed cases (93% unvaccinated or unknown) and 3 deaths in 2025	
Mumps	Approximately 88% after two doses	160,000–200,000 cases/yr, 40–50 deaths/yr	Sporadic outbreaks	
Congenital rubella syndrome	Approximately 97%	20,000 cases and 2160 deaths during peak in 1964–1965	<1 Imported case/yr	
Haemophilus influenzae type b	>95%	Thousands of cases, hundreds of deaths	>99% reduction in incidence	None
Pneumococcal conjugate	Approximately 95% against invasive disease	>200,000 cases/yr	>95% reduction in incidence of invasive disease, 34–51% reduction in incidence of otitis media from any cause, 22% reduction in incidence of clinical pneumonia from any cause	None
Varicella	70–90% overall, >95% against severe disease	4 Million cases/yr, 100–200 deaths/yr	>97% reduction in incidence	None
Hepatitis B	Approximately 95% against infection and near 100% against chronic infection	Approximately 20,000 childhood infections/yr	Almost zero cases per year	None
Hepatitis A	95–100%	Tens of thousands of cases per year	Reduction in incidence by a factor of 17	None
Rotavirus	High effectiveness against severe diarrhea	>50,000 hospitalizations/yr	Markedly reduced hospitalizations	Very rare risk of intussusception found in some studies (approximately 1 case above the background incidence per 100,000 doses) but not others
Human papillomavirus	Very effective against cervical and other cancers	Endemic infection	Reduced incidence of high-grade lesions and cancers	None¶
Influenza	Varies	Millions of outpatient visits and tens of thousands of hospitalizations per year	Substantial decrease in hospitalizations and mortality	None‖
Coronavirus disease 2019	Varies	Millions of outpatient visits and tens of thousands of hospitalizations per year; 20–30% of hospitalized children admitted to intensive care unit	Decreased risk of hospitalization, death, and postacute sequelae	Very rare risk of myocarditis, particularly in male patients 12–39 yr of age, noted in 2021–2022; no increased risk found in recent seasons[48]

Structured Approach to an Effective Conversation with a Vaccine-Hesitant Parent.

Steps for Speaking with Vaccine-Hesitant Parents	Examples
1. Recommend vaccination.	Present vaccination as the norm; if they express concerns or decline the vaccine, go to step 2.
2. Ask them to share their concerns.	
Engage in active listening with few questions or interruptions at the start. Use open-ended questions to understand their top concerns. Acknowledge their concerns. Reflect and summarize to check their understanding.	"Can you please let me know your main concerns, perhaps your top three concerns, about vaccines?" "It is normal to have questions." "It sounds like too many vaccines at once is your biggest concern, is that right?"
3. Share your knowledge.	
Establish your credibility and nonbiased approach. Ask permission to share evidence. Address concerns and offer to look for additional information together or to get back to them later if you are not sure how to answer their questions. Avoid overreassurance and be honest about vaccine side effects. Consider sharing your own experience. Reinforce personal motivation to vaccinate (e.g., going to preschool, having asthma).	"I've received questions about this before and I've looked into it extensively. Would it be okay with you if I share what I know?" "I haven't heard that question before. I will look into it and speak to my colleagues and get back to you. What I can tell you is that I've given this vaccine to thousands of children and have never seen that happen." "Your child has asthma, which makes them more vulnerable to getting very sick from influenza, so the flu vaccine is very important."
4. Reframe discussion to focus on disease severity.	
Return to a discussion of disease severity. Show them local data on vaccine-preventable diseases according to age and year if possible.	"Now that we've gone over some of the safety issues, I'd like to come back to why I recommend these vaccines in the first place — the diseases we're talking about are very serious, and I would feel terrible if one of my patients got sick with one of them. For me, it's really clear that the benefits of preventing these diseases greatly outweigh the risks of side effects." "We have seen rising cases of measles in our region (or state) — the MMR vaccine is important."
5. Facilitate vaccination.	
If they are ready, vaccinate on site that day if possible. Depending on your practice, explain where to go and how to get the vaccine.	Provide a list of practices offering vaccination. Be mindful that some parents work full time and may need after-hours or weekend clinics or may have trouble paying the cost of the appointment.
6. Continue the conversation.	
If they are not ready, allow the conversation to continue at the next appointment. Maintain trust.	"Please take a look at these resources for information on your question and make another appointment to come back and talk to me."

Interventions to Stop the Creation, Spread, and Belief in Misinformation.

Intervention	Examples	Notes
System level (government regulation)	Legislation to reduce the spread of harmful misinformation on social media through data access and transparency Changing of recommendation algorithms and technology standards; demonetizing websites that spread misinformation or deindexing them from search results	May be more effective than individual strategies in reducing spread
Individual level (for clinicians)	Avoiding repeating misinformation without including a correction Tailoring vaccine messaging Supporting local journalism Leveraging trusted sources (e.g., Vaccine Champions)	More effective at changing behavior Builds trust and fills information gaps through investment in local, independent media
Prebunking	Psychological inoculation: teaching people to identify vaccine fallacies and building skills and resilience Strategies: preemptive warnings about misinformation with a correction; games, videos, or messages teaching critical thinking and how to recognize misinformation	May be more effective than debunking Can build public resilience against misinformation and improve vaccine attitudes and intent to get vaccinated Potential to forestall misinformation at scale Scalable and cost-effective
Nudging	Shifting focus from the social and emotional appeal to accuracy to reduce sharing of misinformation Accuracy nudges: considering veracity of information Social-norms nudges: highlighting community standards about reporting information Motivational nudges: rewarding people for being accurate and for not sharing misinformation	Mixed efficacy Multiple nudges in a row are more effective than one; works better when combined with other strategies (e.g., inoculation) Rating accuracy of a single headline reduced sharing of misinformation by 10%[59]; social media platforms can integrate these prompts directly into the sharing user interface
Media literacy education	Digital literacy interventions: may strengthen societal resilience to misinformation through education and teaching analytical reasoning to improve judgment of quality and accuracy of information	Difficult to evaluate because content, duration, and outcomes vary widely Challenges in speed, scale, and targeting May be most effective when paired with debunking
Debunking	Fact-checking and correction of misinformation "Truth sandwich" strategy: stating the fact first, followed by the myth and a detailed refutation of the myth, and ending with the facts	Effective in real-world contexts and across cultures Effects fade over time, requires repeated correction Providers warrant training Education materials alone and scare tactics can backfire

Brief Responses to Common Questions about Vaccine Safety.

Question	Brief, Targeted Response
Is it safe for young children to receive multiple vaccines?	Children receive vaccines when they are most vulnerable to getting sick from the diseases the vaccines protect against. Infants' immune systems respond to many different things all the time. When we give the infant schedule of vaccines, a very small portion of an infant's immune system produces the protective antibodies that help to fight disease. In fact, believe it or not, babies could effectively respond to as many as thousands of vaccines at one time and produce protective antibodies very well. Of course, we would never do that, but it tells us that babies can easily respond to the number of vaccines we give them in the schedule and that their immune systems are not overwhelmed. We also know this by testing the infant vaccines in clinical trials to show both how well the vaccines work and their safety. Children defend themselves against a far greater number of challenges to their immune systems every day from their environment.
Is aluminum in vaccines dangerous?	Aluminum is used in vaccines as an adjuvant, which means it helps to boost the immune response to the vaccine. Using aluminum means smaller quantities of the vaccine and fewer doses can be used for infants to get the same strong immune response. Aluminum is found in many foods including fruits, vegetables, dairy products, and baby formulas. Normally, adults eat about 7 to 9 mg of aluminum a day. In the first 6 months, infants get about 4 mg of aluminum from vaccines but they receive much more than that in their diet (e.g., breast-fed infants get 7 mg and formula-fed infants about 38 mg of aluminum in the first 6 months). So, the amount of aluminum babies get from vaccines is very small and is safe.
Do vaccines cause autism?	Vaccines do not cause autism. This has been shown in many studies that have compared millions of children who did and those who did not get vaccines and showed no difference in the rates of autism. Symptoms of autism, such as difficulties with behavior, social skills, and communication, can start to appear between 1 and 2 years of age. But this does not mean that the MMR vaccine caused these changes even though they may occur during the same period of time that the child receives the first MMR vaccine (at 1 year of age). We do not know all the causes of autism, but we do know that it is highly genetic through studying twins. Just because two things occur during the same time period does not mean that one caused the other.
Do HPV vaccines cause infertility?	No. This was a myth that started online and there is no truth to it. Studies have confirmed that the HPV vaccine does not cause infertility. What we do know, though, is that getting infected with HPV can lead to many problems, including cancer and problems with fertility and childbirth.

Conclusions and Recommendations

The mother in the vignette expressed concern regarding a common, widely debunked myth about the MMR vaccine (see above responses for brief responses to other common concerns). In this scenario, we would proceed with an open-ended question: “Can you tell me more about what you have heard about the MMR vaccine?” After active listening, we would summarize what we heard: “It sounds like you’ve just heard so much about the possibility that MMR might cause autism that you’d prefer to wait for now. Do I have that right?” Then we would validate her feelings and, rather than shaming or judging her for questioning the MMR vaccine, we would use a motivational-interviewing approach of asking permission to share the evidence and facts: “You know, I understand how difficult this decision must be for you. I’ve looked into this issue extensively. Would it be okay to share with you what I’ve found out?”

Chyluria from a Lymphatic–Urinary Fistula

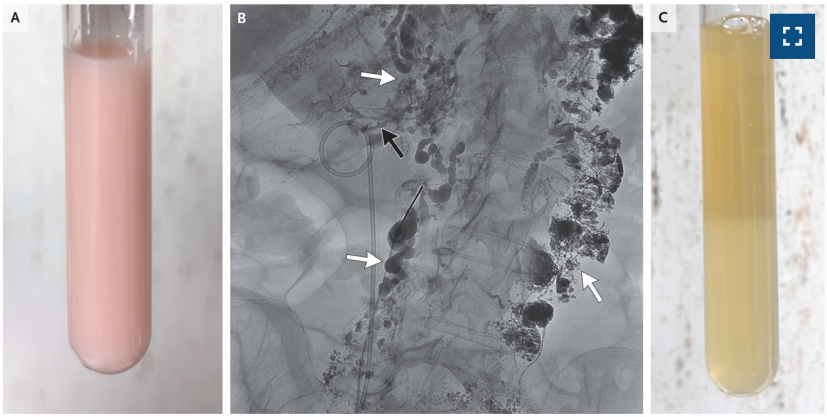

A 56-year-old woman presented to the emergency department with a 3-week history of leg swelling. On physical examination, pitting edema in both legs and a milky appearance to the urine were observed (Panel A). Laboratory studies were notable for a serum albumin level of 18 g per liter (reference range, 35 to 52) and a urinary protein-to-creatinine ratio of 34,958 (with protein measured in milligrams and creatinine measured in grams; reference range, 0 to 200). Further testing of the urine identified elevated levels of chylomicrons and a urinary triglyceride level of 1456 mg per deciliter (reference value, undetectable), findings indicative of chyluria. Chyluria results from abnormal communication between the lymphatic and urinary systems. Possible causes are lymphatic filariasis, congenital lymphatic malformations, post-traumatic lymphatic malformations, and lymphatic compression by tumors. Lymphangiography (after the placement of a right-sided ureteral stent) identified retroperitoneal lymphatic malformations (Panel B, white arrows) with a fistulous communication to the right pyeloureteral junction (Panel B, black arrow). Whether the lymphatic malformations were congenital or acquired was unclear. A diagnosis of chyluria from a lymphatic–urinary fistula was made. The chyluria persisted despite the patient's following a low-fat diet, so the fistula was subsequently closed by percutaneous transabdominal embolization. At follow-up 3 months later, the appearance of the urine had normalized (Panel C; apparent layering is due to a label on the back of the tube), the patient's serum albumin levels had improved, and the edema and proteinuria were markedly reduced.

Dysphagia Lusoria

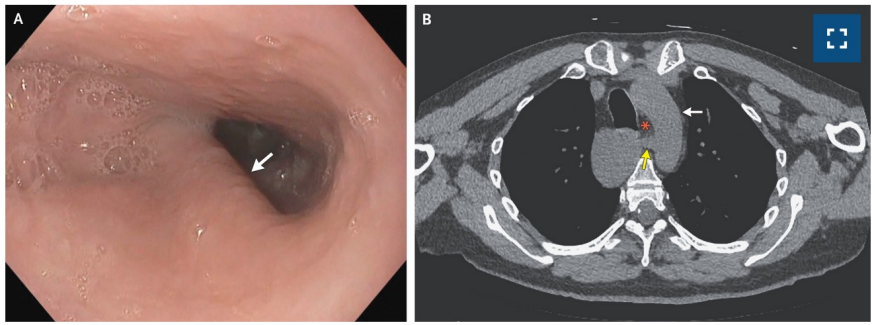

A 44-year-old man with cerebral palsy was referred to the gastroenterology clinic for a 4-year history of choking episodes while eating. Despite treatment for reflux with a proton-pump inhibitor and food-texture modifications to address mild oropharyngeal dysphagia that had been identified in a modified barium-swallow study, the patient's symptoms had persisted. Physical examination was notable only for long-standing spastic quadriplegia and language delay related to his cerebral palsy. Endoscopic examination revealed luminal narrowing of the upper esophagus by a pulsating, cordlike structure in the posterior wall of the esophagus (Panel A, white arrow, and video). A subsequent computed tomographic scan of the chest showed an aberrant right subclavian artery (Panel B, yellow arrow) originating as a fourth branch of the aortic arch (Panel B, white arrow) and coursing posterior to the esophagus (Panel B, asterisk). A diagnosis of dysphagia lusoria — compression of the esophagus by an aberrant right subclavian artery — was made. Although dysphagia lusoria results from a congenital abnormality, it may not cause symptoms until middle age, when vascular stiffening occurs. Nonsurgical management with continued speech–language therapy for swallowing and dietary modifications was selected by the patient's health care proxy. Three months after diagnosis, the patient had less frequent choking episodes, continued to eat orally, and maintained his weight.

VIDEO

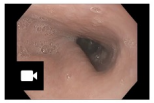

Upper Endoscopy 0m 12s

The Unusual Suspects

A 53-year-old man with Crohn's disease and psoriasis presented to the emergency department with headache, slurred speech, nausea, and vomiting that had persisted for 2 days. His wife reported that he had had yellowing of the skin and eyes and darkening of the urine during the previous 2 weeks. His medications included oral budesonide at a dose of 9 mg daily and intramuscular dupilumab at a dose of 300 mg every 2 weeks; this treatment regimen had remained unchanged for 2 years. He reported no use of tobacco, supplements, or other substances. He consumed four bottles of wine (20 standard drinks) weekly and had maintained this pattern for decades. He lived in New England with his wife. He had traveled to Caribbean islands on two occasions: 4 months before presentation and 3 weeks before presentation. He reported no sick contacts or family history of liver disease.

Dupilumab ist ein monoklonaler Antikörper, der gezielt in das Immunsystem eingreift, um chronische Entzündungen vom Typ 2 zu hemmen. Im Körper spielen die Proteine Interleukin-4 (IL-4) und Interleukin-13 (IL-13) eine Schlüsselrolle bei der Auslösung von Typ-2-Entzündungen. Dupilumab blockiert die Rezeptoren für diese Botenstoffe, wodurch Entzündungsreaktionen, Schleimhautschwellungen, Juckreiz und Atemwegsbeschwerden gelindert werden.

The oral temperature was 36.8°C, the blood pressure 119/79 mm Hg, the heart rate 130 beats per minute and regular, the respiratory rate 18 breaths per minute, and the oxygen saturation 98% while the patient was breathing ambient air. The body-mass index (the weight in kilograms divided by the square of the height in meters) was 31. Scleral icterus and jaundice were present. Cardiovascular examination was notable for a soft, grade 2/6 holosystolic murmur at the apex that radiated to the axilla. The lungs were clear. He had abdominal obesity without tenderness, hepatosplenomegaly, or masses. A nontender papule that measured 5 mm in diameter was present on the left hypothenar eminence, and a tender papule that measured 3 mm in diameter was noted on the left fourth toe. A 2-cm irregular plaque on the right fifth finger was nontender. Two splinter hemorrhages were noted on the right hand. The patient was alert and oriented. His speech was slurred. Cranial nerves II through XII were intact. Nuchal rigidity, pronator drift, and asterixis were absent. Strength, reflexes, and sensation were normal.

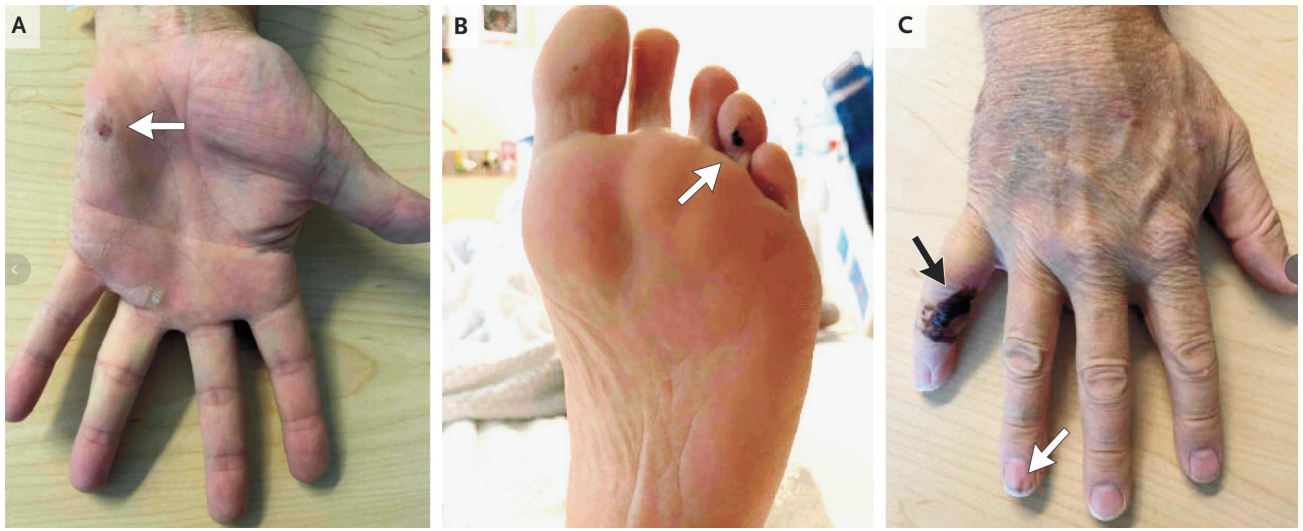

Clinical Photographs.
Skin lesions are present on the left hypothenar eminence (Panel A, arrow), the inferior surface of the left fourth toe (Panel B, arrow), and the dorsum of the right fifth finger (Panel C, black arrow). A splinter hemorrhage is present on the nail of the right fourth finger (Panel C, white arrow).

The white-cell count was 34,000 per microliter, with 79.8% neutrophils, 12.9% bands, and 4.9% metamyelocytes. The hemoglobin level was 12.7 g per deciliter, and the platelet count 130,000 per microliter. The blood level of urea nitrogen was 31 mg per deciliter (11 mmol per liter), and the creatinine level 1.7 mg per deciliter (150 mmol per liter); the estimated glomerular filtration rate was 47.6 ml per minute per 1.73 m^2 of body-surface area (normal value, >60.0). The remainder of the basic metabolic panel was normal. The aspartate aminotransferase (AST) level was 810 IU per liter (normal range, 10 to 40), and the alanine aminotransferase (ALT) level 1965 IU per liter (normal range, 7 to 56). The alkaline phosphatase level was 178 IU per liter (normal range, 44 to 147), and the total bilirubin level 10.2 mg per deciliter (174 µmol per liter; normal range, 0.1 to 1.2 mg per deciliter [2 to 21 µmol per liter]), with a direct bilirubin level of 8 mg per deciliter (137 µmol per liter; normal value, <0.4 mg per deciliter [<7 µmol per liter]). The results of these liver-function tests had been normal 9 months earlier. The albumin level was 3.1 g per deciliter (normal range, 3.5 to 5.0), the ammonia level 25 µmol per liter (43 µg per deciliter; normal range, 11 to 32 µmol per liter [19 to 54 µg per deciliter]), and the lactate level 4.1 mmol per liter (37 mg per deciliter; normal range, 0.5 to 2.2 mmol per liter [5 to 20 mg per deciliter]).

Blood levels of lipase, thyrotropin, and fibrinogen were normal, as was the partial-thromboplastin time; the international normalized ratio was 1.2. The d-dimer level was 3.62 µg per milliliter (normal value, <0.50). Urinalysis showed trace blood, 1+ white cells, and 1+ bilirubin; microscopic examination of the sediment revealed 16 to 20 white cells per high-power field (normal value, <5).

An electrocardiogram showed sinus tachycardia. Computed tomography (CT) of the head, performed without the administration of contrast material, revealed acute subdural and subarachnoid hemorrhages overlying the left frontal lobe. CT of the abdomen, also performed without the administration of contrast material, revealed mild hepatic steatosis without cirrhosis or biliary abnormalities and wedge-shaped renal hypodensities that were suggestive of infarcts. The patient was admitted to the hospital. Blood samples were obtained for culture, treatment with vancomycin and meropenem was initiated, and budesonide (and presumably dupilumab) therapy was interrupted owing to active infection.

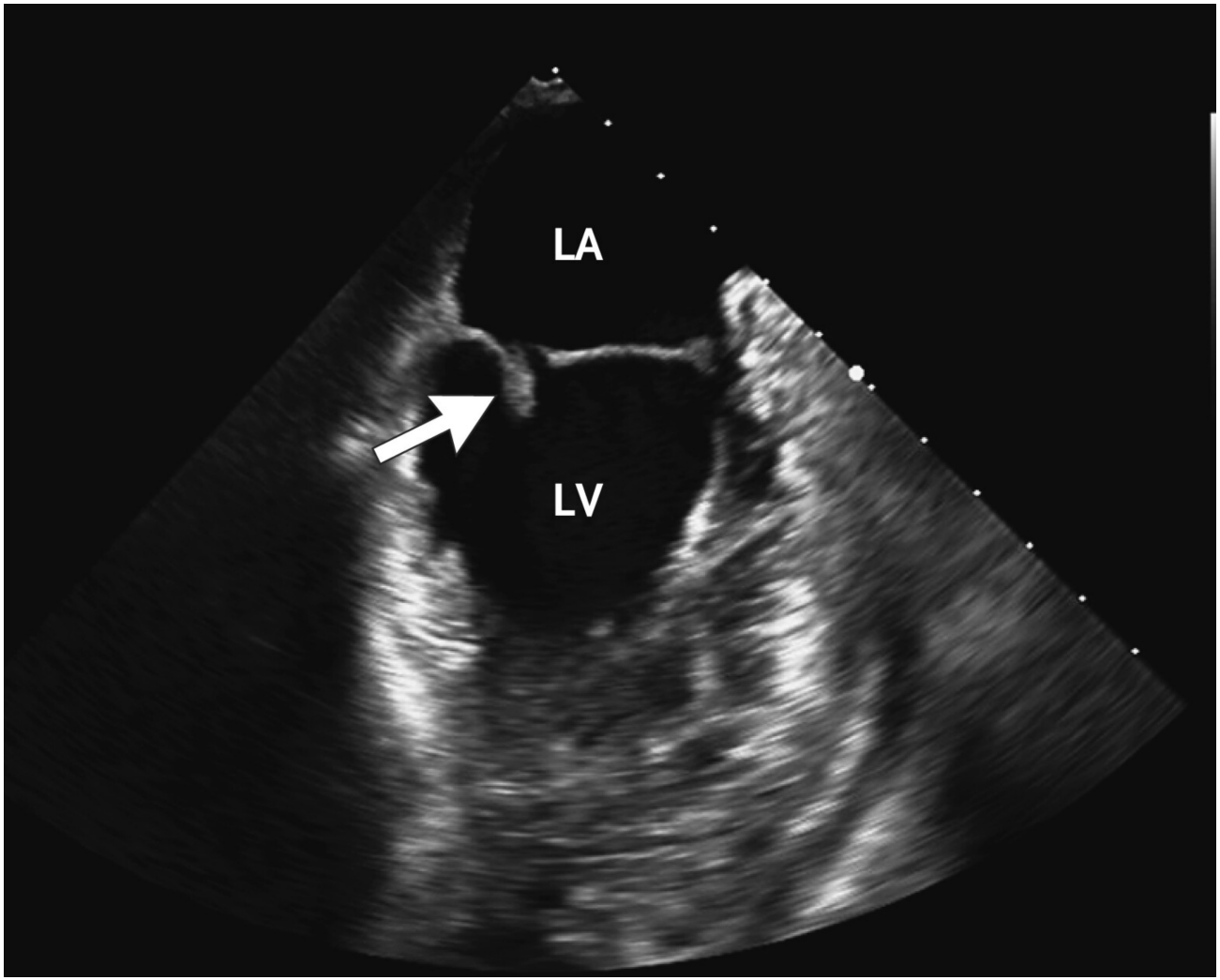

Transesophageal Echocardiogram.

A two-chamber view shows a 1.2-cm, nonmobile vegetation on the body of the anterior leaflet of the mitral valve (arrow). I denotes left atrium, and LV left ventricle.

His blood cultures grew methicillin-sensitive *Staphylococcus aureus*. Viral serologic testing showed no evidence of infection with hepatitis A, B, or C virus. The results of serologic testing for Epstein–Barr virus included undetectable IgM against the viral capsid antigen (a normal result) and elevated IgG levels against viral capsid and nuclear antigens (>750 IU per milliliter and 600 IU per milliliter, respectively; normal value, <18 for both). Testing for cytomegalovirus IgG and IgM was negative. A polymerase-chain-reaction (PCR) test for herpes simplex virus was negative. The level of varicella–zoster virus IgM was 1.26 IU per milliliter (normal value, ≤0.90). Doppler ultrasonography of the abdomen showed patent hepatic vessels, mild hepatic steatosis, and mild thickening of the gallbladder wall. Magnetic resonance imaging of the head confirmed the presence of acute hemorrhages in the left frontal lobe and identified acute infarcts of 5 mm in diameter in the left frontal lobe, the left parietal lobe, and both cerebellar hemispheres that suggested an embolic origin. CT angiography of the head revealed a 2-mm abnormality that was suggestive of a mycotic aneurysm of the left middle cerebral artery, with patent vasculature. Testing for lupus anticoagulant was negative, as was serologic testing for antiphospholipid antibodies and PCR testing for factor V Leiden and prothrombin variants.

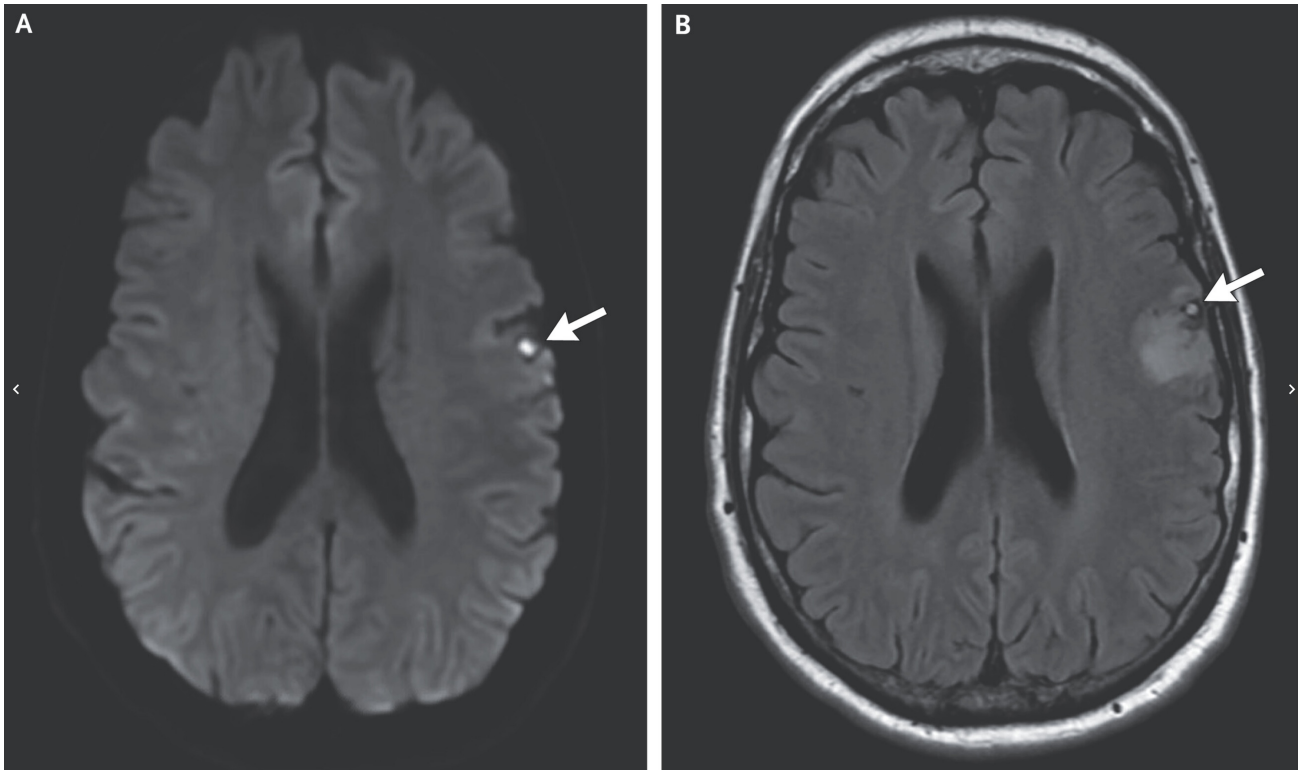

Magnetic Resonance Imaging of the Head.

A diffusion-weighted image (Panel A) shows signal hyperintensity with reduced diffusivity, susceptibility artifact, and heterogeneous enhancement in the left posterior frontal lobe and frontal operculum (arrow). A T2-weighted image (Panel B) shows hyperintensity and associated susceptibility in the left posterior frontal lobe and frontal operculum (arrow), findings that indicate a subacute infarct.

The antinuclear antibody (ANA) titer was 1:320 (normal value, <1:40). The F-actin anti–smooth-muscle IgG level, measured by enzyme-linked immunosorbent assay, was 35 units (normal value, <20), with negative tests for antimitochondrial antibodies and anti–liver–kidney microsomal antibodies. The IgG level was 3238 mg per deciliter (normal range, 700 to 1600), and the IgA level 894 mg per deciliter (normal range, 70 to 400), with a normal IgM level. The phosphatidylethanol level, measured on hospital day 12, was 37 ng per milliliter (a level of <20 suggests absent or low alcohol consumption; a level of >200 suggests heavy consumption). The serum ceruloplasmin level was 39 mg per deciliter (normal range, 18 to 36). The $alpha_1$-antitrypsin level was normal. The ferritin level was 1288 µg per liter (normal range, 30 to 300), and the iron level 167 µg per deciliter (normal range, 60 to 170); the presence of hyperbilirubinemia prevented calculation of the transferrin saturation. Three days after initiation of empirical antibiotic therapy with vancomycin and meropenem, the AST level had decreased to 445 IU per liter, the ALT level to 480 IU per liter, the total bilirubin level to 6.9 mg per deciliter (118 µmol per liter), and the white-cell count to 15,100 per microliter.

Between hospital days 6 and 14, the AST and ALT levels increased again; the AST level rose to a peak of 984 IU per liter, and the ALT level to a peak of 674 IU per liter. The bilirubin and alkaline phosphatase levels trended downward. The leukocytosis decreased. Blood cultures showed no growth after hospital day 7. Repeat echocardiography showed valvular function that was similar to that seen on the initial study. A liver biopsy revealed severe portal and lobular hepatitis; findings included infiltrate containing approximately 40% mononuclear immune cells with numerous clusters of more than 5 plasma cells, severe interface activity, and focal portal–central bridging necrosis without evidence of other liver disease. Together with the patient's laboratory test results, these findings met the criteria for definite autoimmune hepatitis on the basis of a scoring system (the Simplified Autoimmune Hepatitis Score) for diagnosis of autoimmune hepatitis.

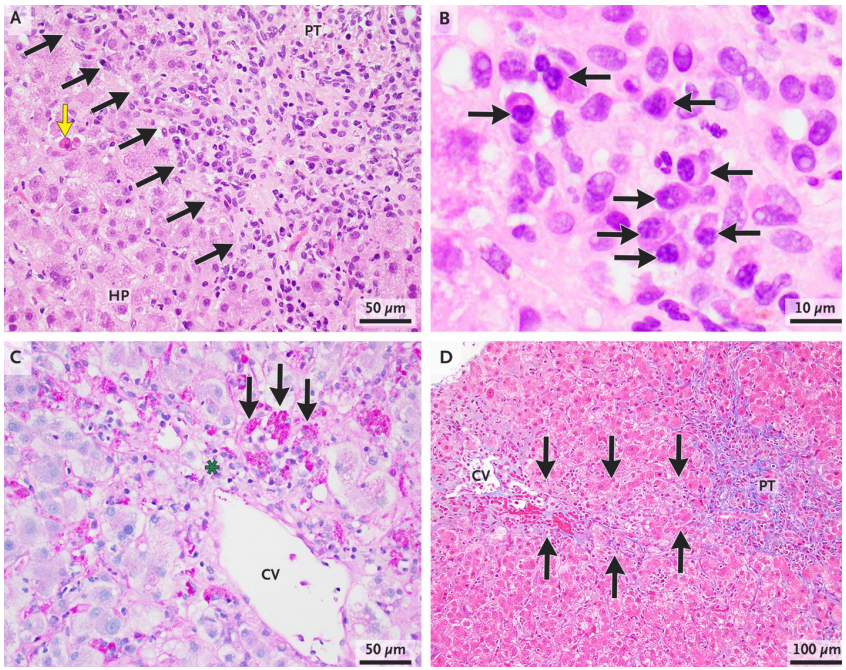

Treatment with azathioprine was added to the prednisone regimen 1 week after hospital discharge and was increased to a dose of 100 mg daily over the course of 1 month. Owing to planned mitral-valve surgery and concerns about the risks associated with glucocorticoids in the context of surgery, the dose of prednisone was rapidly tapered over a period of 2 months and was discontinued 1 week after the levels of liver enzymes had normalized. Bioprosthetic mitral-valve replacement was performed soon after the dose of prednisone was tapered to discontinuation; the patient had no complications from the procedure. The levels of liver enzymes remained normal at a follow-up visit 16 months later.

Commentary

This patient presented with jaundice, headache, slurred speech, and emesis and received a diagnosis of staphylococcal endocarditis and liver injury that incompletely abated with antibiotics. Liver biopsy ultimately led to a diagnosis of autoimmune hepatitis, which had been unmasked by bacterial infection and temporary discontinuation of budesonide therapy for Crohn's disease, followed by resumption of budesonide at a reduced dose.

Discontinuing treatment for one (or two) autoimmune conditions can unmask a third

THE LANCET

Der **Systemische Lupus erythematodes (SLE)** ist eine **chronisch-entzündliche Autoimmunerkrankung**, bei der das Immunsystem fälschlicherweise gesundes, körpereigenes Gewebe angreift. Da die dabei gebildeten Autoantikörper über die Blutbahnen jeden Bereich des Körpers erreichen können, handelt es sich um eine Systemerkrankung, die theoretisch **jedes Organ und Gewebe schädigen kann**. Die Erkrankung ist bis heute **nicht heilbar**, verläuft meistens in unvorhersehbaren Schüben und betrifft zu etwa 90 Prozent Frauen – besonders im gebährfähigen Alter zwischen 20 und 40 Jahren

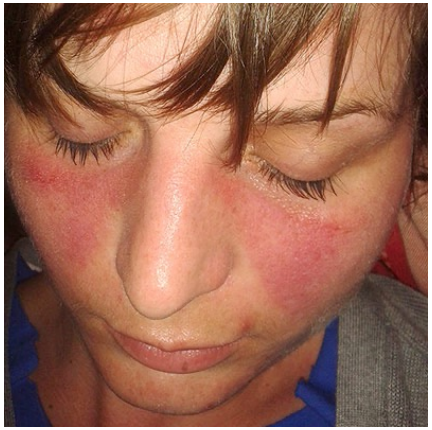

- **Basismedikation:** Nahezu alle Patienten erhalten das Antimalariamittel **Hydroxychloroquin**, da es Schübe nachweislich reduziert und Organe schützt.
- **Akut-Therapie:** Bei akuten Schüben kommen **Glukokortikoide (Kortison)** zum Einsatz, um Entzündungen rasch zu stoppen.
- **Immunsuppressiva:** Bei schweren Verläufen mit Organbeteiligung dämpfen Medikamente wie Azathioprin, Mycophenolat-Mofetil oder moderne Biologika (z. B. Belimumab) das fehlgeleitete Immunsystem.

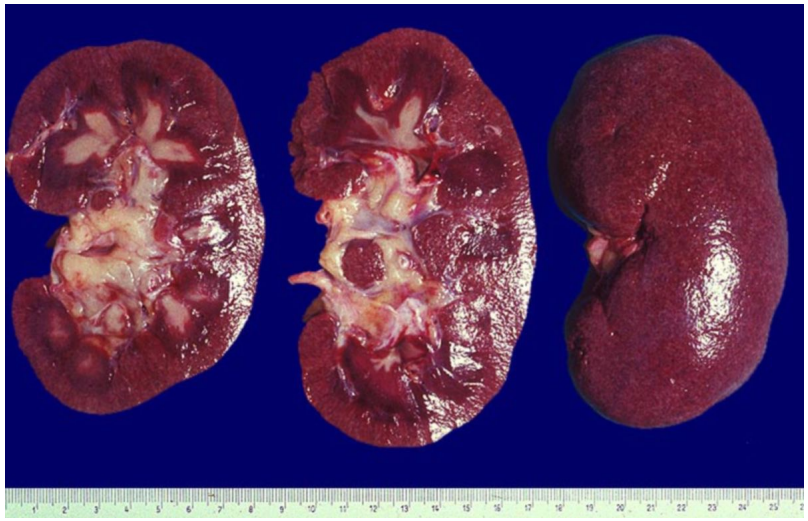

CD40 (Cluster of Differentiation 40) ist ein wichtiges Oberflächenprotein und Rezeptor, der primär auf Zellen des Immunsystems vorkommt (u. a. B-Lymphozyten, Makrophagen und dendritische Zellen). Es spielt eine zentrale Rolle bei der Steuerung der Immunabwehr, Entzündungsreaktionen und der Antikörperproduktion.

Wichtige Funktionen und Mechanismen

- **Kommunikation im Immunsystem:** CD40 wird durch das Protein **CD40L** (CD40-Ligand) aktiviert, das hauptsächlich auf T-Helferzellen exprimiert wird.
- **Aktivierung & Gedächtnis:** Die Bindung zwischen CD40 und CD40L signalisiert den Immunzellen, zu wachsen, sich zu teilen und zielgerichtet Antikörper zu bilden.
- **Krankheitsbilder:** Mutationen im CD40-Gen oder dem CD40L-Gen können zu seltenen Immundefekten wie dem Hyper-IgM-Syndrom (Typ 3) führen.
- **Medizinische Nutzung:** In der modernen Onkologie werden gezielt CD40-Agonisten (Wirkstoffe, die den Rezeptor stimulieren) erforscht. Diese sollen das Immunsystem dazu anregen, Tumorzellen zu erkennen und zu bekämpfen.

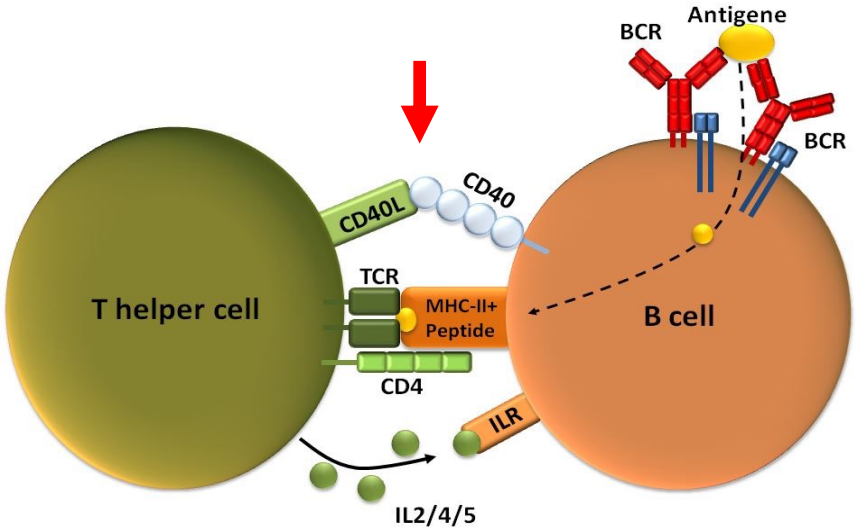

Dapirolizumab Pegol (DZP) ist ein innovatives, biologisches Prüfpräparat zur Behandlung des **systemischen Lupus erythematodes (SLE)**. Es handelt sich dabei um ein monovalentes, Polyethylenglykol-konjugiertes (PEGyliertes) Antikörper-Fab-Fragment, das von den Pharmaunternehmen entwickelt wird.

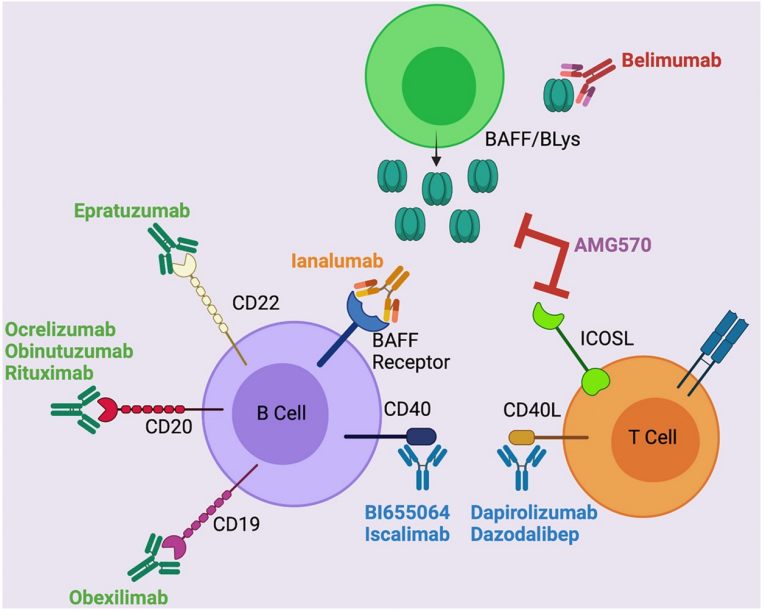

Wirkmechanismus

Der Wirkstoff besitzt ein gezieltes Funktionsprinzip zur Regulation des Immunsystems:

•**CD40L-Inhibition**: Er blockiert spezifisch den CD40-Liganden (CD40L/CD154).

•**Unterbrechung der Interaktion**: Dadurch wird die Interaktivität zwischen T-Zellen und B-Zellen gehemmt.

•**Reduktion von Entzündungen**: Die Bildung entzündungsfördernder Zytokine und Autoantikörper geht zurück.

•**Fehlende Fc-Domäne**: Durch das Design ohne Fc-Teil werden typische thromboembolische Nebenwirkungen älterer CD40L-Inhibitoren vermieden.

Does blocking CD40 signals help SLE?

Efficacy and safety of the CD40 ligand inhibitor dapirolizumab pegol in systemic lupus erythematosus (PHOENYCS GO): a randomised, double-blind, placebo-controlled, phase 3 trial

Summary

Background Dapirolizumab pegol is a novel CD40 ligand inhibitor. In this phase 3 trial, we aimed to evaluate the efficacy and safety of dapirolizumab pegol in patients with systemic lupus erythematosus (SLE).

Methods PHOENYCS GO was a 48-week, randomised, double-blind, placebo-controlled, phase 3 trial conducted in 177 centres (hospitals, private practices, and trial centres) in 25 countries. Patients aged 16 years or older with moderate-to-severe, active SLE despite standard-of-care medication were randomly assigned (2:1), via an interactive web response system, to intravenous dapirolizumab pegol 24 mg/kg or placebo every 4 weeks in addition to standard of care. Patients, investigators, and funders were blinded to treatment assignments. The primary outcome was British Isles Lupus Assessment Group-based Composite Lupus Assessment (BICLA) response at week 48. Efficacy analyses were conducted on a modified intention-to-treat population. Safety analyses included all randomly assigned patients who received at least one study medication dose. This trial is registered with ClinicalTrials.gov (NCT04294667) and is completed.

Findings Between Aug 12, 2020, and June 8, 2023, 643 patients were screened and 321 patients were randomly assigned to dapirolizumab pegol (n=213) or placebo (n=108) plus standard of care. All randomly assigned patients received at least one dose of study medication. Six patients were excluded due to non-compliance of one site with Good Clinical Practice guidelines; therefore, the full-analysis set included 315 patients (293 female, 22 male). A significantly greater proportion of patients receiving dapirolizumab pegol (50% [103/208]) versus placebo (35% [37/107]) had BICLA response at week 48 (p=0·011; difference 14·6; 95% CI 3·3–25·8). Treatment-emergent adverse events occurred in 83% (176/213) of patients receiving dapirolizumab pegol versus 75% (81/108) receiving placebo. Serious treatment-emergent adverse events occurred in 10% (21/213) of patients receiving dapirolizumab pegol versus 15% (16/108) receiving placebo. Hypersensitivity reactions during infusion occurred in 3% (6/213) of patients receiving dapirolizumab pegol. Serious infections occurred in 4% (8/213) and 6% (6/108) of patients receiving dapirolizumab pegol and placebo, respectively. One thromboembolic event (myocardial infarction) occurred in one patient in the dapirolizumab pegol group and one death (gangrene-related sepsis) occurred in another patient in the dapirolizumab pegol group.

Interpretation Dapirolizumab pegol was associated with significant improvement in disease activity in patients with SLE. These findings support the further investigation of dapirolizumab pegol as a treatment option for SLE.

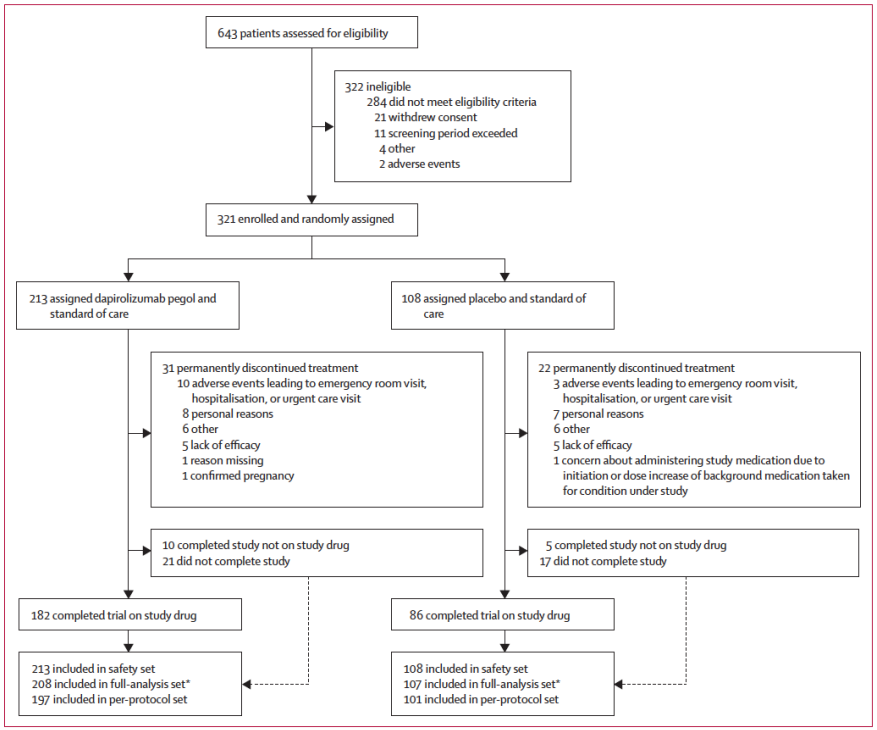

Figure 1: **Trial profile**
*Six patients were excluded from the full-analysis set due to non-compliance with Good Clinical Practice.

	Dapirolizumab pegol (n=208)	Placebo (n=107)
Age, years	43·5 (36·0–52·0)	41·0 (32·0–50·0)
Sex		
Female	193 (93%)	100 (94%)
Male	15 (7%)	7 (7%)
Weight, kg	72·4 (17·9)	69·5 (14·8)
BMI, kg/m²	27·5 (6·0)	26·6 (5·3)
Race		
American Indian or Alaskan Native	20 (10%)	9 (8%)
Asian	18 (9%)	9 (8%)
Black or African American	11 (5%)	9 (8%)
Native Hawaiian or other Pacific Islander	1 (1%)	0
White	128 (62%)	63 (59%)
Other or mixed	30 (14%)	17 (16%)
Ethnicity		
Hispanic or Latino	77 (37%)	40 (37%)
Not Hispanic or Latino	131 (63%)	67 (63%)
Region		
North America	46 (22%)	24 (22%)
Eastern Europe	28 (14%)	8 (8%)
Western Europe	59 (28%)	31 (29%)
Asia-Pacific	16 (8%)	8 (8%)
Latin America	59 (28%)	36 (34%)
Time since SLE diagnosis, years	8·6 (3·7–14·5)	7·0 (3·8–14·0)
SLEDAI-2K score		
Mean	10·7 (3·5)	11·2 (3·4)
<10	68 (33%)	28 (26%)
≥10	140 (67%)	79 (74%)
BILAG-2004 score		
Mean	18·4 (4·0)	18·7 (4·4)
Either ≥1 BILAG-2004 grade A and/or ≥2 BILAG grade Bs	201 (97%)	106 (99%)
≥1 BILAG-2004 grade A	89 (43%)	48 (45%)
≥2 organ systems with BILAG-2004 grade A or B	184 (89%)	96 (90%)
SFI flare		
No flare	46 (22%)	24 (22%)
Mild flare	12 (6%)	6 (6%)
Moderate flare	93 (45%)	43 (40%)
Severe flare	56 (27%)	34 (32%)
Missing	1 (1%)	0
PGA score	58·9 (14·1)	59·7 (14·1)
CLASI-A score	7·0 (4·0–11·0)	6·0 (3·0–10·0)
CLASI-D score	0·0 (0·0–0·0)	0·0 (0·0–0·0)

(Table 1 continues in next column)

	Dapirolizumab pegol (n=208)	Placebo (n=107)
(Continued from previous column)		
Tender joint count*	11·0 (7·0–15·0)	12·0 (5·0–16·0)
Swollen joint count*	7·0 (4·0–10·0)	6·0 (3·0–9·0)
LAMDA PGA of Arthritis	55·5 (18·0)	56·5 (18·7)
SLICC/ACR Damage Index total score	0·6 (0·9)	0·5 (1·1)
FACIT–Fatigue score	28·5 (11·2)	27·7 (10·5)
Concomitant SLE medications at baseline	208 (100%)	107 (100%)
Antimalarials†	166 (80%)	91 (85%)
Systemic glucocorticoids	171 (82%)	87 (81%)
Immunosuppressants	129 (62%)	70 (65%)
Systemic glucocorticoid dose		
Mean, mg/day	7·9 (5·9)	9·6 (8·1)
>7·5 mg/day	105 (51%)	51 (48%)
Anti-dsDNA‡ >10 IU	91 (44%)	62 (58%)
Anti-dsDNA‡ >10 IU and complement C3 <LLN	43 (21%)	34 (32%)
Antinuclear antibody titre§ ≥1:80	206 (99%)	102 (95%)
Complement C3 <LLN	65 (31%)	42 (39%)
Complement C4 <LLN	116 (56%)	57 (53%)
Any antiphospholipid antibodies¶	129 (62%)	64 (60%)
Lupus anticoagulant ratio >ULN‖	16 (8%)	13 (12%)

Data are mean (SD), n (%), or median (IQR). Both groups also received standard-of-care medication. Anti-dsDNA=anti-double stranded DNA. BILAG-2004=British Isles Lupus Assessment Group 2004. CLASI-A=Cutaneous Lupus Erythematosus Disease Area and Severity Index-Activity. CLASI-D=Cutaneous Lupus Erythematosus Disease Area and Severity Index-Damage. FACIT=Functional Assessment of Chronic Illness Therapy. IU=international unit. LAMDA=Lupus Arthritis and Musculoskeletal Disease Activity. LLN=lower limit of normal. PGA=Physician Global Assessment. SFI=Safety of Estrogen in Lupus Erythematosus National Assessment-Systemic Lupus Erythematosus Disease Activity Index Flare Index. SLE=systemic lupus erythematosus. SLEDAI-2K=Systemic Lupus Erythematosus Disease Activity Index-2000. SLICC/ACR=Systemic Lupus International Collaborating Clinics/American College of Rheumatology. ULN=upper limit of normal. *Joint assessments were done on 28 joints. †204 (98%) patients receiving dapirolizumab pegol and 105 (98%) patients receiving placebo were either on antimalarials at baseline or had received antimalarials in the past. ‡Assessed through Phadia EliA. One patient receiving dapirolizumab pegol and one patient receiving placebo had missing data. §Assessed through Indirect Fluorescent Antibody testing with Bio-Rad Kallestad HEp-2 cell line substrate. ¶Antiphospholipid antibodies included anti-phosphatidylserine and anti-prothrombin; includes all patients with >0 antiphospholipid antibodies >ULN or lupus anticoagulant ratio >ULN. ‖The lupus anticoagulant ratio was based on confirmation testing.

Table 1: **Baseline demographics and disease characteristics of the full-analysis set**

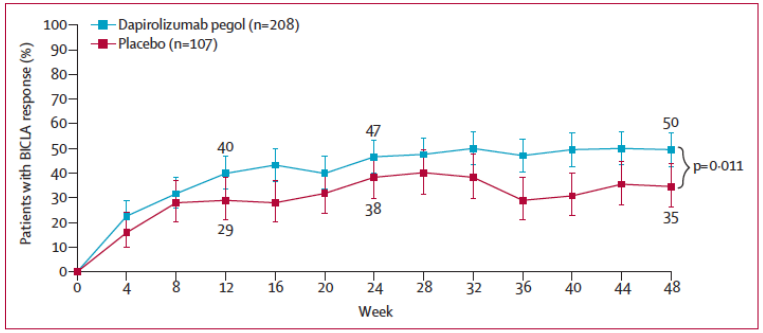

Figure 2: **BICLA response over time in the full-analysis set**
Error bars represent 95% CIs. BICLA=British Isles Lupus Assessment Group-based Composite Lupus Assessment.

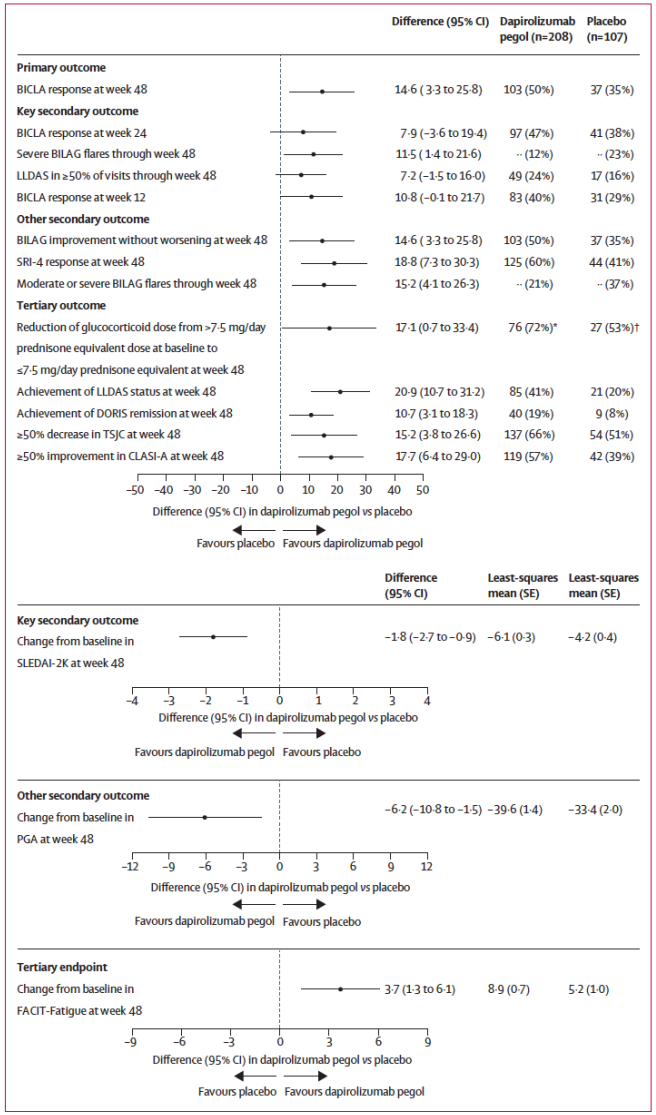

Figure 3: **Primary, secondary, and tertiary outcomes in the full-analysis set**
For BILAG flare outcomes, only percentages are provided and exact patient numbers are not available, given the multiple imputation–missing at random method used. Patients with intercurrent events or missing data cannot be assumed to not have had a flare. BICLA=British Isles Lupus Assessment Group-based Composite Lupus Assessment. BILAG=British Isles Lupus Assessment Group. CLASI-A=Cutaneous Lupus Erythematosus Disease Area and Severity Index–Activity. DORIS=Definition of Remission in Systemic Lupus Erythematosus. FACIT=Functional Assessment of Chronic Illness Therapy. LLDAS=Lupus Low Disease Activity State. PGA=Physician Global Assessment. SLEDAI-2K=Systemic Lupus Erythematosus Disease Activity Index-2000. SRI-4=Systemic Lupus Erythematosus Responder Index-4. TSJC=tender and swollen joint count. *n=105. †n=51.

	Dapirolizumab pegol (n=213)	Placebo (n=108)	Risk difference (95% CI)
Any treatment-emergent adverse event	176 (83%)	81 (75%)	7·6 (−1·5 to 17·6)
Serious treatment-emergent adverse events	21 (10%)	16 (15%)	−5·0 (−13·5 to 2·3)
Anticipated serious adverse events*			
Lower respiratory tract and lung infections	0	2 (2%)	..
Lupus erythematosus	3 (1%)	1 (1%)	..
Urinary tract infections	1 (1%)	0	..
Nephritis	0	0	..
Pain and discomfort	0	1 (1%)	..
Abdominal and gastrointestinal infections	0	2 (2%)	..
Bacterial infections	2 (1%)	1 (1%)	..
Peripheral embolism and thrombosis	0	0	..
Ischaemic coronary artery disorders	1 (1%)	0	..
Herpes viral infections	2 (1%)	1 (1%)	..
Severe treatment-emergent adverse events	13 (6%)	11 (10%)	−4·1 (−11·6 to 1·9)
Permanent discontinuation of drug or study discontinuation due to treatment-emergent adverse events	10 (5%)	4 (4%)	1·0 (−4·8 to 5·3)
Treatment-related treatment-emergent adverse events†	50 (24%)	24 (22%)	1·3 (−8·9 to 10·4)
Deaths‡	1 (1%)	0	0·5 (−3·0 to 2·6)
Most common treatment-emergent adverse events (≥5% of any treatment group by preferred term)			
COVID-19	44 (21%)	17 (16%)	..
Urinary tract infection	29 (14%)	9 (8%)	..
Upper respiratory tract infection	20 (9%)	8 (7%)	..
Nasopharyngitis	18 (9%)	13 (12%)	..
Diarrhoea	15 (7%)	10 (9%)	..
Headache	15 (7%)	7 (7%)	..
Bronchitis	11 (5%)	5 (5%)	..
Nausea	9 (4%)	6 (6%)	..
Herpes zoster	4 (2%)	7 (7%)	..
Oral herpes	4 (2%)	6 (6%)	..
Chest pain	1 (1%)	6 (6%)	..
Treatment-emergent adverse events of special interest	0	1 (1%)	−0·9 (−5·1 to 1·0)
Potential Hy's law§	0	0	..
Malignancies	0	1 (1%)	..
Treatment-emergent adverse events of special monitoring	78 (37%)	26 (24%)	12·5 (1·7–22·3)
Severe infections	3 (1%)	4 (4%)	..
Opportunistic infections¶	6 (3%)‖	1 (1%)**	..
Hypersensitivity treatment-emergent adverse events starting on the day of or the day after an infusion	6 (3%)	0	..
Hypersensitivity treatment-emergent adverse events leading to permanent discontinuation of study treatment	4 (2%)	0	..
Anaphylactic reactions¶††	1 (1%)	0	..
Thromboembolic treatment-emergent adverse events confirmed by adjudication	1 (1%)	0	..
Acute myocardial infarction	1 (1%)	0	..
Neurological events‡‡	0	0	..

(Table 2 continues on next page)

(Continued from previous page)

	Dapirolizumab pegol (n=213)	Placebo (n=108)	Risk difference (95% CI)
Infections and infestations	131 (62%)	56 (52%)	9·7 (−1·7 to 20·9)
Mild	95 (45%)	35 (32%)	..
Moderate	66 (31%)	36 (33%)	..
Severe	3 (1%)	4 (4%)	..
Serious	8 (4%)	6 (6%)	..
Herpes viral infections	13 (6%)	14 (13%)	−6·9 (−14·9 to −0·4)
Herpes zoster	4 (2%)	7 (7%)	..
Ophthalmic herpes zoster	2 (1%)§§	0	..
Herpes ophthalmic	1 (1%)¶¶	0	..

Data are n (%) or risk difference (95% CI). Both groups also received standard-of-care medication. ALP=alkaline phosphatase. ALT=alanine aminotransferase. AST=aspartate aminotransferase. SMQ=Standardised Medical Dictionary for Regulatory Activities Queries. SLE=systemic lupus erythematosus. ULN=upper limit of normal. *The specific serious adverse events displayed are protocol-defined serious adverse events—defined as serious adverse events that can be anticipated in a patient with SLE, irrespective and independent of the study treatment or drug exposure—which were summarised to alert investigators to the possibility of these events occurring in the study population. †Considered related by investigator. ‡Death due to gangrene-related sepsis, which was considered not related to treatment by the investigator. However, per the sponsor, the causal role of the study medication in the final outcome of sepsis could not be completely ruled out. §Potential Hy's law, defined as ALT or AST ≥3 times ULN, with coexisting total bilirubin ≥2 times ULN, in the absence of ALP ≥2 times ULN, with no alternative explanation for the biochemical abnormality. ¶Definition based on the narrow SMQ v24.0. ‖In patients receiving dapirolizumab pegol, there were two cases of ophthalmic herpes zoster, one of herpes ophthalmic, two of disseminated cutaneous herpes zoster, and one case of joint tuberculosis. **One patient receiving placebo had a case of disseminated cutaneous herpes zoster. ††Three patients receiving dapirolizumab pegol had anaphylaxis reactions meeting Sampson's criteria; two patients had infusion-related reactions and one patient had an anaphylactic reaction. ‡‡Prespecified neurological events: severe or serious headache, positional headache, cranial nerve dysfunction, and signs or symptoms of meningitis. §§The two events were reported as "herpes zoster over left eyelid and forehead, V1" and "left herpes zoster ophthlamicus (dermatome V1/V2)". ¶¶Reported as "herpetic queratitis".

Table 2: **Adverse events in the safety set**

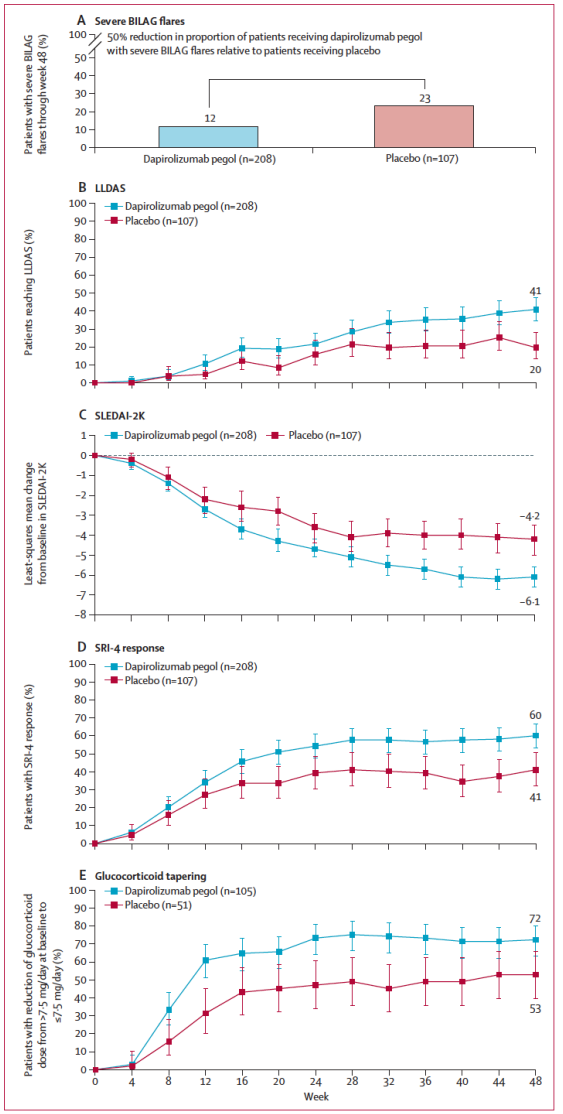

Figure 4: **Select efficacy outcomes over time up to week 48 in the full-analysis set**

Error bars represent 95% CIs. BILAG=British Isles Lupus Assessment Group. LLDAS=Lupus Low Disease Activity State. SLEDAI-2K=Systemic Lupus Erythematosus Disease Activity Index-2000. SRI-4=Systemic Lupus Erythematosus Responder Index-4.

Implications of all the available evidence

As SLE immunopathology is complex and multifaceted, treatments targeting multiple immunological pathways and affecting a range of disease domains could provide benefit over current standard of care. The results of PHOENYCS GO reinforce the potential of targeting CD40–CD40 ligand interactions in the treatment of SLE, and support dapirolizumab pegol as a potential treatment option in patients with moderate-to-severe, active SLE. The ongoing open-label extension (ie, PHOENYCS GLIDE; NCT04976322), and a second confirmatory phase 3 trial (PHOENYCS FLY; NCT06617325) will further assess the efficacy and safety of dapirolizumab pegol in patients with SLE.

Nach einem Gewichtsverlust **verlangsamt sich der Stoffwechsel und der Körper verbrennt insgesamt weniger Kalorien**. Dies ist eine natürliche, biologische Reaktion, die oft als „metabolische Adaptation“ bezeichnet wird. Der Körper versucht damit, die verbleibenden Fettreserven zu schützen und ein weiteres Sinken des Gewichts zu verhindern.

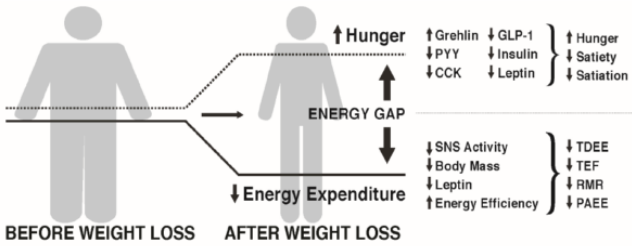

1. Sinken des Grundumsatzes

•**Weniger Masse**: Ein leichterer Körper benötigt im Ruhezustand automatisch weniger Energie, um die Organfunktionen aufrechtzuerhalten.

•**Muskelverlust**: Während einer Diät baut der Körper neben Fett oft auch Muskelmasse ab. Da Muskeln selbst im Ruhezustand viel Energie verbrennen, sinkt der Grundumsatz dadurch zusätzlich.

2. Hormonelle Veränderungen

•**Gesteigerter Hunger**: Das Hormon *Leptin* (welches Sättigung signalisiert) wird in den Fettzellen produziert. Schrumpfen diese Zellen, sinkt der Leptinspiegel drastisch.

•**Mehr Appetit**: Gleichzeitig steigt das Hungerhormon *Ghrelin*. Das Gehirn erhält das Signal „Hungersnot“ und reagiert mit intensivem Appetit, um die Energiespeicher wieder aufzufüllen.

Die langfristige Gewichtserhaltung (Weight Loss Maintenance Therapy) ist die größte Herausforderung bei der Behandlung von Adipositas, da biologische Abwehrmechanismen und veränderte Hormonspiegel den Körper aktiv dazu drängen, verloren gegangenes Gewicht wieder aufzubauen. Eine erfolgreiche Erhaltungstherapie erfordert daher ein dauerhaftes, strukturiertes Zusammenspiel aus medizinischer Betreuung, medikamentösen Ansätzen, Verhaltensänderungen und regelmäßiger Bewegung.

Warum Gewichtserhaltung so schwierig ist

•**Hormonelle Anpassung:** Nach einer Gewichtsabnahme sinkt das Sättigungshormon Leptin, während das Hungerhormon Ghrelin steigt.

•**Reduzierter Energieverbrauch:** Der Stoffwechsel verlangsamt sich oft stärker, als es allein durch den Verlust an Körpermasse zu erklären wäre (metabolische Adaptation).

•**Erhöhter Appetit:** Das Gehirn signalisiert dem Körper über einen langen Zeitraum eine vermehrte Nahrungsaufnahme, um die alten Fettreserven wieder aufzufüllen.

After GLP1, what next?

Tirzepatide for maintenance of bodyweight reduction in people with obesity in the USA (SURMOUNT-MAINTAIN): a multicentre, double-blind, randomised, placebo-controlled trial

Summary

Background Obesity treatment improves long-term health and quality of life outcomes. Weight reduction and its maintenance play an important role in achieving these goals. We evaluated the efficacy and safety of continuing tirzepatide at the maximum tolerated dose (MTD) or lowering the dose to 5 mg compared with switching to placebo on the maintenance of bodyweight reduction obtained with tirzepatide MTD in adults with obesity.

Methods This phase 3b, placebo-controlled, 112-week trial, including a 60-week open-label weight-loss period and a 52-week, double-blind weight maintenance period, was conducted across 20 sites in the USA. After completing the initial weight-loss period with once weekly subcutaneous tirzepatide at the MTD (10 mg or 15 mg), adults (aged ≥18 years) with a BMI of 30 kg/m² and above or 27 kg/m² and above with one or more weight-related comorbidities, and a history of at least one self-reported unsuccessful dietary effort to lose bodyweight were randomly assigned in a 3:3:2 ratio to continue tirzepatide MTD, reduce to tirzepatide 5 mg, or switch to placebo for an additional 52 weeks. Starting at week 84 (24 weeks after random allocation), participants could receive rescue tirzepatide if their weight regain exceeded 50%. The primary endpoint was the percentage change in bodyweight from baseline to week 112. The primary estimand was the modified treatment-regimen estimand, which assumed that participants who initiated rescue tirzepatide would not have gained further benefit from their assigned study treatment and included all randomly allocated participants, regardless of treatment discontinuation or initiation of prohibited medications. The efficacy estimand was supportive. Safety was assessed in all participants who received at least one dose of study drug. This completed trial was registered at ClinicalTrials.gov (NCT06047548).

Findings From Sept 20, 2023, to Jan 20, 2026, 441 patients were enrolled in and took at least one dose of study treatment during the weight-loss period, with 378 participants randomly allocated at week 60 (140 to tirzepatide MTD; 144 to dose-reduction to 5 mg tirzepatide; and 94 to placebo). 372 received at least one dose of study drug during the weight maintenance period (139 for tirzepatide MTD; 142 for 5 mg tirzepatide; and 91 for placebo). 345 (91%) of 378 participants completed the study. The majority of participants were White (67%); 288 (65%) participants were female and 153 (35%) were male; and the mean age was 46·6 years (SD 13·0). At baseline, participants had a mean bodyweight of 113·8 kg (SD 27·0), a BMI of 40·1 kg/m² (SD 8·1), and HbA_{1c} 5·64% (SD 0·4; 38·2 mmol/mol [SD 4·0]). The model-based estimate percent change in bodyweight from baseline to week 112 was –21·9% (95% CI –23·5 to –20·3) with MTD (estimated treatment difference [ETD] –12·0% [95% CI –13·8 to –10·1]), –16·6% (95% CI –18·0 to –15·1) with 5 mg tirzepatide (ETD –6·6 [95% CI –8·3 to –5·0]), versus –9·9% (95% CI –11·1 to –8·8) with placebo ($p<0·0001$ for all comparisons). Among participants who regained at least 50% of lost bodyweight, observed means were 11 (8%) of 138, 35 (25%) of 142, and 60 (67%) of 90 participants received rescue therapy in the tirzepatide MTD, 5 mg tirzepatide, and placebo, respectively. The most common adverse events with tirzepatide were gastrointestinal events, which were mostly mild to moderate in severity and mostly occurred during dose escalation.

Interpretation In adults with obesity, long-term treatment is often necessary to maintain bodyweight reduction and its associated cardiometabolic benefits. In the SURMOUNT-MAINTAIN trial, continuing tirzepatide at MTD maintained bodyweight reduction and health-related benefits. Reducing to 5 mg tirzepatide might provide a valuable alternative to discontinuation, although individuals' treatment response might vary. Together, these findings support the importance of ongoing therapy for long-term obesity management and provide evidence to inform individualised, patient-centred obesity care.

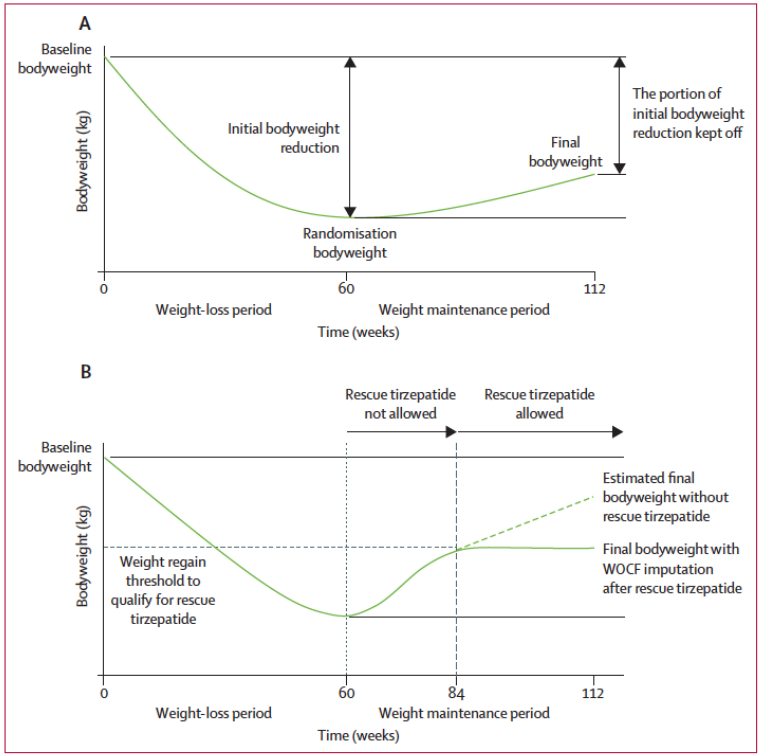

Figure 1: **Conceptual diagram of bodyweight reduction and maintenance (A) and rescue tirzepatide and worse value imputation (B)**
Change in weight=the difference between baseline weight (week 0) and final weight (week 112), expressed in kg. Percentage change in weight=the change in weight from week 0 to week 112, expressed as a percentage of baseline weight. Percentage maintenance=the portion of initial weight reduction kept off at week 112. WOCF=worst observation carried forward.

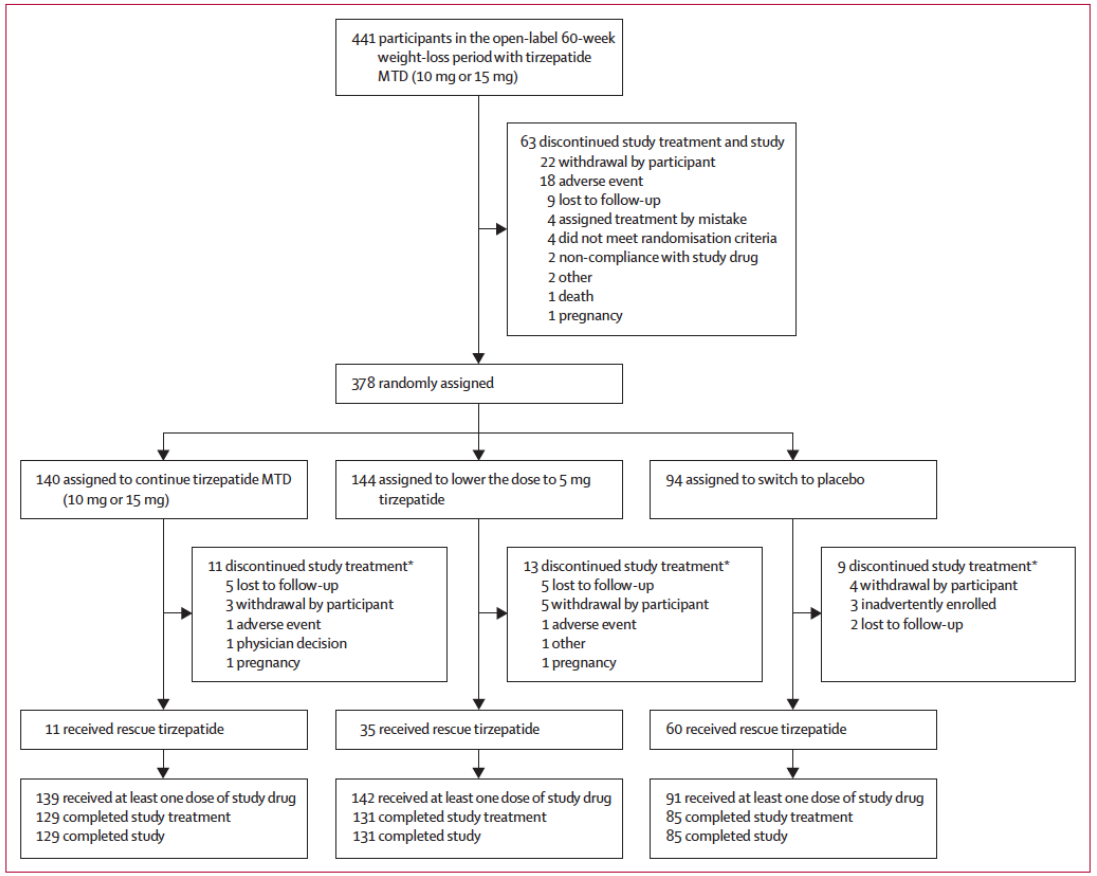

Figure 2: **Trial profile**
MTD=maximum tolerated dose. *All participants who discontinued study treatment also discontinued the study.

	Week 0*	Week 60 (random allocation)		
	Weight-loss period with tirzepatide MTD (n=441)	10 mg or 15 mg tirzepatide, MTD (n=140)	Reduce to 5 mg tirzepatide (n=144)	Switch to placebo (n=94)
Age, years	46·6 (13·0)	48·5 (13·2)	49·4 (12·3)	46·4 (12·6)
<65 years	391 (89%)	119 (85%)	121 (84%)	86 (91%)
≥65 years	50 (11%)	21 (15%)	23 (16%)	8 (9%)
Sex†				
Male	153 (35%)	49 (35%)	50 (35%)	32 (34%)
Female	288 (65%)	91 (65%)	94 (65%)	62 (66%)
Race†				
White	295/438 (67%)	89/139 (64%)	101/144 (70%)	57/92 (62%)
Black or African American	107/438 (24%)	35/139 (25%)	34/144 (24%)	29/92 (32%)
Asian	20/438 (5%)	8/139 (6%)	5/144 (3%)	4/92 (4%)
Multiple	11/438 (3%)	6/139 (4%)	3/144 (2%)	2/92 (2%)
American Indian or Alaska Native	3/438 (1%)	0	1/144 (1%)	0
Native Hawaiian or Other Pacific Islander	2/438 (<1%)	1/139 (1%)	0	0
Ethnicity†				
Hispanic or Latino	99 (22%)	27 (19%)	31 (22%)	25 (27%)
Not Hispanic or Latino	342 (78%)	113 (81%)	113 (78%)	69 (73%)
Duration of obesity, years†	12·8 (5·8–21·9)	13·8 (5·8–23·8)	11·4 (5·8–20·8)	13·3 (6·8–23·8)
Bodyweight, kg	113·8 (27·0)	88·3 (22·3)	88·7 (24·5)	93·7 (27·5)
BMI, kg/m²	40·1 (8·1)	30·8 (6·9)	31·1 (7·2)	33·4 (8·7)
BMI category				
<30	20 (5%)	72 (51%)	76 (53%)	34 (36%)
≥30 to <35	111 (25%)	33 (24%)	36 (25%)	29 (31%)
≥35 to <40	122 (28%)	21 (15%)	14 (10%)	11 (12%)
≥40	188 (43%)	14 (10%)	18 (13%)	20 (21%)
Bodyweight plateau	NA	118 (84%)	120 (83%)	80 (85%)
Percent bodyweight reduction at week 60				
<20%	NA	62 (44%)	64 (44%)	42 (45%)
≥20%	NA	78 (56%)	80 (56%)	52 (55%)
Waist circumference, cm	119·4 (17·5)	99·1 (17·2)	100·0 (17·8)	103·6 (19·9)
HbA1c	5·64% (0·36)	5·16% (0·31)	5·13% (0·33)	5·09% (0·34)
HbA1c, mmol/mol	38·2 (4·0)	32·9 (3·4)	32·6 (3·6)	32·1 (3·7)
Fasting serum glucose, mg/dL	94·7 (11·8)	82·1 (8·0)	82·2 (7·7)	80·5 (6·8)
Fasting serum glucose, mmol/L	5·3 (0·7)	4·6 (0·4)	4·6 (0·4)	4·5 (0·4)
Systolic blood pressure, mm Hg	126·3 (12·8)	116·3 (13·1)	117·4 (14·3)	119·1 (13·8)
Diastolic blood pressure, mm Hg	81·3 (8·2)	77·6 (9·8)	77·9 (9·3)	78·5 (8·4)
Pulse, bpm	71·9 (9·8)	74·9 (9·6)	74·9 (8·4)	75·2 (8·5)

(Table 1 continues on next page)

	Week 0*	Week 60 (random allocation)		
	Weight-loss period with tirzepatide MTD (n=441)	10 mg or 15 mg tirzepatide, MTD (n=140)	Reduce to 5 mg tirzepatide (n=144)	Switch to placebo (n=94)
(Continued from previous page)				
Lipid parameters, mg/dL				
Total cholesterol	192·2 (37·0)	182·0 (40·5)	177·4 (34·6)	184·7 (39·1)
HDL cholesterol	50·7 (13·4)	54·7 (15·0)	54·9 (13·3)	54·6 (14·1)
LDL cholesterol	115·7 (31·1)	110·1 (37·0)	105·2 (29·5)	112·3 (33·8)
VLDL cholesterol	25·2 (11·8)	17·2 (6·6)	17·3 (8·4)	18·1 (9·2)
Triglycerides	128·7 (70·0)	86·3 (33·0)	86·6 (41·9)	90·4 (45·9)
eGFR, mL/min per 1·73 m²‡	89·7 (19·5)	94·5 (19·1)	95·3 (18·4)	95·8 (17·7)
Comorbidities				
Prediabetes	268 (61%)	93 (66%)	89 (62%)	55 (59%)

Data are mean (SD) or n (%), except duration of obesity, which is presented as median (IQR). A full list of comorbidities and number of comorbidities at baseline is provided in appendix 2 (p 10). Baseline SF-36v2 (norm-based) scores are provided in appendix 2 (p 11). bpm=beats per minute. eGFR=estimated glomerular filtration rate. HbA1c=glycated haemoglobin. MTD=maximum tolerated dose. NA=not applicable. SF-36v2=Short Form-36 Health Survey Version 2. *Start of 60-week open-label weight-loss period with tirzepatide MTD. †Sex, race, ethnicity, and duration of obesity were self-reported. The denominator for Race is based on number of participants with no missing data. ‡eGFR was calculated with the serum cystatin-C Chronic Kidney Disease Epidemiology Collaboration equation.

Table 1: **Demographics and clinical characteristics at baseline and random allocation**

	10 mg or 15 mg tirzepatide, MTD (n=138)	Reduce to 5 mg tirzepatide (n=142)	Switch to placebo (n=90)	10 mg or 15 mg tirzepatide, MTD *vs* switch to placebo ETD (95% CI); p value	5 mg tirzepatide *vs* switch to placebo ETD (95% CI); p value
Treatment-regimen estimand					
Primary endpoint in all participants at week 112*					
Percent change from baseline in bodyweight	−21·9% (−23·5 to −20·3)	−16·6% (−18·0 to −15·1)	−9·9% (−11·1 to −8·8)	−12·0% (−13·8 to −10·1); <0·0001	−6·6% (−8·3 to −5·0); <0·0001
Key secondary endpoints in all participants at week 112, unless otherwise noted*					
Change from baseline in bodyweight, kg	−24·6 (−26·6 to −22·6)	−18·8 (−20·5 to −17·2)	−11·3 (−12·6 to −10·0)	−13·3 (−15·5 to −11·2); <0·0001	−7·6 (−9·4 to −5·7); <0·0001
Percent change from random allocation in bodyweight	−0·2% (−1·5 to 1·0)	7·0% (5·8 to 8·2)	15·2% (13·6 to 16·8)	−15·4% (−17·5 to −13·4); <0·0001	−8·2% (−10·1 to −6·2); <0·0001
Change from random allocation in bodyweight, kg	−0·2 (−1·3 to 0·9)	6·0 (5·0 to 7·0)	12·8 (11·5 to 14·1)	−13·0 (−14·7 to −11·3); <0·0001	−6·8 (−8·4 to −5·2); <0·0001
Percent change from baseline in bodyweight at week 84	−22·4% (−23·8 to −21·1)	−18·7% (−20·1 to −17·4)	−12·3% (−13·7 to −10·9)	−10·1% (−11·9 to −8·4); <0·0001	−6·4% (−8·2 to −4·7); <0·0001
Percent maintenance of bodyweight reduction obtained during the 60-week weight-loss period in participants who reached a bodyweight plateau†	96·5% (88·5 to 104·5)	67·9% (61·9 to 73·9)	42·8% (36·5 to 49·1)	53·7% (43·6 to 63·8); <0·0001	25·1% (16·7 to 33·6); <0·0001
Percentage of participants maintaining ≥80% of the bodyweight reduction obtained during the 60-week weight-loss period among those who reached a bodyweight plateau, n/N†	77·5% (3·9) [90/116]	42·4% (4·4) [50/118]	10·4% (3·5) [8/76]	67·1% (56·7 to 77·5); <0·0001	32·0% (21·0 to 43·0); <0·0001

(Table 2 continues on next page)

	10 mg or 15 mg tirzepatide, MTD (n=138)	Reduce to 5 mg tirzepatide (n=142)	Switch to placebo (n=90)	10 mg or 15 mg tirzepatide, MTD *vs* switch to placebo ETD (95% CI); p value	5 mg tirzepatide *vs* switch to placebo ETD (95% CI); p value
(Continued from previous page)					
Efficacy estimand					
Additional secondary endpoints in all participants at week 112, unless otherwise noted‡					
Change from random allocation in waist circumference, cm	−0·6 (−1·6 to 0·4)	3·8 (2·7 to 4·8)	9·3 (7·9 to 10·6)	−9·9 (−11·6 to −8·1)	−5·5 (−7·2 to −3·7)
Percent maintenance of bodyweight reduction obtained during the 60-week weight-loss period	102·4% (96·5 to 108·2)	71·7% (67·4 to 76·1)	44·6% (39·5 to 49·7)	57·8% (50·0 to 65·5)	27·1% (20·4 to 33·8)
Percent maintenance of bodyweight reduction obtained during the 60-week weight-loss period at week 84 in participants who reached a bodyweight plateau†	101·9% (97·4 to 106·5)	81·7% (76·9 to 86·6)	52·6% (46·7 to 58·6)	49·3% (41·8 to 56·8)	29·1% (21·5 to 36·8)
Maintenance of ≥15% bodyweight reduction among those who have already lost ≥15% bodyweight at random allocation†	94·2% (2·4) [100/106]	64·9% (4·3) [71/109]	22·3% (4·8) [16/71]	71·9% (61·3 to 82·4)	42·6% (30·1 to 55·0)
Exploratory endpoints in all participants at week 112‡					
Use of rescue tirzepatide for weight regain ≥50% of the bodyweight reduction obtained at random allocation, n/N	7·9% (2·3) [11/138]	24·6% (3·5 [35/142]	67·9% (4·9) [60/90]	−60·0% (−70·6 to −49·4)	−43·3% (−55·0 to −31·6)
Change from baseline in BMI, kg/m²	−9·0 (−9·6 to −8·4)	−6·8 (−7·3 to −6·3)	−4·1 (−4·5 to −3·6)	−4·9 (−5·6 to −4·2)	−2·7 (−3·4 to −2·1)
Change from baseline in waist circumference, cm	−20·1 (−21·5 to −18·6)	−16·0 (−17·4 to −14·5)	−8·4 (−10·0 to −6·9)	−11·6 (−13·8 to −9·5)	−7·5 (−9·7 to −5·4)
Percent change from baseline in triglycerides, mg/dL	−27·2% (−31·4 to −22·8)	−19·0% (−23·5 to −14·2)	−9·6% (−15·6 to −3·3)	−19·5% (−26·4 to −11·9)	−10·4% (−18·0 to −2·0)
Percent change from baseline in HDL cholesterol, mg/dL	12·6% (9·9 to 15·3)	13·9% (10·9 to 17·0)	11·9% (8·6 to 15·3)	0·6% (−3·1 to 4·5)	1·8% (−2·2 to 6·0)
Percent change from baseline in VLDL cholesterol, mg/dL	−26·7% (−30·9 to −22·2)	−18·8% (−23·4 to −13·9)	−9·2% (−15·2 to −2·7)	−19·3% (−26·3 to −11·6)	−10·6% (−18·3 to −2·2)
Percent change from baseline in non-HDL, mg/dL	−11·7% (−15·4 to −7·8)	−7·2% (−10·3 to −4·1)	−1·5% (−5·3 to 2·4)	−10·4% (−15·4 to −5·0)	−5·8% (−10·6 to −0·8)
Change from baseline in systolic blood pressure, mm Hg	−8·7 (−10·5 to −6·8)	−4·7 (−6·6 to −2·7)	−0·4 (−2·8 to 2·1)	−8·3 (−11·4 to −5·2)	−4·3 (−7·4 to −1·2)
Change from baseline in diastolic blood pressure, mm Hg	−3·8 (−5·2 to −2·4)	−2·7 (−4·0 to −1·3)	−0·1 (−1·6 to 1·5)	−3·7 (−5·8 to −1·7)	−2·6 (−4·6 to −0·6)
Change from baseline in HbA1c, %	−0·53% (−0·57 to −0·49)	−0·41% (−0·45 to −0·36)	−0·19% (−0·24 to −0·15)	−0·34% (−0·40 to −0·27)	−0·21% (−0·28 to −0·15)
Change from baseline in HbA1c, mmol/mol	−5·8 (−6·3 to −5·3)	−4·4 (−5·0 to −3·9)	−2·1 (−2·6 to −1·6)	−3·7 (−4·4 to −3·0)	−2·3 (−3·1 to −1·6)
Change from baseline in fasting serum glucose, mg/dL	−10·6 (−12·1 to −9·1)	−7·4 (−9·3 to −5·5)	−2·6 (−4·5 to −0·8)	−8·0 (−10·4 to −5·6)	−4·8 (−7·4 to −2·2)
Percent change from baseline in fasting insulin, pmol/L	−44·9% (−50·6 to −38·5)	−33·0% (−39·7 to −25·7)	−18·4% (−26·0 to −10·0)	−32·5% (−41·7 to −21·8)	−18·0% (−28·9 to −5·3)
Change from baseline in physical component summary score	6·0 (5·0 to 7·0)	4·6 (3·7 to 5·4)	3·4 (2·0 to 4·8)	2·6 (0·9 to 4·3)	1·2 (−0·4 to 2·8)
Change from baseline in mental component summary score	−0·0 (−1·3 to 1·3)	−0·1 (−1·2 to 0·9)	−1·6 (−2·8 to −0·4)	1·6 (−0·2 to 3·4)	1·5 (−0·2 to 3·1)
Maintenance of ≥20% bodyweight reduction among those who have already lost ≥20% bodyweight at random allocation, n/N†	84·7% (4·2) [65/77]	66·5% (5·4) [53/79]	13·3% (4·8) [7/51]	71·5% (59·0 to 84·0)	53·3% (39·2 to 67·4)

Data are model-based estimates (95% CI) assessed using analysis of covariance from the modified treatment-regimen estimand for primary and key secondary endpoints and using MMRM for the efficacy estimand for additional secondary and exploratory endpoints. Lipids and fasting insulin are estimate (95% CI) using log transformation. Maintenance of bodyweight reduction endpoints and use of rescue tirzepatide are presented as percentage (SE). CIs were not adjusted for multiplicity and should not be used for hypothesis testing. ETD=estimated treatment difference. HbA1c=glycated haemoglobin. HDL=high-density lipoprotein. MMRM=mixed model for repeated measures. MTD=maximum tolerated dose. VLDL=very low-density lipoprotein. *The primary and key secondary endpoints were tested under type 1 error procedure using an overall two-sided nominal significance level of 0·05. †The denominator includes participants who reached bodyweight plateau at random allocation (week 60). ‡Not controlled for multiplicity.

Table 2: **Primary and secondary endpoints by treatment group**

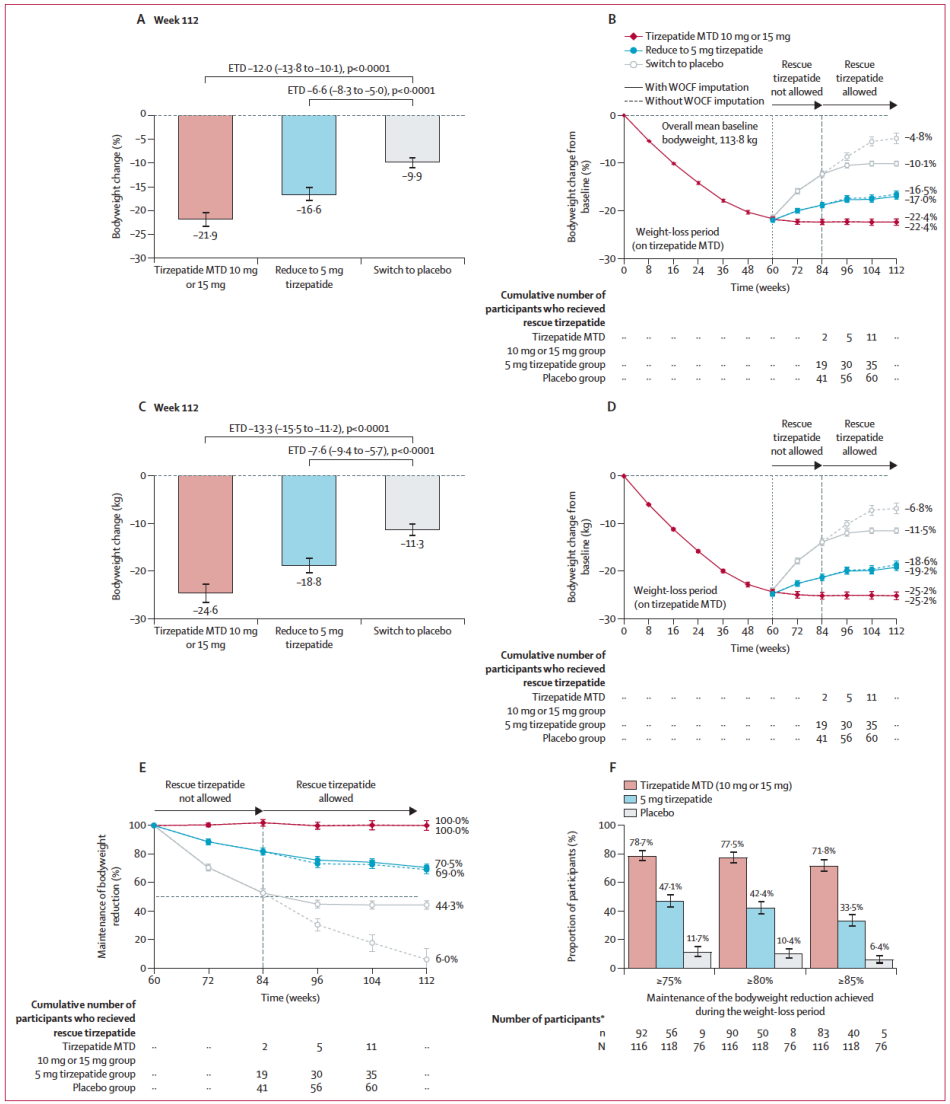

	Pre-random allocation	Weight maintenance period				Risk difference (95% CI)	
	Weight-loss period with MTD tirzepatide (n=441)	10 mg or 15 mg tirzepatide, MTD (n=139)	Reduce to 5 mg tirzepatide (n=142)	Switch to placebo (n=91)	Total (n=372)	10 mg or 15 mg tirzepatide, MTD *vs* switch to placebo	5 mg tirzepatide *vs* switch to placebo
Any adverse event emerging during treatment	359 (81%)	78 (56%)	71 (50%)	41 (45%)	190 (51%)	11·1 (−2·1 to 24·2)	4·9 (−8·2 to 18·1)
Deaths*	1 (<1%)	0	0	0	0	0	0
Serious adverse events	20 (5%)	0	2 (1%)	1 (1%)	3 (1%)	−1·1 (−3·2 to 1·0)	0·3 (−2·6 to 3·2)
Adverse events or death leading to discontinuation of study treatment	20 (5%)*	0	1 (1%)	0	1 (<1%)	0	0·7 (−0·7 to 2·1)
Gastrointestinal disorders leading to discontinuation of study treatment	11 (2%)	0	0	0	0	0	0
Nausea	3 (1%)	0	0	0	0	0	0
Vomiting	3 (1%)	0	0	0	0	0	0
Constipation	2 (<1%)	0	0	0	0	0	0
Diarrhoea	1 (<1%)	0	0	0	0	0	0
Abdominal pain, upper	1 (<1%)	0	0	0	0	0	0
Obstructive pancreatitis	1 (<1%)	0	0	0	0	0	0
Adverse events that emerged during treatment and occurred in ≥5% of participants in any treatment group							
Nausea	156 (35%)	8 (6%)	6 (4%)	2 (2%)	16 (4%)	3·6 (−1·3 to 8·5)	2·0 (−2·4 to 6·5)
Vomiting	73 (17%)	9 (6%)	1 (1%)	0	10 (3%)	6·5 (2·4 to 10·6)	0·7 (−0·7 to 2·1)
Diarrhoea	106 (24%)	10 (7%)	7 (5%)	1 (1%)	18 (5%)	6·1 (1·3 to 10·9)	3·8 (−0·3 to 8·0)
Constipation	136 (31%)	1 (1%)	5 (4%)	4 (4%)	10 (3%)	−3·7 (−8·1 to 0·8)	−0·9 (−6·1 to 4·3)
Eructation	34 (8%)	4 (3%)	1 (1%)	0	5 (1%)	2·9 (0·1 to 5·7)	0·7 (−0·7 to 2·1)
Dyspepsia	31 (7%)	3 (2%)	1 (1%)	0	4 (1%)	2·2 (−0·3 to 4·6)	0·7 (−0·7 to 2·1)
Gastro-oesophageal reflux disease	31 (7%)	2 (1%)	1 (1%)	1 (1%)	4 (1%)	0·3 (−2·6 to 3·3)	−0·4 (−2·9 to 2·2)
Abdominal pain	27 (6%)	2 (1%)	2 (1%)	0	4 (1%)	1·4 (−0·5 to 3·4)	1·4 (−0·5 to 3·3)
Abdominal distension	23 (5%)	4 (3%)	2 (1%)	1 (1%)	7 (2%)	1·8 (−1·7 to 5·3)	0·3 (−2·6 to 3·2)
Upper respiratory tract infection	32 (7%)	2 (1%)	5 (4%)	2 (2%)	9 (2%)	−0·8 (−4·4 to 2·9)	1·3 (−3·0 to 5·6)
COVID-19	30 (7%)	2 (1%)	4 (3%)	0	6 (2%)	1·4 (−0·5 to 3·4)	2·8 (0·1 to 5·5)
Influenza	23 (5%)	6 (4%)	2 (1%)	4 (4%)	12 (3%)	−0·1 (−5·5 to 5·3)	−3·0 (−7·6 to 1·7)
Sinusitis	12 (3%)	7 (5%)	7 (5%)	0	14 (4%)	5·0 (1·4 to 8·7)	4·9 (1·4 to 8·5)
Urinary tract infection	12 (3%)	7 (5%)	2 (1%)	0	9 (2%)	5·0 (1·4 to 8·7)	1·4 (−0·5 to 3·3)
Injection site reaction	40 (9%)	8 (6%)	3 (2%)	0	11 (3%)	5·8 (1·9 to 9·6)	2·1 (−0·3 to 4·5)
Fatigue	45 (10%)	2 (1%)	0	0	2 (1%)	1·4 (−0·5 to 3·4)	0
Headache	41 (9%)	3 (2%)	5 (4%)	3 (3%)	11 (3%)	−1·1 (−5·5 to 3·3)	0·2 (−4·5 to 5·0)
Dizziness	32 (7%)	2 (1%)	1 (1%)	0	3 (1%)	1·4 (−0·5 to 3·4)	0·7 (−0·7 to 2·1)
Decreased appetite	24 (5%)	0	0	0	0	0	0
Alopecia	41 (9%)	1 (1%)	0	0	1 (<1%)	0·7 (−0·7 to 2·1)	0
Adverse events of special interest occurring in one or more participants							
Severe or serious gastrointestinal events	8 (2%)	1 (1%)	2 (1%)	0	3 (1%)	NA	NA
Malignancies	4 (1%)	0	1 (1%)	0	1 (<1%)	NA	NA
Adjudication-confirmed MACE	2 (<1%)	0	0	1 (1%)	1 (<1%)	NA	NA
Adjudication-confirmed pancreatic events	0	0	0	0	0	NA	NA

Data are number of participants (%). Data obtained during the weight maintenance period after rescue were excluded. The total N for the open-label weight-loss period includes anyone who got treatment, whereas the total N for the double-blind weight maintenance period includes anyone who received treatment during the double-blind period only. Additional information is provided in appendix 2 (p 15). MACE=major adverse cardiovascular event. NA=not available. *Deaths were also counted as serious adverse events.

Table 3: **Adverse events**

Implications of all the available evidence

Together with previous evidence, these findings underscore the importance of continued therapy for the long-term management of obesity and demonstrate that staying on tirzepatide MTD resulted in superior maintenance of bodyweight reduction and associated cardiometabolic benefits versus placebo. In addition, this is the first incretin-based obesity medication trial of its kind providing data to elucidate clinical considerations associated with reducing treatment intensity such as dose lowering to maintain a majority of the bodyweight reduction and to provide evidence to inform individualised, patient-centred obesity care.

Die **koronare Flussreserve** (engl. *Coronary Flow Reserve*, kurz **CFR** oder **Koronarreserve**) beschreibt die Fähigkeit der Herzkranzgefäße, die Herzdurchblutung bei steigendem Sauerstoffbedarf (z. B. unter körperlicher Belastung) im Vergleich zum Ruhezustand maximal zu steigern. Sie wird als Quotient aus dem maximalen Blutfluss unter medikamentöser oder physischer Belastung und dem Blutfluss in Ruhe berechnet.

$$\underset{\text{(Coronary Flow Reserve)}}{\text{CFR}} = \frac{\text{Hyperemic flow}}{\text{Resting Flow}} = \frac{1/\text{Tmn\_Hyp}}{1/\text{Tmn\_Rest}} = \frac{\text{Tmn\_Rest}}{\text{Tmn\_Hyp}}$$

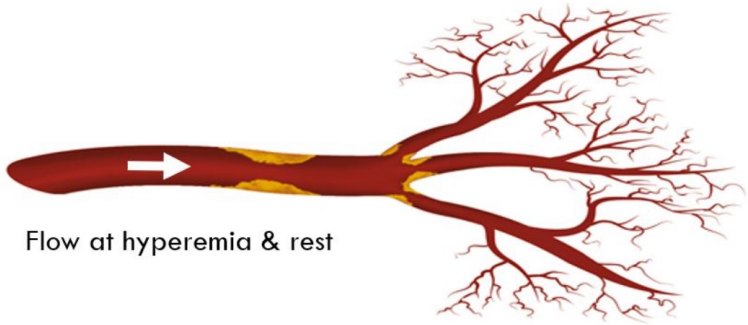

Die CFR wird nach folgender Formel ermittelt:

$$\text{CFR} = \frac{\text{maximaler Koronarblutfluss (Hyperämie)}}{\text{Koronarblutfluss in Ruhe}}$$

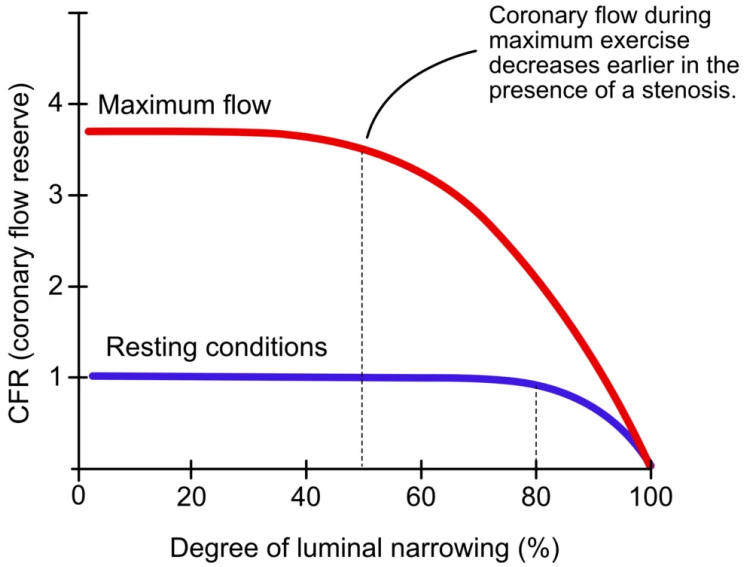

•**Gesunder Normwert:** Liegt typischerweise **über 3,5** (oft zwischen 4 und 6). Das bedeutet, das Herz kann seine Durchblutung bei Bedarf problemlos vervierfachen bis versechsfachen.

•**Pathologischer Wert:** Ein Wert **unter 2,0** gilt als deutlich erniedrigt und deutet auf eine Durchblutungsstörung hin.

Adenosin wird injiziert oder infundiert, um die koronare Flussreserve (Coronary Flow Reserve, CFR) zu messen.

Funktion von Adenosin bei der CFR-Messung

•**Maximale Vasodilatation**: Adenosin erweitert die kleinen Widerstandsgefäße (Mikrozirkulation) des Herzens maximal.

•**Hyperämie**: Es erzeugt einen Zustand künstlicher, maximaler Durchblutung (Hyperämie).

•**Vergleich von Flussraten**: Die Messung vergleicht den Blutfluss unter dieser maximalen Belastung mit dem Blutfluss in Ruhe.

•**Index des Mikrozirkulationswiderstands (IMR)**: Misst den physischen Widerstand in den kleinsten Gefäßen während der simulierten Belastung. Ein **IMR ≥ 25** gilt als pathologisch und bestätigt eine CMD.

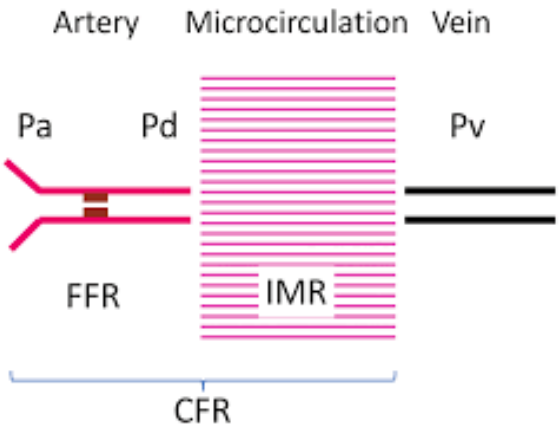

Coronary microvascular dysfunction worth it?

Coronary microvascular dysfunction and cardiovascular outcomes (Multicenter FLOW-CMD Registry): a prospective, multicentre cohort study in South Korea

Summary

Background Coronary microvascular dysfunction often coexists with epicardial coronary artery disease. Data regarding its prevalence and prognosis in patients undergoing invasive coronary angiography are scarce. This study aimed to evaluate the prevalence and prognosis of coronary microvascular dysfunction in patients undergoing clinically indicated invasive coronary angiography in routine practice.

Methods In this prospective, multicentre cohort study done in seven tertiary medical hospitals in South Korea, consecutive patients aged 18 years and older who were referred for clinically indicated invasive coronary angiography were systematically screened and evaluated by coronary physiological assessment. Obstructive epicardial coronary artery disease was defined as an intermediate stenosis (40–90% diameter stenosis), with fractional flow reserve of 0·80 or less or severe stenosis (>90% of diameter stenosis) treated with revascularisation without fractional flow reserve measurement. Coronary microvascular dysfunction was identified as coronary flow reserve below 2·0 and index of microcirculatory resistance of ≥25. The primary endpoint was a composite of all-cause death, myocardial infarction, clinically driven repeat revascularisation, or hospitalisation for heart failure. The Multicenter FLOW-CMD Registry study is registered with ClinicalTrials.gov (NCT05369182).

Findings Between April 22, 2022, and Nov 19, 2024, 5764 patients were screened and 1003 patients were enrolled (756 men and 247 women). Among these patients, coronary microvascular dysfunction was observed in 123 (21·5%) of 573 patients with obstructive epicardial coronary artery disease and in 40 (9·3%) of 430 patients without obstructive epicardial coronary artery disease. At a median follow-up of 1·9 years, the primary endpoint occurred in 26 patients (2-year Kaplan–Meier estimate 18·8%) with coronary microvascular dysfunction and 70 patients (2-year Kaplan–Meier estimate 10·5%) with preserved microvascular function (hazard ratio 1·91 [95% CI 1·22–2·99]; p=0·0047).

Interpretation In patients with suspected ischaemic heart disease undergoing invasive coronary angiography, coronary microvascular dysfunction coexisted with epicardial coronary artery disease and was associated with a higher risk of the composite of all-cause death, myocardial infarction, clinically driven repeat revascularisation, or hospitalisation for heart failure.

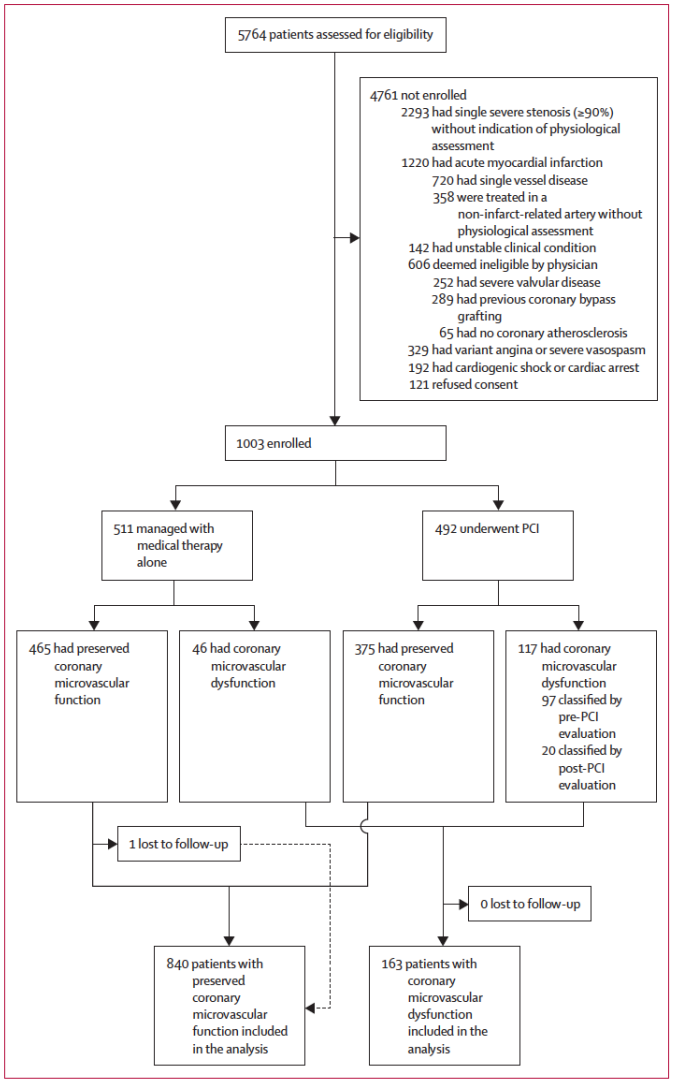

Figure 1: **Study selection**
PCI=percutaneous coronary intervention.

	Study population (n=1003)
Median age (years)	65·0 (58·0–72·0)
Sex	
Male	756 (75·4%)
Female	247 (24·6%)
Median BMI (kg/m²)	24·5 (22·7–26·8)
Initial presentation	
Chronic coronary syndrome	664 (66·2%)
Acute coronary syndrome	339 (33·8%)
Unstable angina	200 (19·9%)
Acute myocardial infarction	139 (13·9%)
Non-ST-segment elevation myocardial infarction	86 (8·6%)
ST-segment elevation myocardial infarction	53 (5·3%)
Initial symptom	
Typical chest pain on exertion	635 (63·3%)
Atypical symptoms	368 (36·7%)
Medical history	
Hypertension	702 (70·0%)
Diabetes	406 (40·5%)
Insulin-treated diabetes	53 (5·3%)
Dyslipidaemia	870 (86·7%)
Current smoking	132 (13·2%)
Chronic renal insufficiency	104 (10·4%)
Previous percutaneous coronary intervention	194 (19·3%)
Previous myocardial infarction	86 (8·6%)
Previous stroke	104 (10·4%)
Peripheral arterial disease	22 (2·2%)
Atrial fibrillation or flutter	106 (10·6%)
Non-invasive tests before coronary angiography*	478 (47·7%)
Coronary CT angiography	422 (42·1%)
Exercise treadmill test	36 (3·6%)
Exercise stress echocardiography	21 (2·1%)
Single-photon emission CT	12 (1·2%)
Nitrogen-13 ammonia PET	8 (0·8%)
Cardiac MRI	4 (0·4%)
Non-invasive tests results	
Abnormal results	457/478 (95·6%)
Normal results	21/478 (4·4%)
Laboratory test	
Median LDL cholesterol (mg/dL)	74·0 (56·0–106·0)
Median glycated haemoglobin (%)	6·0 (5·7–6·7)
Median estimated creatinine clearance (mL/min per 1·73 m²)	76·4 (57·9–97·2)
NT-proBNP (pg/mL)	125·0 (41·2–606·0)

(Table 1 continues in next column)

	Study population (n=1003)
(Continued from previous column)	
Median left ventricle ejection fraction (%)	62·7 (57·7–66·6)
Angiographic disease extent	
Insignificant disease	162 (16·2%)
Single-vessel disease	406 (40·5%)
Two-vessel disease	295 (29·4%)
Three-vessel disease	140 (14·0%)
Intervention	
Fractional flow reserve ≤0·80 at least one vessel	444 (44·3%)
Percutaneous coronary intervention at least one vessel	492 (49·1%)
Drug-eluting stents	365/492 (74·2%)
Drug-coated balloon	69/492 (14·0%)
Both	58/492 (11·8%)
Intravascular imaging devices used	246/492 (50·0%)
Discharge medications	
Aspirin	565 (56·3%)
$P2Y_{12}$ inhibitor	
Any	737 (73·5%)
Clopidogrel	637 (63·5%)
Ticagrelor	25 (2·5%)
Prasugrel	75 (7·5%)
Oral anticoagulant	71 (7·1%)
Statin	952 (94·9%)
Ezetimibe	741 (73·9%)
β blocker	358 (35·7%)
ACE inhibitor or ARB	574 (57·2%)
Calcium channel blocker	420 (41·9%)
Other angina medications (eg, trimetazidine, nicorandil)	302 (30·1%)
SGLT2 inhibitors	230 (22·9%)

Data are median (IQR) or n (%). ACE=angiotensin-converting enzyme. ARB=angiotensin receptor blocker. *25 patients had more than one non-invasive test.

Table 1: **Baseline characteristics**

	Lesions (n=1615)
Location of lesion	
Left main artery	18 (1·1%)
Left anterior descending artery	977 (60·5%)
Left circumflex artery	288 (17·8%)
Right coronary artery	332 (20·6%)
Culprit lesion in acute coronary syndrome	323 (20·0%)
Pre-PCI TIMI flow grade (n=1248)*	
TIMI 2	9 (0·7%)
TIMI 3	1239 (99·3%)
Pre-PCI quantitative coronary angiography (n=1432)†	
Mean proximal reference diameter (mm)	3·4 (0·6)
Mean distal reference diameter (mm)	2·8 (0·6)
Mean minimal lumen diameter (mm)	1·6 (0·7)
Mean diameter stenosis (%)	49·7 (17·2)
Mean lesion length (mm)	25·9 (11·6)
Pre-PCI physiological characteristics (n=1248)*	
Mean resting Pd/Pa	0·93 (0·07)
Mean FFR	0·82 (0·10)
Mean resting Tmn (s)	0·93 (0·51)
Mean hyperaemic Tmn (s)	0·36 (0·21)
Mean CFR	2·9 (1·5)
Mean IMR	23·8 (13·1)
Procedural characteristics	
No PCI	873 (54·1%)
Suboptimal PCI	3 (0·2%)
Successful PCI	739 (45·9%)
Devices	
Drug-coated balloons	170/742 (22·9%)
Drug-eluting stents	567/742 (76·4%)
Both	5/742 (0·7%)
Mean device size (mm)	3·0 (0·5)
Mean number of stents	1·1 (0·4)
Mean length of stents (mm)	32·2 (13·9)
Post-adjunctive balloon	478/742 (64·4%)
Mean size of post-adjunctive balloon (mm)	3·3 (0·6)
Mean maximum pressure (atmosphere)	19·8 (4·6)

(Table 2 continues in next column)

	Lesions (n=1615)
(Continued from previous column)	
Intravascular imaging devices	
No intravascular imaging devices used	434/742 (58·5%)
IVUS	179/742 (24·1%)
OCT	129/742 (17·4%)
Timing of intravascular imaging devices	
Before PCI	16/308 (5·2%)
After PCI	34/308 (11·0%)
Both	258/308 (83·8%)
Post-PCI TIMI flow grade	
TIMI 3	742/742 (100%)
Post-PCI quantitative coronary angiography (n=689)‡	
Mean proximal reference diameter (mm)	3·3 (0·6)
Mean distal reference diameter (mm)	2·9 (0·5)
Mean minimal lumen diameter (mm)	2·5 (0·6)
Mean diameter stenosis (%)	14·9 (12·7)
Post-PCI physiological characteristics (n=347)§	
Mean resting Pd/Pa	0·93 (0·04)
Mean FFR	0·85 (0·06)
Mean resting Tmn (s)	0·79 (0·44)
Mean hyperaemic Tmn (s)	0·31 (0·17)
Mean CFR	2·8 (1·3)
Mean IMR	22·2 (13·2)

Data are n (%), mean (SD), or n/N (%). CFR=coronary flow reserve. FFR=fractional flow reserve. IMR=index of microcirculatory resistance. IVUS=intravascular ultrasound. OCT=optical coherence tomography. Pa=aortic pressure. Pd=distal coronary pressure. PCI=percutaneous coronary intervention. Tmn=mean transit time. TIMI=thrombolysis in myocardial infarction. *At baseline, coronary physiological assessment was not done in 367 lesions due to chronic total occlusion, critical stenosis with decreased coronary flow, culprit vessel of acute myocardial infarction, or technical reasons. Among 144 patients who underwent multivessel physiological assessment, 20 vessels had incomplete sets of CFR, IMR, or FFR measurements. These vessels were included in total lesion counts. The proportion of pre-PCI TIMI flow grades was presented only for the target vessels that were evaluated by invasive physiological assessment. †183 lesions and ‡53 lesions could not be analysed due to technical reasons such as vessel overlapping, insufficient contrast filling, or inaccurate calibration. §395 lesions were not evaluated by post-PCI coronary physiological assessment.

Table 2: **Lesion and procedural characteristics**

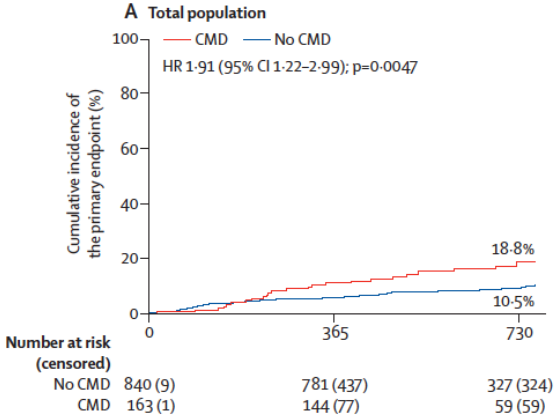

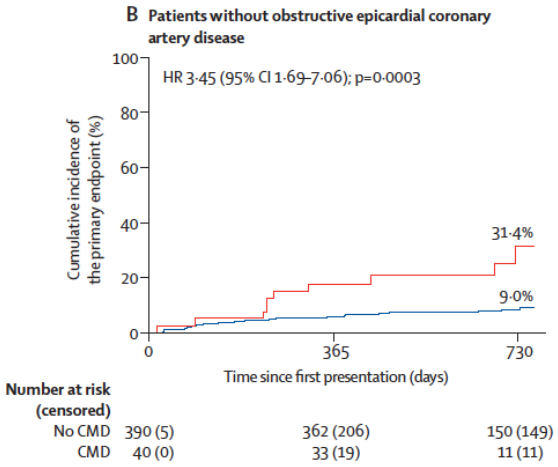

Figure 2: **Cumulative incidences of primary endpoint**
(A) Cumulative incidence for the total population. (B) The primary endpoint is compared according to the presence of coronary microvascular dysfunction among patients without epicardial coronary artery disease, defined by fractional flow reserve of 0·80 or more and deferred revascularisation. CMD=coronary microvascular dysfunction. HR=hazard ratio.

	Number of patients (2-year Kaplan–Meier estimates; %)			Absolute risk difference (95% CI)	Hazard ratio (95% CI)	p value
	Total (n=1003)	No CMD (n=840)	CMD (n=163)			
Primary endpoint						
Patient-oriented composite outcome*	96 (11·8%)	70 (10·5%)	26 (18·8%)	8·3 (1·1 to 15·6)	1·91 (1·22–2·99)	0·0047
Secondary endpoints†						
All-cause death	33 (4·8%)	23 (4·4%)	10 (7·7%)	3·5 (–1·6 to 8·6)	2·20 (1·05–4·61)	0·038
Cardiac death	20 (2·9%)	12 (2·2%)	8 (6·5%)	4·3 (–0·3 to 9·0)	3·38 (1·38–8·26)	0·0077
Non-cardiac death	13 (1·9%)	11 (2·0%)	2 (1·2%)	–0·8 (–3·1 to 1·4)	0·91 (0·20–4·12)	0·91
Cardiac death or myocardial infarction	31 (4·0%)	22 (3·5%)	9 (6·9%)	3·5 (–1·3 to 8·2)	2·08 (0·96–4·51)	0·065
Myocardial infarction‡	12 (1·3%)	10 (1·3%)	2 (1·2%)	–0·1 (–1·9 to 1·9)	1·03 (0·23–4·69)	0·97
Target vessel-related myocardial infarction	9 (1·0%)	8 (1·0%)	1 (0·6%)	–0·4 (–1·8 to 1·0)	0·64 (0·08–5·13)	0·68
Non-target vessel-related myocardial infarction	3 (0·3%)	2 (0·2%)	1 (0·6%)	0·4 (–0·9 to 1·7)	2·59 (0·23–28·53)	0·44
Deferred vessel myocardial infarction	8 (0·9%)	7 (0·9%)	1 (0·6%)	–0·3 (–1·7 to 1·1)	0·74 (0·09–5·98)	0·77
Repeat revascularisation§	39 (4·8%)	27 (4·0%)	12 (8·8%)	4·9 (–0·3 to 10·0)	2·30 (1·17–4·55)	0·016
Target vessel revascularisation	33 (4·0%)	25 (3·6%)	8 (6·1%)	2·4 (–2·0 to 6·9)	1·66 (0·75–3·68)	0·21
Non-target vessel revascularisation	12 (1·6%)	6 (1·0%)	6 (4·6%)	3·6 (–0·2 to 7·4)	5·21 (1·68–16·16)	0·0042
Deferred vessel revascularisation	27 (3·3%)	18 (2·7%)	9 (6·5%)	3·8 (–0·6 to 8·2)	2·60 (1·17–5·78)	0·019
Hospitalisation for heart failure¶	28 (2·9%)	21 (2·5%)	7 (4·9%)	2·4 (–1·5 to 6·3)	1·71 (0·73–4·03)	0·22
Stroke (ischaemic or haemorrhagic)	20 (2·1%)	19 (2·4%)	1 (0·6%)	–1·8 (–3·5 to –0·2)	0·27 (0·04–2·02)	0·20

Data are n (%) unless otherwise stated. The database for the analysis was locked on Nov 18, 2025. Clinical endpoints were evaluated during the overall study period. Percentages are the Kaplan–Meier estimates at 2 years. CMD=coronary microvascular dysfunction. PCI=percutaneous coronary intervention. *The number needed to harm regarding primary endpoint was 12·0 (95% CI 1·0–15·6). †The individual endpoints listed are the first occurrence of that event. ‡Myocardial infarction was defined with the Fourth Universal Definition of Myocardial Infarction.[17] Deferred vessel myocardial infarction is the myocardial infarction occurring in the vessel with deferred PCI at index procedure. §Repeat revascularisation includes all first clinically driven elective, urgent, or emergent revascularisation procedures that were not planned during the index hospitalisation during the overall study period. Target vessel denotes the vessel that was evaluated by physiological assessment at index procedure. Deferred vessel revascularisation is the revascularisation occurring at the vessel with deferred PCI at index procedure. ¶Hospitalisation for heart failure should include all of these criteria: (1) hospitalisation with primary diagnosis of heart failure, (2) duration of hospitalisation of at least 12 h, (3) new or worsening symptoms of heart failure, (4) objective evidence of new or worsening heart failure on physical examination or laboratory findings, and (5) initiation or intensification of heart failure treatment.

Table 3: **Cumulative rates of primary and secondary endpoints**

Implications of all the available evidence

Taken together with existing evidence, these findings suggest that coronary microvascular dysfunction might represent an important component of ischaemic heart disease that is not fully captured by assessment of epicardial coronary artery disease alone. Although the observational design precludes causal inference, these results support the potential value of incorporating microvascular functional assessment for risk stratification in patients undergoing invasive coronary evaluation. Further studies are needed to establish whether diagnostic and therapeutic strategies targeting coronary microvascular dysfunction can improve clinical outcomes and to define the role of integrated epicardial and microvascular assessment in routine clinical practice.

Das **polyendokrine metabolische Ovarsyndrom (PMOS)** – im Deutschen auch als **Polyendokrines metabolisches Ovarsyndrom** bezeichnet – ist der neue offizielle Name für das bisher bekannte **Polycystic Ovary Syndrome (PCOS)** bzw. Polycystische Ovarsyndrom. Im Mai 2026 einigten sich 56 weltweite medizinische Fachgesellschaften und Patientengruppen auf diese Umbenennung. Der alte Name galt als ungenau und irreführend, da die typischen Bläschen im Ultraschall keine echten, gefährlichen Gewebezysten sind, sondern lediglich unreife Eibläschen (Follikel). Zudem verdeutlicht der neue Name viel besser, dass es sich um eine komplexe hormonelle und stoffwechselbedingte Erkrankung handelt, die den gesamten Körper betrifft

- **Polyendokrin**: Betrifft mehrere Hormonsysteme parallel (z. B. erhöhtes Testosteron und erhöhte Insulinwerte).
- **Metabolisch**: Signalisiert die enge Verknüpfung mit dem Stoffwechsel und Risiken wie Insulinresistenz.
- **Ovarian / Ovar**: Bestätigt, dass die Funktion der Eierstöcke gestört ist, ohne fälschlicherweise „Zysten“ als Hauptursache zu benennen.

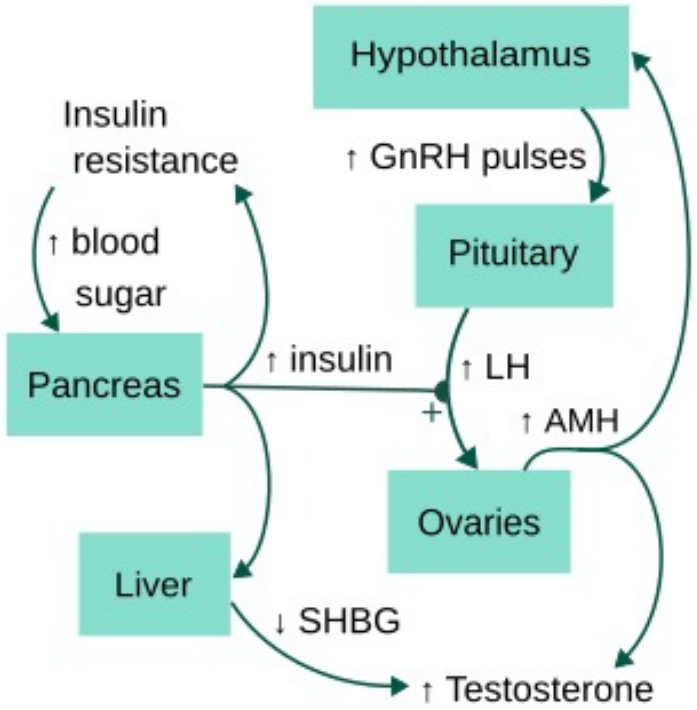

Why the name change?

Polyendocrine metabolic ovarian syndrome, the new name for polycystic ovary syndrome: a multistep global consensus process

Polyendocrine metabolic ovarian syndrome (PMOS), previously named polycystic ovary syndrome (PCOS), affects one in eight women. However, the term PCOS is inaccurate, implying pathological ovarian cysts, obscuring diverse endocrine and metabolic features, and contributing to delayed diagnosis, fragmented care, and stigma, while curtailing research and policy framing. Building on an international mandate for change, we outline an unprecedented, rigorous, multistep global consensus process for the name change. Funding and governance were established with engagement of 56 leading academic, clinical, and patient organisations. Using iterative global surveys (with responses from 14 360 people with PCOS and multidisciplinary health professionals from all world regions), modified Delphi methods, nominal group technique workshops, and marketing and implementation analyses, we identified principles prioritising scientific accuracy, clarity, stigma avoidance, cultural appropriateness, and implementation feasibility. An accurate new name was prioritised over retaining the PCOS acronym or a generic name. Implementation approaches prioritised evolution rather than transformation. Preferred terms were polyendocrine, metabolic, and ovarian, reflecting the condition's multisystem pathophysiology, and polyendocrine metabolic ovarian syndrome was the consensus new name. Accuracy was improved by omitting cysts and by capturing endocrine, metabolic, and ovarian dysfunction. A co-designed global implementation strategy, including a transition period, education, and alignment with health systems and disease classification, is under way.

The review concerns primarily the strategy behind the name change

Key messages

- Polycystic ovary syndrome affects more than 170 million women globally, yet its current name is inaccurate and misleading, obscuring the condition's multisystem endocrine and metabolic features, reinforcing stigma, delaying diagnosis, and hindering effective clinical care, research, and policy alignment.
- Through an unprecedented, rigorous global consensus process engaging patients, multidisciplinary health professionals, and organisations across world regions, a new name—polyendocrine metabolic ovarian syndrome—was agreed, omitting the misleading reference to ovarian cysts and accurately reflecting the diverse features of the condition.
- Consensus for the new name was built by use of robust, transparent methods, including modified Delphi survey processes, nominal group technique workshops, and implementation and marketing analyses, ensuring scientific accuracy, cultural appropriateness, stigma avoidance, and feasibility of adoption. These processes optimised representativeness, legitimacy, and transparency, and served to enhance engagement to underpin implementation.
- Coordinated implementation is under way in health systems, research institutions, funding bodies, education providers, clinical guidelines, and disease classification systems (including ICD coding), and is supported by a global transition period and continuous evaluation.
- Aligning nomenclature with scientific evolution and improving accuracy will enhance awareness, diagnosis, care quality, research coherence, and patient experience, strengthening policy, advocacy, and health outcomes globally.

Panel 1: Context and the case for a new name

The term polycystic ovary syndrome (PCOS) has long been recognised as inaccurate and potentially harmful. The following evidence-based considerations informed the need for a new name:

- The term polycystic ovary implies the presence of pathological ovarian cysts, which are not a feature of the condition. This misnomer contributes to misunderstandings among patients, clinicians, policy makers, and the public.
- PCOS encompasses diverse endocrine, metabolic, reproductive, psychological, and dermatological features. The current name reflects only one organ and fails to capture the disorder's multisystem nature.
- Confusion arising from the current name can delay diagnosis and hinder effective communication between patients and health professionals, contributing to patient dissatisfaction with care.
- The reproductive focus of the name can reinforce stigma, particularly in sociocultural contexts where fertility carries high value. Many individuals report distress associated with the name itself.
- The misnomer complicates epidemiological classification, research comparability, and health system coding. A more accurate name is expected to improve scientific coherence, research funding, and policy alignment.
- International guidelines, expert groups, and patient organisations have repeatedly called for renaming, with serial surveys and workshops culminating in a mandate to change the name through a rigorous, global consensus process.
- A new name must support long-term clinical care, research, and global adoption, and enable a smooth transition from existing terminology.

Panel 2: Overview of the consensus process

We conducted a structured, multistep global process to establish a new name for polycystic ovary syndrome, incorporating patient and professional perspectives across all world regions. Key stages included:

- Funding: we obtained resources for the name change process and translation (in September, 2024)
- Governance and stakeholder engagement: we established an international governance framework and recruited patient organisations, professional societies, and lived experience and multidisciplinary health professional experts (in December, 2024)
- Delphi surveys: building on 7708 previous survey responses, two further global surveys (launched in April, 2025, and January, 2026,) generated a further 14 360 responses from 10 411 patients and 3949 health professionals, that identified principles, approaches, terminology, and combinations for a new name
- Nominal group workshops: in November, 2025, and February, 2026, we held serial online workshops with participants from all world regions for systematic iterative testing of endocrine, metabolic, and reproductive terms, combinations, and acronyms, with prioritisation based on accuracy, acceptability, and cultural appropriateness
- Marketing and communication analysis: we applied branding and communication frameworks to assess feasibility, clarity, and transition strategies for candidate names in December, 2025
- Prioritised outcome: agreement among patients and health professionals on the new name (polyendocrine metabolic ovarian syndrome) occurred in February, 2026
- Implementation strategy: in 2025 and 2026, we developed a transition roadmap to support adoption across clinical practice, research, education, and public communication

	Survey A (n=3656)	Workshop registrations* (n=60)	Survey B (n=293)
Obstetrics and gynaecology	1183	16	117
Reproductive endocrinology	664	15	94
Endocrinology	366	13	50
Primary care	267	3	36
Nutrition or exercise	215	2	64
Nursing or midwifery	136	2	39
Paediatrics	62	5	17
Dermatology	8	1	2
Psychology	34	1	24
Academia or laboratory work	292	2	81

Questions in surveys A and B were not mandatory, and multiple responses were allowed. Totals therefore might not equal the number of respondents.
*Five participants who attended workshop A were unable to attend workshop B.

Table 1: **Health professional disciplines represented across workshops and surveys A and B**

	Survey A		Survey B	
	Patients (n=9358)	Health professionals (n=3656)	Patients (n=1053)	Health professionals (n=293)
Age, years				
18–25	1563 (19%)	103 (3%)	116 (11%)	3 (1%)
26–35	4230 (50%)	724 (24%)	461 (44%)	38 (13%)
36–45	1866 (22%)	866 (28%)	292 (28%)	82 (28%)
46–55	523 (6%)	696 (23%)	112 (11%)	93 (32%)
≥56	187 (2%)	612 (20%)	57 (5%)	74 (25%)
Prefer not to say	75 (1%)	47 (2%)	6 (1%)	2 (1%)
Duration of PCOS, years				
<1	1052 (14%)	NA	43 (4%)	NA
1–5	2450 (31%)	NA	299 (31%)	NA
6–10	1564 (20%)	NA	199 (20%)	NA
≥11	2736 (35%)	NA	440 (45%)	NA
PCOS care, years				
≤5	NA	812 (27%)	NA	105 (24%)
6–10	NA	624 (21%)	NA	84 (19%)
11–20	NA	716 (24%)	NA	118 (27%)
>20	NA	845 (28%)	NA	134 (30%)

Percentages are calculated based on available responses for each variable; denominators therefore vary due to non-response. NA=not applicable. PCOS=polycystic ovary syndrome.

Table 2: **Participant characteristics across surveys**

Panel 3: Summary of naming principles

Principles guiding the development of a new name for polycystic ovary syndrome were established through global Delphi surveys and multistakeholder workshops.

- Support for clinical care, research, and improved health outcomes: the name should facilitate diagnosis, improve awareness, optimise care, and enhance research and understanding of the condition to improve health outcomes
- Scientific and medical accuracy: the name must reflect the underlying endocrine and metabolic pathophysiology and avoid inaccurately including ovarian cysts.
- Clarity and communication: the terminology should be readily understood by patients, clinicians, researchers, and the public
- Avoidance of stigma: terms perceived as potentially stigmatising—particularly those linked directly to reproduction or fertility—should be avoided
- Cultural and linguistic appropriateness: the name must be acceptable and interpretable across diverse cultural, linguistic, and regional contexts.
- Feasibility of implementation: the name should allow for a practical transition in clinical, research, and policy environments

	Survey A (April to October, 2025; support %)	Workshop A (November, 2025; ranked first %)*	Survey B (January, 2026; ranked first %)	Workshop B (February, 2026; ranked first %)
Naming principles				
Scientific accuracy	67%	✓	✓	✓
Patients	60%	..	..	..
Health professionals	86%	..	..	..
Ease of communication	68%	✓	✓	✓
Patients	62%	..	..	..
Health professionals	85%	..	..	..
Avoidance of stigma	71%	✓	✓	✓
Patients	66%	..	..	..
Health professionals	85%	..	..	..
Cultural appropriateness	60%	✓	✓	✓
Patients	53%	..	..	..
Health professionals	80%	..	..	..
Naming approaches				
Generic name	48%	NA	NA	NA
Patients	46%	NA	NA	NA
Health professionals	54%	NA	NA	NA
Unchanged PCOS acronym, new terms	25%	NA	NA	NA
Patients	20%	NA	NA	NA
Health professionals	39%	NA	NA	NA
Accurate name	82%	✓	✓	✓
Patients	86%	..	..	..
Health professionals	70%	..	..	..
Key terms				
Endocrine features				
Endocrine	85%	65%	✓	NA
Patients	89%	NA	..	NA
Health professionals	74%	NA	..	NA
Polyendocrine	81%	35%	NA	✓
Patients	88%	NA	NA	..
Health professionals	60%	NA	NA	..
Metabolic features				
Cardiometabolic	52%	21%	NA	NA
Patients	52%	NA	NA	NA
Health professionals	52%	NA	NA	NA
Metabolic	76%	79%	✓	✓
Patients	74%	NA	..	..
Health professionals	80%	NA	..	..
Reproductive features				
Reproductive	54%	40%	NA	NA
Patients	52%	NA	NA	NA
Health professionals	63%	NA	NA	NA

(Table 3 continues on next page)

	Survey A (April to October, 2025; support %)	Workshop A (November, 2025; ranked first %)*	Survey B (January, 2026; ranked first %)	Workshop B (February, 2026; ranked first %)
(Continued from previous page)				
Ovary	42%	NA	NA	25%
Patients	38%	NA	NA	8%
Health professionals	53%	NA	NA	30%
Ovulatory	54%	60%	51%	5%
Patients	51%	NA	49%	8%
Health professionals	64%	NA	64%	5%
Gynaecological	NA	NA	37%	NA
Patients	NA	NA	40%	NA
Health professionals	NA	NA	27%	NA
Repro†	NA	NA	13%	NA
Patients	NA	NA	11%	NA
Health professionals	NA	NA	9%	NA
Ovarian	NA	NA	NA	70%
Patients	NA	NA	NA	85%
Health professionals	NA	NA	NA	65%
Names and acronyms for combination of terms				
Endocrine metabolic ovulatory syndrome	NA	NA	22%	NA
Patients	NA	NA	22%	NA
Health professionals	NA	NA	24%	NA
Ovulatory metabolic endocrine syndrome	NA	NA	11%	NA
Patients	NA	NA	10%	NA
Health professionals	NA	NA	19%	NA
Polyendocrine metabolic ovarian syndrome‡	NA	NA	66%	✓
Patients	NA	NA	69%	..
Health professionals	NA	NA	57%	..

Tick marks indicate the option was prioritised and carried forward to the next stage of the consensus process. NA=not assessed. PCOS=polycystic ovary syndrome. *Ranked first indicates the percentage of respondents who selected the option as their highest-ranked (most preferred) choice. †Repro was provided as an option for reproductive, with examples including repro-endocrine or repro-metabolic. ‡Polyendocrine metabolic ovarian syndrome was substituted for endocrine metabolic ovulatory syndrome given its majority support in survey A workshop A, marketing recommendations and cultural considerations, and to address challenges associated with the acronym of endocrine metabolic ovulatory syndrome (EMOS).

Table 3: **Iterative development of naming components across surveys and workshops**

Panel 4: Eight stages for global implementation of the new name for polycystic ovary syndrome, polyendocrine metabolic ovarian syndrome

The implementation strategy was informed by considerations highlighted in survey responses, and was co-designed with consumers, marketing and implementation experts, and governance bodies (including health professional experts), and was based on implementation science frameworks.

Stage 1: publication and academic dissemination
Publication of this Health Policy, supported by accompanying commentaries, clinical reviews, editorial correspondence, and updates to textbooks and educational materials.

Stage 2: resource development
Co-design of patient and health professional resources in multiple languages and for diverse platforms and delivery modes.

Stage 3: global communication and engagement
Implementation of a structured communication strategy, including society toolkits, multilingual patient and clinician resources, multimedia dissemination, professional education programmes, and coordinated events for patients and health professionals worldwide.

Stage 4: integration within health care and health information systems
Incorporation of the new terminology into electronic health records, including within Systematized Nomenclature of Medicine—Clinical Terms, and engagement with major electronic medical record vendors and key stakeholders in health-care provider education (eg, universities and textbook publishers).

Stage 5: policy and research alignment
Engagement with governments, research funders, journal editors, regulators, and the health-care industry (including the pharmaceutical industry), to support adoption across research classifications, publication processes, and funding systems.

Stage 6: international classification and global bodies
Formal engagement with international bodies, including WHO, to progress integration into disease classification systems, including the ICD.

Stage 7: transition and future refinement
A managed transition period of 3 years with monitoring and evaluation, consideration of emerging evidence on subtypes, and refinement of terminology as scientific understanding evolves.

Stage 8: guidelines
Integration into the International Guideline, which is already used in 195 countries and will next be updated in 2028.

Polyendocrine metabolic ovarian syndrome

PMOS

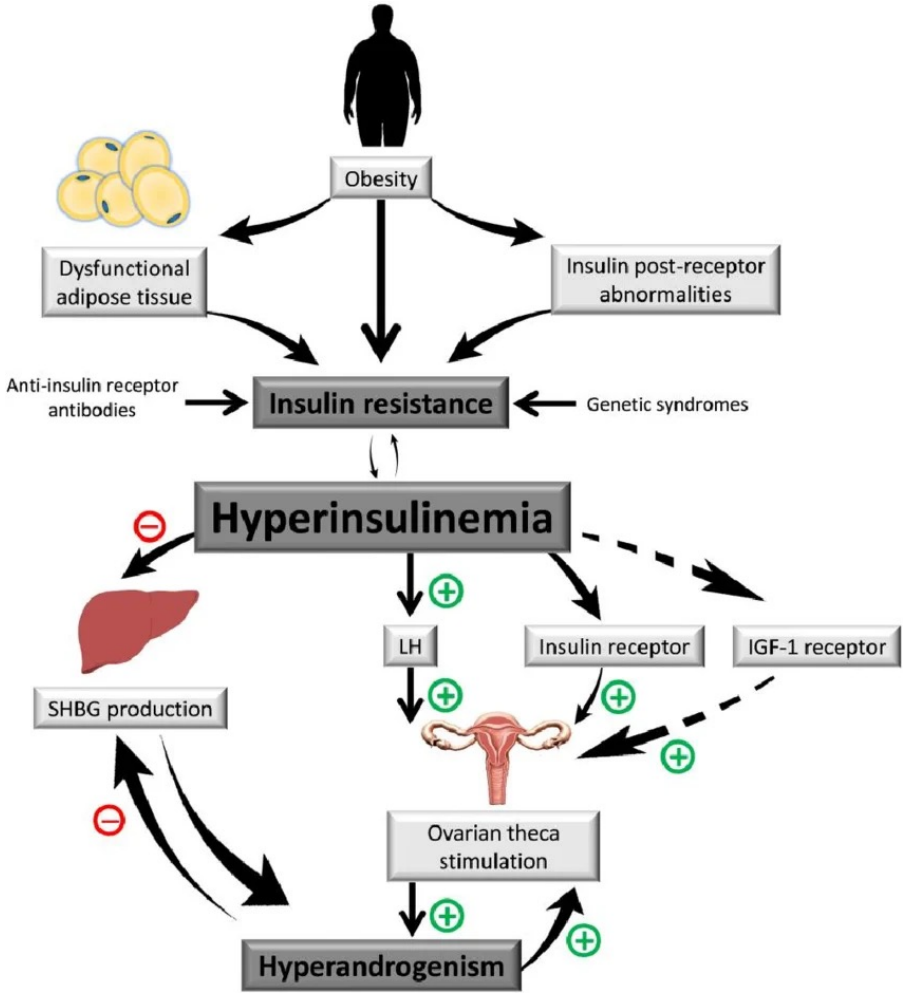

Troponin I (TnI) ist ein Strukturprotein der Skelett- und Herzmuskulatur, das die **Muskelkontraktion reguliert, indem es im entspannten Zustand des Muskels das Aneinanderbinden von Aktin und Myosin blockiert**. Das Kürzel „**I**“ steht hierbei für **inhibitorisch** (hemmend).

Die biologische Funktion im Muskel

Im ruhenden Muskel sorgt Troponin I gemeinsam mit zwei anderen Proteinen (Troponin T und Troponin C) und dem Fadenprotein Tropomyosin für den Entspannungszustand:

•**Blockade (Ruhezustand)**: Liegt keine Muskelaktivität vor, bindet Troponin I direkt an die Aktinfilamente. Dadurch stabilisiert es den umliegenden Komplex und verdeckt die Bindungsstellen für die Myosinköpfchen. Der Muskel kann sich nicht zusammenziehen.

•**Aktivierung (Kontraktion)**: Erhält der Muskel ein elektrisches Signal, strömen Calcium-Ionen (Ca^{2+}) in die Muskelzelle und binden an Troponin C.

•**Freigabe**: Diese Bindung führt zu einer strukturellen Verformung des gesamten Troponin-Komplexes. Troponin I gibt die Bindungsstelle frei, und Tropomyosin verschiebt sich. Die Myosinköpfchen können nun an das Aktin andocken und die Muskelkontraktion (das Zusammenziehen) beginnt.

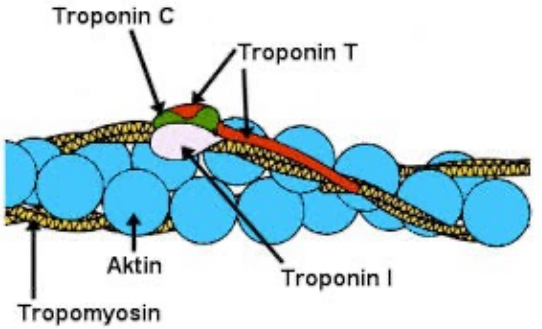

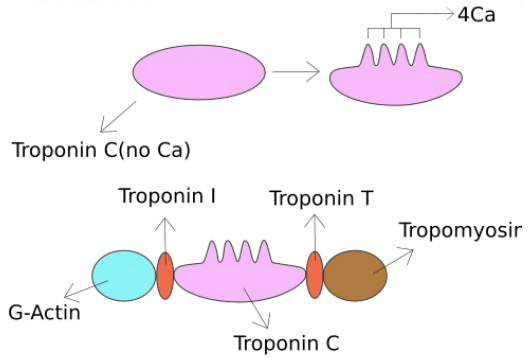

•**Troponin C (Calcium-bindend):** Bindet Kalziumionen, was den Startschuss für die Muskelkontraktion gibt.
•**Troponin I (Inhibitorisch):** Hemmt im Ruhezustand die Verbindung von Aktin und Myosin, sodass der Muskel entspannt bleibt.
•**Troponin T (Tropomyosin-bindend):** Verankert den gesamten Troponin-Komplex am Tropomyosin auf dem Muskel-Aktinfilament

Die Rolle im Detail

•**Grundfunktion:** Die grundsätzliche Aufgabe von Troponin I (einem Protein des Troponin-Komplexes) besteht darin, in Ruhesituationen die Bindung zwischen Aktin und Myosin zu verhindern, wodurch der Muskel erschlaffen kann. Bei Calciumeinstrom wird dieser "Block" aufgehoben und der Herzmuskel zieht sich zusammen.

•**Die Funktion der Phosphorylierung (Feinabstimmung):** Unter körperlicher Belastung oder Stress (z. B. durch Adrenalin) wird Troponin I an bestimmten Aminosäuren phosphoryliert. Dies verändert seine Struktur.

•**Auswirkung:** Die Phosphorylierung verringert die Empfindlichkeit des Herzmuskels für Calcium. Dadurch löst sich das Calcium schneller wieder von Troponin C, was eine **schnellere Erschlaffung (Relaxation)** des Herzmuskels bewirkt.

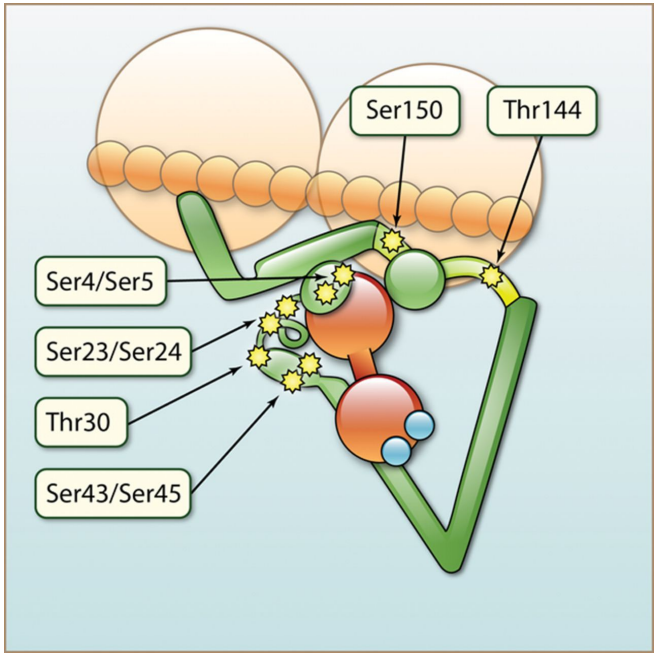

Warum das wichtig ist

Für ein gesundes Herz ist dieser Mechanismus essenziell. Bei schnellem Herzschlag muss sich die Herzkammer erst entspannen, um sich wieder mit Blut füllen zu können, bevor der nächste Schlag erfolgt. Ohne die Phosphorylierung von Troponin I (beispielsweise bei bestimmten Herzerkrankungen) ist diese schnelle Entspannung beeinträchtigt

Severe obesity in human HFpEF alters contractile protein function and organization

INTRODUCTION: More than half of heart failure patients have normalappearing contraction as reflected by the percent of blood ejected with each heartbeat, the ejection fraction (EF). This syndrome, known as heart failure with preserved ejection fraction (HFpEF), confers substantial morbidity and mortality and has few effective treatments. It historically affected elderly individuals with hypertension and thickened hearts, but most HFpEF patients now have obesity, often severe, that is associated with worse clinical outcomes. Underlying cellular abnormalities in human HFpEF heart muscle and any potential impacts of coexisting severe obesity remain largely unknown. In addition, there are no data from human heart muscle of individuals without heart failure but with similarly severe obesity to determine whether and how this itself affects myocyte function.

RATIONALE: We hypothesized that function and structure of the contractile apparatus (sarcomeres) in single cardiomyocytes from patients with HFpEF are adversely affected by the coexistence of severe obesity. We further proposed that such changes correlate with body mass index (BMI) and clinical exercise parameters, may be ameliorated after weight loss, and in part relate to sarcomere protein modifications. This study examined demembranated myocytes and myofibrils from small cardiac biopsies of patients with HFpEF and nonfailing (NF) controls with a broad BMI range.

RESULTS: We measured ~30 different rest and reserve functional and structural parameters of cardiomyocytes-myofibrils from patients with HFpEF. Unsupervised machine learning identified two subgroups whose primary clinical difference was their BMI (31 kg/m^2 in Group 1 (G1), 43 in G2, $P < 10^{-12}$). Myocytes from more obese G2-HFpEF patients had markedly reduced calcium-stimulated and length-dependent tension and peak power like that in heart failure with reduced EF (such as from patients undergoing heart transplantation). G1-HFpEF data were similar to NF controls.

Myosin crossbridge detachment was slowed and myofibrillar relaxation prolonged in both HFpEF groups, whereas resting stiffness was higher in less-obese G1 versus G2 or NF hearts. X-ray diffraction structural analysis revealed myosin deactivation in very obese G2-HFpEF patients. These abnormalities were not present in myocytes obtained from hearts of similarly obese but NF controls. Depressed myocyte contractility correlated with lower exercise work capacity that occurred with higher exercise-induced heart pressures. In patients with HFpEF treated with weight-loss therapy, the extent of BMI reduction correlated with enhanced myocyte contractility, suggesting that these abnormalities may be reversible. Finally, phosphorylation of sarcomere proteins increased in G2-HFpEF, and reducing it with phosphatase 2a (PP2a) improved contractility in this subgroup. Phosphorylation of cardiac troponin I at threonine 181 positively correlated with BMI in heart failure but was unchanged in NF myocardium. Mutating the threonine to mimic its phosphorylation depressed contractility in myocytes, as in G2-HFpEF patients.

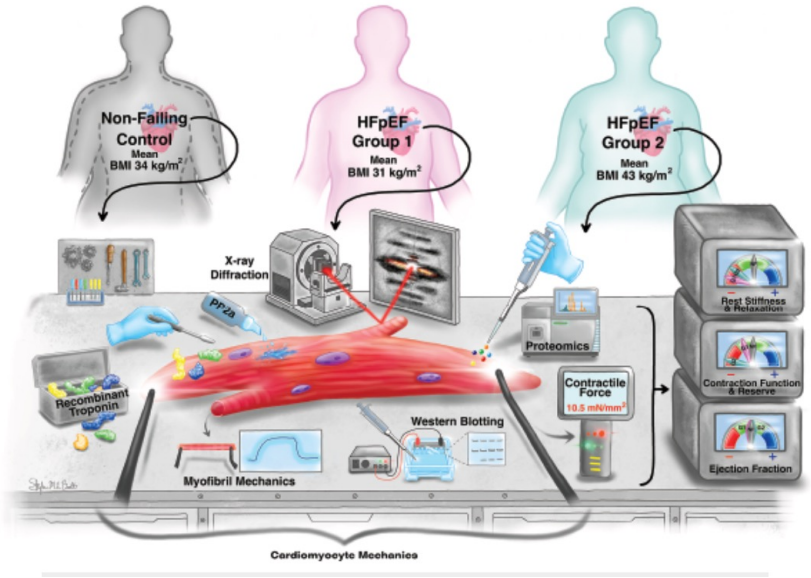

Cardiac myocytes from biopsies of human HFpEF and NF control hearts were subjected to an array of mechanical, structural, and molecular measurements. Despite all patients having normal-range ejection fraction, active myocyte contractile function, reserve, and structural motor-protein activation were very reduced in severely obese HFpEF (G2), whereas diastolic abnormalities were somewhat greater in less-obese HFpEF patients (G1). Abnormal troponin I phosphorylation likely plays a role.

CONCLUSION: The combination of HFpEF and severe obesity reduces heart muscle cell contractile function and reserve and impairs myofilament structural activation in ways not found with severe obesity alone. These defects indicate that negative modulators of sarcomere function should be used cautiously or avoided in patients with severe obesity and in HFpEF patients, whereas weight loss and/or therapies targeting underlying sarcomere abnormalities may prove more effective.

Diabetes researchers ejected from conference after criticizing White House

Five diabetes researchers, including the editor of a leading journal, were removed from the field's premier conference in New Orleans on Friday morning, after handing out copies of an editorial criticizing the Trump administration's "dismantling" of the biomedical research enterprise.

The incident occurred outside a conference hall where a keynote address had originally been scheduled to be given by Jay Bhattacharya, director of the National Institutes of Health, at a gathering organized by the American Diabetes Association. A group of about 10 researchers, including some of the field's leaders, were quietly handing out printouts of an editorial published in Diabetes Care, a journal the association publishes, according to three of the participants. Security and police told them to leave at the direction of event organizers and confiscated some of their lanyards and ability to attend the conference.

One of those ejected from the meeting was Steven Kahn, a University of Washington professor of medicine who is the editor in chief of Diabetes Care and the director of a federally funded diabetes research center. Kahn said in an interview that he had 1,000 copies made of an editorial that he had co-authored that called scientists to action to oppose changes to federal biomedical research funding that endangered diabetes research.

"A number of people who come to this meeting are scientists, who feel their livelihoods are threatened by what NIH is doing to science," Kahn said.

The editor of *Diabetes Care*

Ballroom donors won $50B in contracts after giving to Trump project, watchdog group finds

More than half of the publicly identified donors to President Donald Trump's White House ballroom project have won new or expanded federal contracts worth more than $50 billion during the past six months, according to a report released Thursday by a government watchdog group.

Fourteen of the 27 known corporate donors to the $400 million project, which would replace the East Wing that Trump demolished in October, have seen their government business grow in that window, according to the report from Public Citizen, a nonprofit. Most of those same companies are also facing federal enforcement actions over alleged wrongdoing or have had such actions suspended by the Trump administration since the start of Trump's second term, the nonprofit found.